

CRANFIELD UNIVERSITY

CAROLINE AMY HEPBURN

Removal of Siloxanes from Biogas

SCHOOL OF ENERGY, ENVIRONMENT AND AGRIFOOD
Cranfield Water Science Institute

PhD
Academic Year: 2011 - 2014

Supervisors: Ewan McAdam and Nigel Simms
October 2014

CRANFIELD UNIVERSITY

SCHOOL OF ENERGY, ENVIRONMENT AND AGRIFOOD
Cranfield Water Science Institute

PhD

Academic Year: 2011 - 2014

CAROLINE AMY HEPBURN

Removal of Siloxanes from Biogas

Supervisors: Ewan McAdam and Nigel Simms
October 2014

This thesis is submitted in partial fulfilment of the requirements for
the degree of Doctor of Philosophy

© Cranfield University 2014. All rights reserved. No part of this
publication may be reproduced without the written permission of the
copyright owner.

ABSTRACT

Economic utilisation of biogas arising from sewage sludge is hampered by the need to remove siloxanes, which damage gas engines upon combustion. This thesis applies on-line Fourier transform infrared spectroscopy to measure siloxanes in biogas upstream and downstream of the activated carbon vessels designed to adsorb siloxanes. On-line analysis provides accurate measurement of siloxane concentrations with a detection limit below the siloxane limits set by engine manufacturers, high data intensity and timely identification of breakthrough. Cost savings of up to £0.007 kWh⁻¹ may be realised compared to existing grab sampling. Using on-line analysis, the performance of full-scale and bench-scale carbon vessels were measured. Full-scale carbon contactors are typically operated at Reynold's numbers close to the boundary between the laminar and transitional regimes ($Re = 40 - 55$). This thesis demonstrates, at full- and bench-scale, that increasing the Reynold's number to site the adsorption process in the transitional regime increases media capacity, by 36% in dry gas and by 400% at 80% humidity. It is postulated that the change in gas velocity profile which occurs as Reynold's number increases reduces the resistance to siloxane transport caused by gas and water films around the carbon particles, and therefore increases the rate of the overall adsorption process. In the laminar regime ($Re = 31$) increasing humidity from zero to 80% led to the classical stepwise reduction in adsorption capacity observed by other researchers, caused by the increasing thickness of the water film, but in the transitional regime ($Re = 73$) increasing humidity had no effect as no significant water film develops. It is therefore recommended that siloxane adsorption vessels should be designed to operate at Reynold's numbers above 55. By choosing a high aspect ratio (tall and thin) both Reynold's number and contact time can be optimised.

Keywords: *Activated carbon; Adsorption; Anaerobic digestion; FTIR spectroscopy; Hydrodynamic regime*

ACKNOWLEDGEMENTS

First of all, a great big thank you to my supervisors, Ewan McAdam and Nigel Simms, for keeping me on the straight and narrow when I was lost in realms of inexplicable data and encouraging me when it seemed my test rig should be consigned to the scrap heap.

Thanks also to the rest of my thesis committee, Pete Jarvis and Paul Morantz, for pushing me to know my mechanisms and golden nuggets, and ensuring that I kept to my Gantt chart (more or less).

Thanks to the EPSRC and Severn Trent Water for funding this project and thanks to my contacts at STW, especially Pete Vale and John Griffiths, for tolerating my requests for carbon samples, data and more. I'm keeping the hard hat.

Many people have helped me in more informal roles – too many to name – but thanks to all the CWSI technicians, especially Rukhsana, Nigel, Alan and Paul, for suggesting better ways to do things when I was tapping a measuring cylinder on the bench for hours and finding a lighter coolbox when I broke my wrist and struggled to lift the big one. Thanks to everyone in the Pilot Hall and the PhD office for assistance and companionship and helping me realise it wasn't just me... especial thanks goes to Rachel, Siobhán and Catherine – girly coffees kept me sane!

Finally, thanks to my parents for supporting and encouraging me through a long three years, and to Alex for feeding me up when I was down and dragging me away to the hills by bike and on foot (but not electric tram).

TABLE OF CONTENTS

ABSTRACT	i
ACKNOWLEDGEMENTS.....	iii
LIST OF FIGURES.....	viii
LIST OF TABLES	xii
LIST OF EQUATIONS.....	xiv
LIST OF ABBREVIATIONS.....	xv
1 Introduction.....	1
1.1 Background.....	1
1.2 Aim and objectives.....	6
1.3 Thesis structure	7
2 Adsorbent selection for environmental gas applications.....	9
Abstract.....	9
2.1 Introduction	10
2.2 General process characterisation	11
2.3 Adsorbent characteristics.....	15
2.4 Adsorbate characteristics.....	17
2.5 Conclusions	25
3 On-line siloxane detection for adsorption vessel characterisation using FTIR spectroscopy	27
Abstract.....	27
3.1 Introduction	28
3.2 Materials and Methods.....	31
3.2.1 Instrument and set up.....	31
3.2.2 Calibration and verification	32
3.2.3 Data analysis.....	34
3.3 Results.....	34
3.3.1 FTIR calibration using reference gas and real biogas	34
3.3.2 Volatile organic carbons in biogas samples	40
3.3.3 Finalised calibration using partial least squares analysis and verification using external reference gas.....	40
3.3.4 Application to full scale contactors	42
3.4 Discussion	42
3.5 Conclusions	49
3.6 Acknowledgements.....	49
4 On-line management of siloxane breakthrough in carbon contactors using changepoint detection	51
Abstract.....	51
4.1 Introduction	52
4.2 Materials and Methods.....	54
4.2.1 The FTIR spectrometer and case study site.....	54

4.2.2	The changepoint detection algorithm and calculations.....	54
4.3	Results and discussion	56
4.3.1	Changepoint detection for broad-fronted breakthrough curves	56
4.3.2	Changepoint detection for sharp-fronted breakthrough curves	59
4.3.3	Effectiveness of changepoint detection algorithm	61
4.4	Implementing changepoint detection for broad-fronted breakthrough profiles	63
4.5	Conclusions	65
5	Characterisation of Full Scale Carbon Contactors for Siloxane Removal from Biogas using On-line Fourier Transform Infrared Spectroscopy.....	67
	Abstract.....	67
5.1	Introduction	68
5.2	Materials and Methods.....	69
5.2.1	Site description.....	69
5.2.2	On-line Fourier transform infrared (FTIR) analysis	70
5.2.3	Data analysis.....	72
5.3	Results.....	72
5.3.1	Evaluation of siloxane concentration in the treated biogas.....	72
5.3.2	Analysis of siloxane uptake in the GAC contactors	75
5.3.3	Analysis of GAC contactor operational conditions.....	77
5.4	Discussion	77
5.5	Conclusions	84
6	Siloxane adsorption from biogas in the transitional regime	85
	Abstract.....	85
6.1	Introduction	86
6.2	Materials and Methods.....	88
6.2.1	Test rig	88
6.2.2	FTIR	91
6.3	Results.....	91
6.3.1	Effect of EBCT and Reynold's number on uptake in dry gas.....	91
6.3.2	Influence of humidity	95
6.3.3	Influence of competition between siloxane species.....	97
6.4	Discussion	99
6.5	Supporting information.....	103
6.5.1	Materials and methods.....	103
6.5.2	Capillary condensation	104
6.5.3	Use of the modified Wheeler equation to calculate rate constants.	107
7	Practical implementation	109
7.1	Is on-line FTIR assessment an effective tool?	109
7.2	How do we best enhance media capacity in practice?.....	114
7.3	What is the optimum carbon vessel design for siloxane removal?.....	117
7.3.1	For new carbon contactors.....	117

7.3.2 Adapting existing vessels	120
7.3.3 Vessel layouts	121
7.4 How is this understanding of contactor deign integrated into existing practice?	123
8 Conclusions and Future Work	124
8.1 Conclusions	124
8.2 Future Work	125
REFERENCES	127

LIST OF FIGURES

- Figure 1-1 Distribution of siloxanes (D4, D5, D6) at a UK sewage treatment works, showing that most siloxanes are removed in settling tanks as they sorb onto solids. Data from van Egmond et al. (2013)..... 4
- Figure 1-2 Siloxane removal vessels pre-treat biogas from anaerobic digester before it is combusted in a CHP engine. If the siloxane removal vessel is not in use, biogas may be sent directly to the engine or flared..... 5
- Figure 1-3. Thesis road map 8
- Figure 2-1. Relationship between molecular weight and Dubinin-Radushkevich affinity coefficient for selected VOCs (using L2 as reference compound).. 19
- Figure 3-1. Infrared absorbance spectra for (a) D5 in nitrogen and (b) biogas. The main peaks are labelled with the corresponding chemical bonds (Stuart, 2004). Note the difference in y-axis scale – the peaks caused by D5 are 1/50th of the height of the large peaks caused by the bulk gases (CH₄ and CO₂)..... 30
- Figure 3-2. Comparison between expected D5 concentrations in reference gas (N₂) and absorbance peak heights in FTIR spectra. $r^2 = 0.99$ for both correlations..... 36
- Figure 3-3. Comparison between expected D5 concentrations in reference gas (CO₂) and FTIR readings. The dashed line represents $y = x$ 36
- Figure 3-4. FTIR readings compared to GC-MS measurements in synthetic reference gas. $r^2 = 0.99$ for D5 in N₂ and $r^2 = 0.98$ for D5 in CO₂. The dashed line represents $y = x$ 37
- Figure 3-5. FTIR reading for cyclic siloxanes compared to total cyclic siloxanes measured from gas bag samples by GC-MS from biogas (a) upstream of carbon vessel and (b) downstream of carbon vessel. The dashed lines show the 95% confidence limits..... 38
- Figure 3-6: Volatile organic compounds found in the biogas samples from upstream and downstream of a carbon vessel. (a) Concentration; (b) molar ratio to D5. *Nonane, decane and carbon disulphide, do not contain bonds which are thought to contribute to interference in the FTIR readings. 39
- Figure 3-7. An example breakthrough curve for a carbon vessel (1.21 m³, 450 kg_{carbon}). The area under the outlet concentration graph can be used to calculate the mass of siloxane entering the engine as follows: light grey - 0.94 kg over 18 days before breakthrough; mid grey - 0.94 kg over three days after breakthrough; dark grey - a further 2.72 kg over eight days before the carbon is changed. 43
- Figure 4-1. A broad-fronted breakthrough curve with (a) Waukesha siloxane limit (30 mg m⁻³) superimposed (dotted line) and (b) showing changepoints

detected by changepoint detection algorithm (dotted lines) and the time at which the changepoint was detected (solid lines).....	57
Figure 4-2. Three breakthrough curves from vessels exhibiting broad-fronted profiles. The Waukesha siloxane limit (30 mg m^{-3}) is superimposed (dotted line) and for each curve the detection time of the first changepoint is labelled.....	58
Figure 4-3. A sharp-fronted breakthrough curve with (a) Waukesha siloxane limit (30 mg m^{-3}) superimposed (dotted line) and (b) showing changepoints detected by changepoint detection algorithm (dotted lines) and the time at which the changepoint was detected (solid lines).....	60
Figure 4-4. Two breakthrough curves from vessels exhibiting sharp-fronted profiles. The Waukesha siloxane limit (30 mg m^{-3}) is superimposed (dotted line) and for each curve the detection time of the first changepoint is labelled.....	62
Figure 4-5. Comparison of the time taken to exceed the siloxane limit imposed by Waukesha and the time that the first changepoint was detected by the changepoint detection algorithm. $Y = x$ is shown (dotted line) to demonstrate the “early warning” potential of the change point detection algorithm.....	62
Figure 5-1. Inlet and outlet siloxane concentrations for one of the carbon contactors during a single exhaustion cycle (run time, 706 h between media changes). The solid and dashed lines represent the Jenbacher and Waukesha siloxane limits.	73
Figure 5-2. Cumulative frequency curves developed using outlet siloxane data from GAC 1 to ascertain conformity to proposed warranty specification (Table 5-1). Data is provided from five consecutive exhaustion cycles.	74
Figure 5-3. Cumulative frequency curves developed using outlet siloxane data from all five GAC contactors to ascertain conformity to proposed warranty specifications (Table 5-1). Data is from a single exhaustion cycle in which all five contactors are assessed simultaneously.	74
Figure 5-4. Breakthrough curves for four of the GAC contactors which experienced breakthrough. Breakthrough is defined as the outlet concentration exceeding 30 mg m^{-3} for the third consecutive reading (equivalent to the Waukesha warranty limit, Table 5-1).....	76
Figure 5-5. Media sampled at breakthrough, cross-sectioned (at centre) and analysed for Si to determine Si deposition in media operated at low Re_p (GAC4, $Re = 30$) and high Re_p (GAC1, $Re = 81$).	76
Figure 5-6. Evaluating the role of empty bed contact time (EBCT) in determining the number of bed volumes of biogas that can be treated before breakthrough. EBCT is determined by contactor length/superficial velocity.....	78

Figure 5-7. Evaluating the role of the modified Reynold's number (Re_p) in determining the number of bed volumes of biogas that can be treated before breakthrough. The modified Re_p was calculated based on specific contactor and media dimensions. 78

Figure 6-1. Breakthrough curves showing the effect of varying empty bed contact time (EBCT) and Reynold's number. At EBCTs above 0.05 s (and Reynold's numbers below 55) the curves are nearly identical. At lower EBCTs (higher Re), the breakthrough curves are progressively less steep. (Inlet concentration = $70 \text{ mg}_{D5} \text{ m}^{-3} \text{ CO}_2$; humidity = 0%; $Re = 31 - 107$; EBCT = 0.02 – 0.15 s.)..... 92

Figure 6-2. The relationship between the Reynolds number and specific media capacity. When Re is increased from 31 to 107 the media capacity increases from 138 to $191 \text{ g}_{D5} \text{ kg}^{-1} \text{ carbon}$, an increase of 38%. 93

Figure 6-3. Comparison of the effects of changing EBCT and Re separately. a) EBCT is held constant whilst Re is changed from 32 to 73, resulting in an increase in media specific capacity from 70.3 to $165 \text{ g}_{D5} \text{ kg}^{-1} \text{ carbon}$. b) Re is held constant whilst EBCT is increased from 0.014s to 0.031s, resulting in specific media capacity increasing from $76.4 \text{ g}_{D5} \text{ kg}^{-1} \text{ carbon}$ to $165 \text{ g}_{D5} \text{ kg}^{-1} \text{ carbon}$. (Inlet concentration = $70 \text{ mg}_{D5} \text{ m}^{-3} \text{ CO}_2$; humidity = 0%.)..... 94

Figure 6-4. Breakthrough curves showing the effect of humidity at a Reynold's number of 31 (near-laminar flow regime). As humidity increases from 0% to 80% the media siloxane capacity decreases from 135 to $69.3 \text{ g}_{D5} \text{ kg}^{-1} \text{ carbon}$. (Inlet concentration = $70 \text{ mg}_{D5} \text{ m}^{-3} \text{ CO}_2$; humidity = 0 – 80%; $Re = 31$; EBCT = 0.077 s.) 96

Figure 6-5. Breakthrough curves showing the effect of humidity at a Reynold's number of 73 (transitional flow regime). Adding 10% humidity has no effect on media capacity compared to dry gas. Adding 30 – 80% humidity increases the media capacity by $39 \text{ g}_{D5} \text{ kg}^{-1} \text{ carbon}$ (12%). The differences between 30 – 80% humidity are within experimental error. (Inlet concentration = $70 \text{ mg}_{D5} \text{ m}^{-3} \text{ CO}_2$; humidity = 0 – 80%; $Re = 73$; EBCT = 0.031 s.)..... 96

Figure 6-6. Breakthrough curves for L2 and D5 in the same gas showing competition between the two species. (Humidity = 0%; $Re = 3.6$; EBCT = 2.7 s.)..... 97

Figure 6-7. The effect of humidity on two siloxanes (a) L2 and (b) D5. (Humidity = 0 – 100%; $Re = 3.6$; EBCT = 2.7 s.) 98

Figure S6-8. Test rig schematic 103

Figure S6-9. Comparison of two breakthrough curves generated using the test rig under the same conditions on different dates, demonstrating the repeatability of data generated using the test rig. The adsorption capacities calculated from these curves are $354 \text{ g}_{D5} \text{ kg}^{-1} \text{ carbon}$ and $342 \text{ g}_{D5} \text{ kg}^{-1} \text{ carbon}$

(4% error). (Inlet concentration = $70 \text{ mg}_{\text{D5}} \text{ m}^{-3} \text{ CO}_2$; humidity = 80%; $\text{Re} = 73$; EBCT = 0.031 s.)	105
Figure S6-10. Pore size distribution of activated carbon	106
Figure S6-11. The Kelvin equation may be used to calculate the relative humidity required to cause capillary condensation in a pore of a given diameter.....	106
Figure S6-12. Breakthrough curves showing the effect of varying empty bed contact time (EBCT) and Reynold's number. (Inlet concentration = $70 \text{ mg}_{\text{D5}} \text{ m}^{-3} \text{ CO}_2$; humidity = 0%; $\text{Re} = 31 - 107$; EBCT = 0.02 – 0.15 s.)	107
Figure 7-1. Schematic showing the outcomes of this project	110
Figure 7-2. Proposed contactor layouts.....	122

LIST OF TABLES

Table 1-1 Names and molecular structures of low molecular weight siloxanes and polymethyldisiloxane (Chandra, 1997; Royal Society of Chemistry, 2014)	2
Table 1-2 Uses of siloxanes and silicones presented in the literature	3
Table 2-1 Operational parameters of bench-scale and full-scale siloxane adsorption studies	12
Table 2-2. Parameters of VOC column experiments from the literature	21
Table 2-3. Bench-scale siloxane adsorption experiments from the literature ...	22
Table 2-4. Physical properties of adsorbents	23
Table 2-5. Physical properties of adsorbates	24
Table 3-1. Infrared absorbance peaks for siloxanes.....	32
Table 3-2. Speciated siloxanes measured by GC-MS from gas bag samples from sewage treatment works (n = 9).	35
Table 3-3. VOC species present in biogas samples and associated infrared absorbance peaks (Stuart, 2004). The italicised peaks may fall into the zones monitored by the FTIR spectrometer and cause positive interference.	41
Table 3-4. Comparison of total siloxanes measured in real biogas samples using a variety of sampling and analytical procedures.	45
Table 3-5. Costs of siloxane monitoring and removal and CHP engine maintenance (estimated considering a carbon vessel containing 3000 kg of carbon protecting five 1MW CHP engines).....	48
Table 4-1. Comparison of change points and detection times to the time the warranty specification is first exceeded for carbon vessels exhibiting broad-fronted breakthrough curves.....	59
Table 4-2. Comparison of change points and detection times to the time the warranty specification is first exceeded for carbon vessels exhibiting sharp-fronted breakthrough curves.....	61
Table 4-3. Benefits of using on-line analysis and the changepoint detection algorithm or warranty specification for different vessel layouts.....	64
Table 5-1. Maximum silicon levels recommended by gas engine manufacturers	68
Table 5-2. Design parameters of contactors and media characterisation.....	70
Table 5-3. Operational conditions used in studies contactors (mean reported, n = 5-17)	71

Table 5-4. Estimated mass balance of GAC4 for fully speciated siloxanes and competing VOCs using a UKAS accredited GCMS trace analysis suite....	80
Table 5-5. Estimation of full scale carbon vessel operation from the literature compared to this study.....	82
Table 7-1. Instruments available for on-line measurement of siloxanes in biogas.....	111

LIST OF EQUATIONS

(4-1).....	54
(4-2).....	55
(4-3).....	55
(4-4).....	63
(4-5).....	63
(5-1).....	68
(5-2).....	72
(5-3).....	72
(5-4).....	72
(6-1).....	88
(6-2).....	90
(S6-3).....	104

LIST OF ABBREVIATIONS

AD	Anaerobic digestion
ATEX	94/9/EC directive: Equipment and protective systems intended for use in potentially explosive atmospheres
BET	Brunauer, Emmett, Teller (surface area)
BTEX	Benzene, toluene, ethylbenzene, xylenes
BTX	Benzene, toluene, xylenes
BvBB	Bed volumes (of gas treated) before breakthrough
CHP	Combined heat and power
EBCT	Empty bed contact time
EU	European Union
FTIR	Fourier transform infrared (spectrometer)
FTIR	Fourier transform infrared (spectroscopy)
GAC	Granular activated carbon
GAC1-5	Siloxane removal vessels 1 – 5 at Minworth sewage treatment works
GC	Gas chromatograph
GC	Gas chromatography
GC-MS	Gas chromatography – mass spectrometry
i.d.	Internal diameter
IUPAC	International Union of Pure and applied Chemistry
L	Length
LOD	Limit of detection
MTZ	Mass transfer zone
MW	megawatt
Re	Reynold's number
STW	Severn Trent Water
STW	Sewage treatment works
UKAS	United Kingdom accreditation service
VMS	Volatile methyl siloxane
VOC	Volatile organic carbon
W	Width

L2	Hexamethyldisiloxane
D3	Hexamethylcyclotrisiloxane
D4	Octamethylcyclotetrasiloxane
D5	Decamethylcyclopentasiloxane
D6	Dodecamethylcyclohexasiloxane
PDMS	Polydimethylsiloxane
K_{oc}	Organic carbon - water partition coefficient
K_{ow}	Octanol-water partition coefficient
β	Dubin-Radushkevich affinity coefficient

1 Introduction

1.1 Background

Siloxanes are anthropogenic compounds with an alternating silicon-oxygen backbone and associated methyl groups (Smith, 1991). Volatile methyl siloxanes (hereafter referred to as “siloxanes”) are the smallest members of this group, and take two distinct structures: linear and cyclic (Table 1-1). Siloxanes and their polymers (polydimethylsiloxane, PDMS, silicone) are almost ubiquitous in industry, healthcare, the office and the home (Table 1-2), due to their useful properties which include minimal biological activity, high resistance to UV radiation, hydrophobicity, good electrical insulation, low surface tension, and excellent thermal properties (Smith, 1991). They also make very good release agents (Smith, 1991). As a result of their widespread use, siloxanes and silicones are found in many wastewater streams. Due to their hydrophobicity, the majority of the siloxanes adsorb to the sewage sludge during the wastewater treatment process (Figure 1-1) (Bletsou et al., 2013; van Egmond et al., 2013). Some of the larger polymer molecules (PDMS) are degraded to smaller siloxane molecules (Bletsou et al., 2013; Ducom et al., 2013; Ohannessian et al., 2008). During the anaerobic digestion of sewage sludge, some of the smaller siloxanes volatilise and partition into the biogas (Surita and Tansel, 2013; Xu et al., 2013). Similarly, siloxanes from solid waste are found in landfill gas. Biogas is a valuable renewable energy resource with a calorific value of approximately 2.2 kWh m^{-3} (Read and Hofmann, 2011). Increasingly, water utilities are creating additional revenue by utilising biogas in combined heat and power (CHP) engines. In 2013 Severn Trent Water had 40 MW of capacity in CHP engines installed over 35 sites which they used to generate 23% of their annual electricity demand. The UK Anaerobic Digestion Action Plan sets the target of generating 3 - 5 TWh from biogas by 2020 (DEFRA, 2011), so there is plenty of interest in improving this process. To enable its economic utilisation, biogas must be pre-treated to remove siloxanes, which cause damage to CHP engines.

Table 1-1 Names and molecular structures of low molecular weight siloxanes and polymethyldisiloxane (Chandra, 1997; Royal Society of Chemistry, 2014)

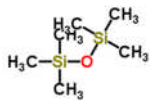
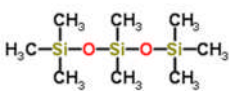
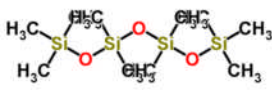
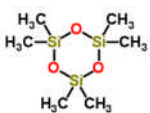
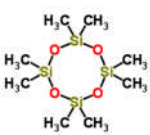
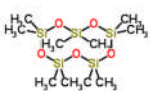
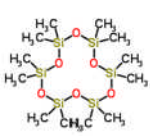
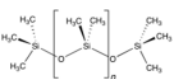
IUPAC name	Other name(s)	Structural formula	Molecular weight (g mol ⁻¹)
Hexamethyldisiloxane	L2; MM		162
Octamethyltrisiloxane	L3; MDM		236
Decamethyltetrasiloxane	L4; MD ₂ M		310
Hexamethylcyclotrisiloxane	D3		222
Octamethylcyclotetrasiloxane	D4		297
Decamethylcyclopentasiloxane	D5		371
Dodecamethylcyclohexasiloxane	D6		445
Polymethyldisiloxane	PMDS		-

Table 1-2 Uses of siloxanes and silicones presented in the literature

Category	Example uses
Medical	Implants in cosmetic surgery ^{3;11} Tracheotomy tubes ³ Prostheses and devices ¹²
Industrial	Feedstock chemicals ³ Wastage from factories making products ^{3; 5} "Eco" dry cleaning chemicals (alternative to chlorinated hydrocarbons) ³ Replacement for organic solvents ^{6; 8} Lubricants ^{6;12} Stopcock grease ¹³ Mould release agent in manufacture of rubber or plastic ¹³ Silicone rubber ¹³ Caulking material ¹² Coupling agents ¹²
Coatings	Paints ^{3;11} and coatings ^{1;12} Surfactants ^{10;12} Adhesives ^{6;11;12;13} Pressure sensitive adhesives (e.g. for self-adhering labels) ^{12;13}
Gels	Barrier creams ³
Office/home	Ink ⁶ Printing inks ¹² Washing paint brushes ³ Washing off excess sealants from tools ^{3;6;14} Furniture and car polishes ^{7;13} Car waxes ⁷ Paper products ^{2;3; 11}
Personal care	Personal toiletries ³ Skin creams ^{4;6;8;9;11;12} Deodorants ^{3; 4;6;8;10;14} and antiperspirants ⁵ Cosmetics ^{1;2;3;5;6;11;12;14} Shampoo ^{1;2; 6;9-11} and conditioners ^{3;8}
	Coating hypodermic needles ^{3;6} Coating bottle stops ^{3;6} Coating pacemakers ³ Cleaning agents ¹⁰ Gas chromatography column substrates ¹² Heat transfer fluids ¹² Organic synthesis aids ¹² Foaming agents ¹² Anti-foamers ^{3;7} Extensive usage as carrier oils ³ Penetrating oils ³ Isolation products ¹¹ Fire retardants ³ Waterproofing agents ^{3;8;11} Textiles ^{2;3;10} Textile finishes ¹² Silicone components and tubing ³ Nappies ³ Cleaning agents ^{7;10} such as detergents ^{2;6;14} Fabric softeners ³ Double glazing sealants ³ Food additives ^{3;9} Lubricants ^{1;8} Electrical insulation ¹³ Fuel additives ⁷ Hair styling products ¹⁴ such as gels ¹⁰ and sprays ³ Shaving creams ³ Toothpaste ⁹ Pharmaceuticals ^{3; 6;12}

¹(Arnold and Kajolinna, 2010); ²(Dewil et al., 2007); ³(Dewil et al., 2006); ⁴(Glus et al., 1999); ⁵(Lee et al., 2001); ⁶(McBean, 2008); ⁷(Narros et al., 2009); ⁸(Oshita et al., 2010); ⁹(Rasi et al., 2011); ¹⁰(Rasi et al., 2010); ¹¹(Ricaurte Ortega and Subrenat, 2009b); ¹²(Smith, 1991); ¹³(Smith and Parker, 1991); ¹⁴(Soreanu et al., 2011)

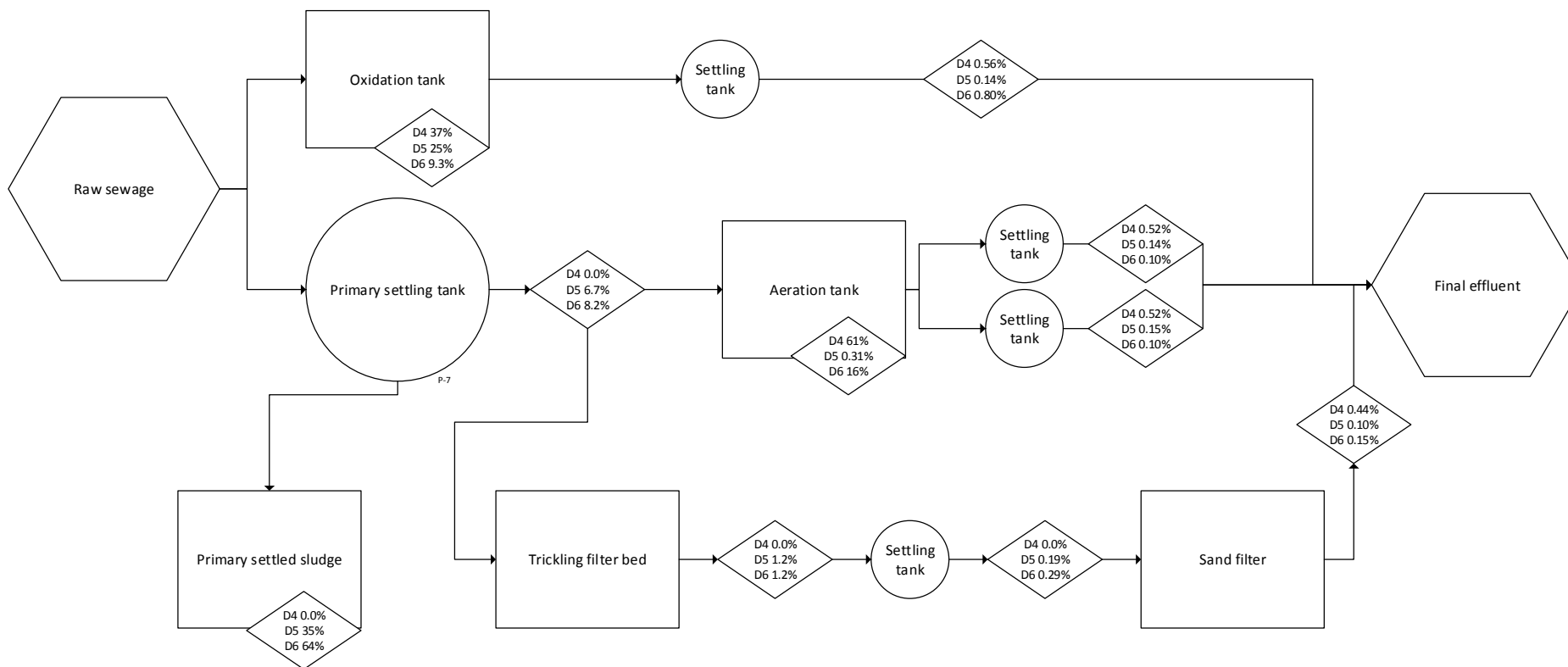


Figure 1-1 Distribution of siloxanes (D4, D5, D6) at a UK sewage treatment works, showing that most siloxanes are removed in settling tanks as they sorb onto solids. Data from van Egmond et al. (2013).

When combusted in a CHP engine, siloxanes form hard micro-crystalline silica which abrades the inner surfaces of the combustion chamber (Schweigkofler and Niessner, 2001), clogs valves (Accettola et al., 2008) and reduces engine efficiency (Ohannessian et al., 2008), causing significant additional maintenance costs and engine downtime. A range of technologies have been considered for siloxane removal as described in the comprehensive reviews by Ajhar et al. (2010a) and Sorenau et al. (2011), but the technology most commonly employed at large scale to date is siloxane adsorption onto activated carbon (Figure 1-2). To date, nineteen bench-scale studies have been published regarding siloxane adsorption (see chapter 2), the majority of which have focused on comparing different adsorption media, including a variety of activated carbons and some alternative media such as silica gel, zeolites and vermiculite. A few studies have considered operational conditions such as temperature (Boulinguez and Le Cloirec, 2010; Sigot et al., 2014) and humidity (Schweigkofler and Niessner, 2001; Boulinguez and Le Cloirec, 2010; Sigot et al., 2014; Cabrera-Codony et al., 2014) but, to the author's knowledge, there has been no rigorous investigation into the design of adsorption beds specifically tailored to siloxane removal.

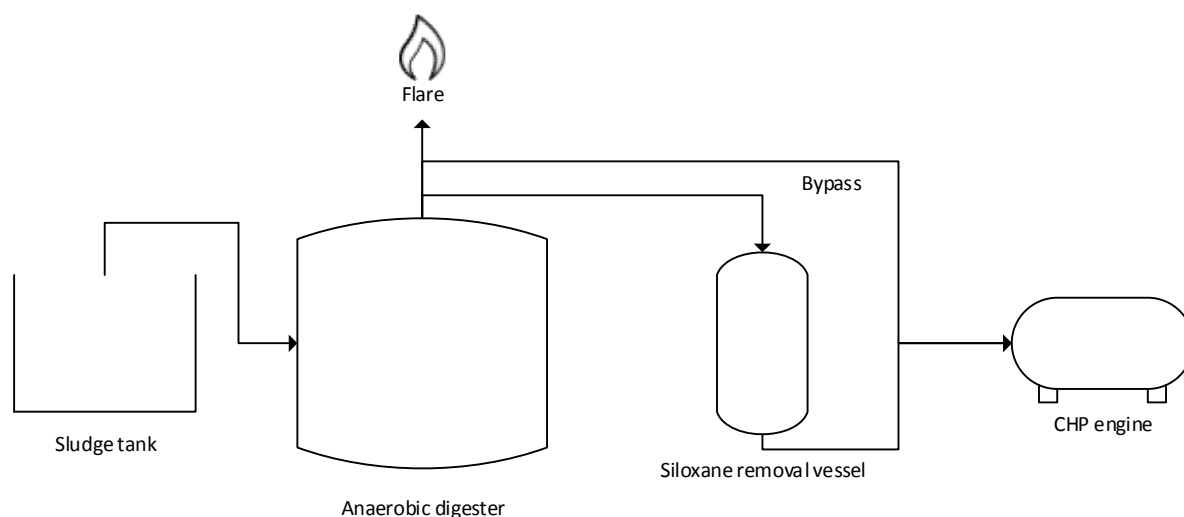


Figure 1-2 Siloxane removal vessels pre-treat biogas from anaerobic digester before it is combusted in a CHP engine. If the siloxane removal vessel is not in use, biogas may be sent directly to the engine or flared.

The relative paucity of data pertaining to siloxane removal from biogas may be partially due to difficulties in measuring siloxanes. Currently there is no standard method of measuring siloxane concentrations in biogas, but most methods employ either grab or integrated sampling, with analysis carried out at an external laboratory (Dewil et al., 2007; Rasi et al., 2010; Hayes et al., 2003). This leads to a lag of up to four days between sampling and receiving results, which, coupled with infrequent sampling, means that effective process performance monitoring is impossible. Recently, the concept of on-line monitoring of siloxanes has been introduced by Arnold and Kajolinna (2010), Bramston-Cook and Bramston-Cook (2012) and Oshita et al. (2010) (see chapter three). In this thesis, the application of on-line monitoring of siloxanes has been extended to cover siloxane analysis both upstream and downstream of activated carbon adsorption vessels (full-scale and bench-scale), using a Fourier transform infrared spectrometer to enable comprehensive evaluation of operational and design characteristics of adsorption vessels.

1.2 Aim and objectives

The aim of this project is to develop an optimum design envelope for removing siloxanes from biogas to reduce CHP operation costs.

This aim was achieved by carrying out the following objectives:

- 1) To investigate whether industry ready Fourier transform infrared spectroscopy can be adapted as an on-line method for siloxane analysis to monitor carbon contactor performance.
- 2) To understand the benefits of on-line siloxane measurement in terms of providing engine protection and managing carbon contactors, and to perform a cost-benefit analysis for the FTIR spectrometer.
- 3) To investigate the potential for using statistical tools to take advantage of the enhanced data intensity provided by on-line analysis to provide early-warning of siloxane breakthrough in a carbon contactor.
- 4) To investigate the performance of full-scale siloxane adsorption processes at Minworth Sewage Treatment Works and understand the

implications of contactor design, leading to design guidelines for future contactors.

- 5) To use bench-scale experiments to investigate the mechanisms underpinning the findings at full-scale, with particular emphasis on the hydrodynamic regime and the effects of humidity and competition on the adsorption capacity of activated carbon.

1.3 Thesis structure

This thesis is presented as a series of chapters formatted as journal papers. All chapters were written by the first author, Caroline A. Hepburn, and edited by Dr Ewan J. McAdam. All experimental work was undertaken by Caroline A. Hepburn, with the exception of modifications to the FTIR calibration in chapter three which were supported by Mr Jay Roberts (Thermofisher Inc.); the development of the changepoint detection algorithm in chapter four which was supported by Dr Ali Daneshkhah; and the electron microscopy in chapter five, which was conducted by Dr Ben Martin.

This thesis begins with a review of the literature (chapter two), “Adsorbent selection for environmental gas applications”, which summarises bench-scale studies carried out relating to removal of trace gases in ambient pressure adsorption processes, with particular emphasis on siloxanes.

Chapters three to six cover the technical content of the thesis. Chapters three and four focus on the application of on-line analysis to siloxanes in biogas. Chapter three evaluates the capability of a Fourier transform infrared spectrometer to provide useful on-line siloxane concentration data in biogas upstream and downstream of activated carbon vessels. Chapter four investigates how to integrate this data into a process control system.

Chapters five and six investigate the design and operation of activated carbon vessels for siloxane adsorption. Chapter five compares breakthrough curves from full-scale carbon vessels of different designs subjected to the same feed gas and chapter six uses bench-scale experiments to investigate the effects of

gas flow rates, humidity and competition between siloxane species under controlled conditions.

The thesis concludes in chapters seven and eight with a discussion of the practical implications of full-scale implementation, before reaching conclusions and proposing further work. The structure of this thesis is summarised in the thesis road map (Figure 1-3).

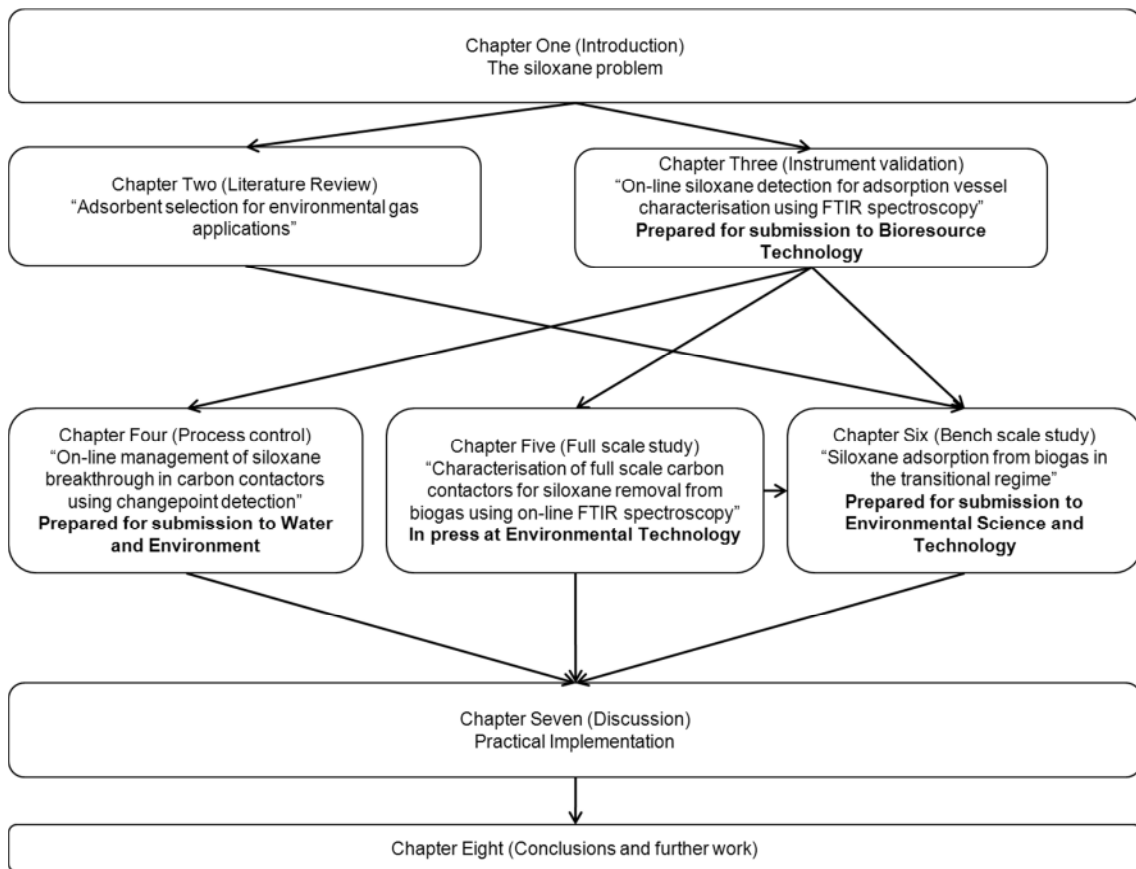


Figure 1-3. Thesis road map

2 Adsorbent selection for environmental gas applications

C.A. Hepburn^a, N.J. Simms^b, E.J. McAdam^a

^aCranfield Water Science Institute, Cranfield University, Cranfield, Bedfordshire, MK43 0AL, UK

^bCentre for Power Engineering, Cranfield University, Cranfield, Bedfordshire, MK43 0AL, UK

Abstract

Adsorption processes for the purification of gases in environmental applications differ from industrial gas separation or purification processes as they are run at ambient temperature and pressure. These processes are therefore low energy and low capital cost. Adsorption may be used for economic reasons (e.g. removal of siloxanes from biogas) or to meet environmental regulations (e.g. removal of volatile organic carbons (VOCs) from air-scrubbing off-gas). This review assimilates technical papers relating to the adsorption of VOCs under ambient conditions, with particular emphasis on siloxane and BTEX (benzene, toluene, ethylbenzene, xylenes) removal. The relationship between the size of the adsorbate molecule and adsorbent pores was found to have a significant influence of the suitability of an adsorbent, with smaller pores providing more surface area for adsorption but only if the adsorbate molecule is sufficiently small to enter or travel along the pores. The optimum pore diameter may be two to three times the adsorbate molecule's diameter. The hydrophobicity of the adsorbent should also be matched to the adsorbate as hydrophilic compounds (e.g. silica gel) were found to have greater affinity for less hydrophobic adsorbates (e.g. hexamethyldisiloxane compared to decamethylcyclopentasiloxane). These findings may be used as a preliminary screening tool to choose appropriate adsorbents for a particular application before bench-scale tests are carried out.

Keywords: *Activated carbon; Adsorption; BTEX; Purification; Siloxane; VOC*

2.1 Introduction

The ability of charcoal to adsorb unpleasant odours has been known for over a century and came into widespread use during WWI when charcoal was used in gas masks to remove poisonous gases from air (Crittenden and Thomas, 1998). Adsorption of trace gases is now a well-established industrial practice with applications broadly characterised into two groups: gas purification and pollution abatement.

In the environmental field, a key example of process improvement is the application of adsorption technology for biogas preconditioning. To enable economic utilisation of biogas in combined heat and power (CHP) engines, some trace gases, including hydrogen sulphide and siloxanes, must be removed as they cause damage to the engines (Arnold, 2009). When exposed to ignition within the CHP engine, siloxanes are oxidised to microcrystalline quartz causing significant wear and irregular operating conditions which reduce engine efficiency and increase operational cost (Ajhar et al., 2010a). At the Trecatti landfill in the UK, a major engine failure occurred after 200 h of operation due to high (up to 400 mg m^{-3}) siloxane levels (Appels et al., 2008). Increasingly stringent environmental regulation has also increased demand for efficient pollution reduction technology (Hand et al., 1999). Off-gases from processes such as vapour extraction for contaminated land treatment or air-stripping during drinking water treatment commonly contain volatile organic compounds (VOCs) including the BTEX compounds (benzene, toluene, ethylbenzene and xylene) and chlorinated solvents (Hand et al., 1999). Many VOCs are carcinogenic or otherwise harmful to human health and permissible levels are low (World Health Organisation, 2010). As part of the Thematic Strategy on Air Pollution, the European Parliament aims to reduce VOC emissions to 49% of 2000 levels by 2020 (European Parliament, 2012).

Adsorption is an effective technology for treating these gases because it is a relatively low energy, low cost process and is effective at low contaminant concentrations (Yang, 1997). The key characteristic of these adsorption processes is that, unlike industrial separation processes which are commonly run at pressures of 2 – 4 atm or higher (Yang, 1997; Tagliabue et al., 2009), they are all run at

ambient pressure. Although elevated pressure increases adsorption rates and capacities (Brunauer et al., 1938), the cost of raising the pressure is usually prohibitive. Also, raising the pressure is problematic in many processes, for example if the pressure is raised in an air-stripping off-gas treatment process, the back pressure will shift the equilibrium position of the air-stripping process and reduce the efficiency (Hand et al., 1999). High pressure can also be undesirable upstream of the application, for example the pressure range specified for a Jenbacher gas engine is 80-200 mbar (GE Jenbacher, 2006) so if gas was pressurised for siloxane adsorption, it would need to be subsequently depressurised before being fed to the engine.

The low cost of adsorption is critical for environmental applications as these are often run at high gas flows and very low cost margins. Adsorbent media are often not regenerable, due perhaps to chemical reactions which occur on the adsorbent surface. For example, Finocchio et al. (2009) found that hexamethylcyclotrisiloxane (D3) partially polymerised to polydimethylsiloxane on the surface of their activated carbon. Consequentially, the amount of target gas adsorbed by the media before adsorbate breakthrough and media replacement is important. This paper reviews the literature relating to bench-scale adsorption of VOCs, focussing particularly on siloxanes and BTEX compounds. The aim of the review is to relate adsorbent and adsorbate properties to assist in choosing the optimum adsorbent for a particular application.

2.2 General process characterisation

Most studies have been very small scale with adsorbent masses between 0.2 g and 2.0 g (Table 2-2 and Table 2-3). Three larger bench-scale studies have been performed with 150 g (Matsui and Imamura, 2010), 250 g and 500 g (Silvestre-Albero et al., 2010), and 295 g (Khandaker and Seto, 2010) of adsorbent. Liang et al. (2001) ran a pilot scale test with 96 kg of activated carbon. Contactor volumes have varied in proportion to adsorbent masses but contactor aspect ratios have ranged from 3.6 (Shin et al., 2002) to 50 (Finocchio et al., 2009; Montanari et al., 2010). Volumetric flow rates have varied giving linear velocities from 0.06 m min⁻¹ (Khandaker and Seto, 2010) to 59.5 m min⁻¹ (Shin et al., 2002) but most linear

velocities fell in the range 2 – 6 m min⁻¹. Empty bed contact times similarly range from 0.1 s (Gaur et al., 2010) to 192 s (Khandaker and Seto, 2010) but most lie in the range 1 – 4 s. Siloxane studies have typically been operated in the laminar regime (Re = 0.2 – 16.4) with the exception of the Liang et al. (2001) study which operated at a Reynold’s number of 125 (Table 2-1). Full scale siloxane adsorption studies have typically been carried out at higher Reynold’s numbers (70.5, Tower and Wetzal, 2004; 86.7, Pirnie et al., 2011), putting them (and Liang et al.’s study) in the transitional flow regime (Re > 40-55 (Chilton and Colburn, 1931)). Studies using BTEX compounds have typically operated at much higher Reynold’s numbers (190 – 555) although Sager and Schmidt (2010) and Anfruns et al. (2011) operated in the laminar regime (Re = 1.1 and Re = 36.4 respectively). Reynold’s number affects mass transport processes, particularly axial dispersion (Cussler, 2009), so matching full scale and lab scale Reynold’s numbers is likely to be important for understanding adsorption, in particular when Reynold’s numbers near the laminar/transitional boundary are used, as in these experiments. Busmundrud (1993) identified a correlation between a rate constant and linear velocity using the modified Wheeler equation over a similar Reynold’s number range. It has been demonstrated by Wakao and Funazkri (1978) and Urban and Gomezplata (1969) that the axial Peclet number asymptotically approaches a value of 2 at Reynold’s number of approximately 100, indicating that operating at higher Reynold’s numbers will bring no increase in mass transfer rate or media capacity.

A wide range of adsorbent capacities have been reported. The highest capacities (> 800 g_{adsorbate} kg⁻¹_{adsorbent}) were achieved with specially modified adsorbents, including activated carbon impregnated with copper salts (878 mg g⁻¹, Finocchio et al., 2009; Montanari et al., 2010) and silica aerogel (900-950 mg g⁻¹, Štandeker et al., 2009).

Table 2-1 Operational parameters of bench-scale and full-scale siloxane adsorption studies

Parameter	Bench scale range	Full scale range
Empty bed contact time	0.06 – 3.5 s	0.25 – 28 s
Linear velocity	0.06 – 12.4 m min ⁻¹	5.1 -8.4 m min ⁻¹
Reynold’s number	0.2 – 16.4	70.5 – 86.7

Standard activated carbon capacities range from 4 mg g⁻¹ (Shin et al., 2002; Gaur et al., 2010) to 720 mg g⁻¹ (Shin et al., 2002; Balanay et al., 2011). Khandaker and Seto (2010) achieved 99% removal of siloxanes from real biogas using activated carbon and 62 – 92% removal using vermiculite whilst Hagmann et al. (2001) achieved > 99.1% removal with activated carbon, indicating that adsorption is still a viable technology at low siloxane concentrations (<10 ppmv). However, the adsorption capacities achieved when using real biogas are much lower. Liang et al. (2001) reported an adsorption capacity of 44.5 g_{siloxane} kg⁻¹_{adsorbent} for siloxanes onto activated carbon, using real biogas in a pilot scale study. When landfill gas was used in Guar et al.'s (2010) and Shin et al.'s (2002) experiments, they achieved capacities for BTEX an order of magnitude lower than those achieved by other researchers using synthetic gases. Matsui and Imamura (2010) proposed interspecies competition for adsorption sites as an explanation for the reduction in siloxane adsorption capacity they also found when using real biogas instead of model biogas.

Adsorption is an exothermic process (Crittenden and Thomas, 1998) so, in general, the capacity of an adsorbent decreases as temperature increases. Ricautre Ortega and Subrenat (2009b) confirmed this for siloxanes by carrying out batch experiments at 25°C and 60°C. The adsorption capacities of activated carbon for hexamethyldisiloxane (L2) and octamethylcyclotetrasiloxane (D4) decreased by approximately 20% following this temperature increase. Sigot et al. (2014) demonstrated the same principle in a dynamic system, finding that increasing the temperature by 20°C caused the adsorption capacity of silica gel for D4 to decrease by 15%. Ramiez et al. (2005) notes that increasing the temperature from 20°C to 60°C decreased the adsorption capacity of activated carbon for benzene by 20-60%. All other studies found have been carried out at or close to room temperature, with the exception of Matsui and Imamura (2010) whose experiments were run at 35°C – the approximate temperature of biogas in an anaerobic digester (Song et al., 2004). Following production in the digester, biogas subsequently travels through long uninsulated pipework to the CHP gas engine during which the temperature rapidly decreases to ambient; off-gas temperatures are also close to ambient during the

adsorption process, so conducting experiments at ambient temperatures is appropriate.

Most siloxane studies were carried out with dry gas, with the exception of Finocchio et al. (2009) and Montanari et al. (2010) who used a carrier gas saturated with water vapour. Biogas is normally saturated with water when it leaves an anaerobic digester (Persson and Wellinger, 2006). Temperature changes between the digester and CHP can result in the presence of free water, although this is usually removed using knock-out pots. Other processing steps such as chilling or gas drying can lead to a variety of humidities being present on different commercial sites. Ricaurte Ortega and Subrenat (2009b) ran batch experiments using L2 at 0% and 70% humidity. They found the change in humidity had little effect on the adsorption capacity of zeolite (due to its hydrophobic nature) and activated carbon fibre cloth, but increasing humidity decreased the capacity of granular activated carbon. The greatest effect was on silica gel, the capacity of which was decreased by 50%. Schwegkofler and Niessner (2001) and Sigot et al. (2014) also found that increased humidity had a detrimental effect on siloxane adsorption onto silica gel. This is to be expected: at elevated humidities, a water film develops on the adsorbent which the hydrophobic siloxanes must pass through in order to be adsorbed (Habuka et al., 2013; McCoy and Rolston, 1992). Silica gel is more hydrophilic than granular activated carbon so it forms a thicker water film. Capillary condensation may also play a part at high humidities, but at lower humidities (e.g. 0-50% as used by Schwegkofler and Niessner (2001)) capillary condensation is unlikely to be significant. As mentioned above, a wide variety of humidities can be found in biogases so further investigation into the effect of humidity on the adsorption of siloxanes would be welcome.

The effects of humidity on BTEX adsorption have been more thoroughly studied. Activated carbon capacity for benzene, toluene and xylene decreases as humidity in the bulk gas increases (Carrasco-Marín et al., 2009; Li et al., 2010; Long et al., 2012; Veksha et al., 2012), and allowing activated carbon to equilibrate with moisture before exposure to VOCs also leads to shorter breakthrough times (Abiko et al., 2010). Interestingly, some studies found a threshold effect. Pei and Zhang (2012) found no significant difference in the capacity of activated carbon with 20% or 50%

relative humidity, but raising the humidity to 80% dramatically decreased the capacity of the carbon for toluene. They estimated that significant capillary condensation occurred in the pores of their activated carbon at a humidity of 80%, making it difficult for hydrophobic toluene to access adsorption sites. Similarly, Sager and Schmidt (2010) reported only a small effect on the capacity of activated carbon for toluene below 50% humidity, but increasing the humidity to 70% and 90% reduces the capacity by up to 50%. An analogous observation was made using n-butane, but in this case the adsorption capacity reduced by around 90% at 70% humidity. The concentration of the adsorbate can change the effect of humidity. Lorimier et al. (2005) found that although raising the humidity reduced the capacity of activated carbon for toluene at a toluene concentration of 30mg m^{-3} , at a very high toluene concentration (307 mg m^{-3}) humidity had little effect. Shin et al. (2002) tested benzene, toluene and ethylbenzene at 400 ppmv and 600 ppmv and found that at the lower concentration adsorption capacities for all three compounds decreased rapidly at humidities above 60%. The greatest effect was on benzene adsorption with capacity decreasing by 71% when humidity was increased from zero to 90%. At 600 ppmv the effect of humidity on all three compounds was smaller, with the capacity for benzene decreasing by 65% when humidity was increased from zero to 90%. This reduction in the effect of humidity at higher adsorbate concentrations also holds true for other VOCs, including butanone (methyl ethyl ketone) and n-hexane (Vizhemehr et al., 2011), and tetrachloromethane (carbon tetrachloride, Kim et al., 2004; Srivastava et al., 2012). Concentration gradient provides the driving force for adsorbate transport (Welty et al., 2001), so a higher adsorbate concentration in the bulk gas (which leads to a larger concentration gradient between the bulk gas and the adsorbent surface) results in a greater driving force for the adsorbent to overcome the resistance provided by the water film. This indicates that removing humidity is more important when adsorbate concentrations are very low, as is often the case in environmental applications.

2.3 Adsorbent characteristics

The porous structure of adsorbents is very important (Table 2-4). Most of the surface area in a porous adsorbent is provided by the micropores (Yang, 1997) so a common finding is that the capacity of adsorbents for adsorbates is related to

micropore volume. For example, Silvestre-Albero et al. (2010) found a linear relationship between adsorption capacity and micropore volume for benzene adsorbed onto activated carbon aerogels. The size of the micropores is also important. In experiments with benzene, toluene and xylene (BTX) adsorbed onto monolithic carbon aerogels, Fairen-Jimenez (2007) found a good linear relationship between BTX adsorbed and volume of micropores between 0.7 nm and 1.05 nm wide. For micropores less than 0.7 nm wide there was no relationship, perhaps because these are too narrow for BTX molecules to enter (the molecular diameter of benzene is 0.6 nm). Micropores wider than 1.05 nm were found to be less important. However micropores are not the only important structural feature of an adsorbent – the mesopores provide access to the micropores where adsorption takes place (Anfruns et al., 2011). This makes mesopores important in non-equilibrium processes as they increase the rate of adsorption by facilitating transport processes (Branton and Bradley, 2011).

The importance of relative sizes of pores and adsorbates becomes even more important when larger molecules, such as siloxanes, are considered. Oshita et al. (2010) compared the adsorption capacity of eleven adsorbents for octamethylcyclotetrasiloxane (D4) and decamethylcyclopentasiloxane (D5). They found no relationship between the adsorbent capacity and micropore surface area. The molecular diameter of a D5 molecule is approximately 1.1 nm and D4 is approximately 1.0 nm and the mean free paths for D5 and D4 in carbon dioxide at room temperature and pressure are 113 nm and 132 nm respectively. Micropores are classified as pores below 2 nm in diameter (Crittenden and Thomas, 1998), so these results demonstrate that Knudsen diffusion is dominant and will limit the mass transfer rate and likely also the capacity in a dynamic process. Oshita et al. (2010) instead identified positive relationships between adsorbent capacity and BET-specific surface area (which takes into account macropores and mesopores in addition to micropores) and external surface area. This suggests that large molecules such as D4 and D5 adsorb mainly on the outside of adsorbent particles and in the large and mid-sized pores.

2.4 Adsorbate characteristics

Most siloxane studies have either used one or two individual siloxane species in model gas or focused on total siloxane removal from real biogas (Table 2-3). The most common siloxanes tested are D4 and D5 which are the siloxanes of highest concentration in most biogases originating in sewage treatment works (Oshita et al., 2010). L2 is also considered in some studies (Ricaurte Ortega and Subrenat, 2009b; Schweigkofler and Niessner, 2001; Ricaurte Ortega and Subrenat, 2009a) since it forms a large proportion of the siloxane content of landfill gases (Rasi et al., 2007). The research group of Finocchio and Montanari (Finocchio et al., 2009; Montanari et al., 2010) are the only group to have used D3 in their experiments. Of the BTEX compounds, the smaller molecules, benzene and toluene, are most commonly used in investigations (Table 2-2). Of the 25 papers evaluated, sixteen discuss toluene, twelve discuss benzene and only four and two discuss xylene and ethylbenzene respectively.

The siloxane concentrations of model gases used in experiments tend to be higher ($250 - 4500 \text{ mg m}^{-3}$, Oshita et al., 2010; Matsui and Imamura, 2010) than the concentrations found in real biogas (Table 2-3). For example, Schweigkofler and Niessner (2001) used 4 g m^{-3} in their experiments with silica gel and 1 g m^{-3} in their other experiments. The highest concentration ($83,000 \text{ mg m}^{-3}$) was used by Finocchio et al. (2009) and Montanari et al. (2010). Khandaker and Seto (2010) reported concentrations of $3.5 - 20 \text{ mg m}^{-3}$ of individual siloxanes in their (real) biogas and Rasi et al. (2007) reported a maximum of 10.6 mg m^{-3} for an individual siloxane species over 17 landfill and wastewater treatment plants. These concentrations identified in real gas are 2-3 orders of magnitude smaller than those used in laboratory experiments. The only study to have used an environmentally relevant siloxane concentration was Cabrera-Codony et al. (2014), who used 18 mg m^{-3} . Concentration gradient is the driving force for the mass transfer stages of adsorption and affects the position of equilibrium, so it is appropriate to investigate adsorption at low siloxane concentrations where possible. There may also be a change in mechanism at high concentrations for some siloxanes: D4 exhibits a type IV isotherm on activated carbon suggesting intergranular condensation occurs at high concentrations (Boulinguez and Cloirec, 2009), although Ricaurte Ortega and

Subrenat (2009b; 2009a) found the adsorption of L2 was best described by a Type I isotherm, indicating single monolayer adsorption (Crittenden and Thomas, 1998). Type I isotherms are commonly observed when the pore sizes of the adsorbent are not much larger than the molecular diameter of the adsorbate (Crittenden and Thomas, 1998). Type I isotherms have consistently been found for toluene on activated carbon (Boulinguez and Le Cloirec, 2010; Balanay et al., 2011; Boulinguez and Le Cloirec, 2009; Foster et al., 1992; Kim et al., 2006; Yi et al., 2009), except for Bouhamra et al. (2009) who report a Type IV isotherm. Isotherms for other BTEX compounds have not been explicitly plotted, but Guar et al. (2010) and Ramiez et al. (2005) agree that the adsorption capacity of activated carbon for benzene increases at higher benzene concentrations. Guar et al. (2010) further state that this is also the case for ethylbenzene adsorbed on activated carbon. Toluene also gives a Type I isotherm on silica alumina (Bouhamra et al., 2009).

Generally, the adsorption capacity of an adsorbent for a particular adsorbate increases with molecular weight. Ricaurte Ortega and Subrenat (2009b) found that more D4 was adsorbed than L2 ($360 \text{ g}_{\text{D4}} \text{ kg}^{-1}_{\text{media}}$ vs $270 \text{ g}_{\text{L2}} \text{ kg}^{-1}_{\text{media}}$) on activated carbon cloth in batch experiments and Schwegkofler and Niessner (2001) showed that molecular sieve 13X and activated charcoal exhibited greater adsorption capacities for D5 than L2. Oshita et al. (2010) found that 10 - 48% less D4 was adsorbed than D5 on all activated carbons tested. Silica gel adsorbed 8% less D5 than D4 and the difference between D4 and D5 uptake for zeolite was minimal. Khandaker and Seto (2010) found that activated carbon and vermiculite gave a greater removal percentage for D5 and dodecamethylcyclohexasiloxane (D6) (> 99% removal) compared to D4 (78% removal) from real biogas. This relationship between molecular weight and adsorbability agrees with the method of Dubinin-Radushkevich for predicting the adsorbability of an adsorbate on a particular adsorbent. An affinity coefficient, β , must be calculated which is linearly related to the molar volume of the adsorbate (Crittenden et al., 1989), and therefore correlates with the molecular weight (Figure 2-1). The research group of Gaur et al. (2010) and Shin et al. (2002) found that in dynamic column experiments with model gases, the capacity of activated carbon for BTEX compounds also increased with molecular weight, i.e. ethylbenzene > toluene > benzene (xylene was not tested), as

demonstrated for siloxanes. However, when landfill gas (i.e. a multicomponent mixture) was used, the capacity was in the order toluene > xylene > ethylbenzene > benzene. Benzene was displaced by the other compounds when the carbon neared saturation, which supports the notion that it is the most weakly adsorbing compound. However toluene was not expected to have the largest capacity. Guar et al. (2010) suggest the size of the ethylbenzene and xylene molecules may be the limiting factor. Matsui and Imamura (2010) also noticed competition effects in real biogas: when measuring D4 and D5 concentrations they found that concentrations of D4 at the exit exceeded those at the inlet when the adsorbent neared saturation, indicating that D5 was displacing D4 when empty adsorption sites were scarce.

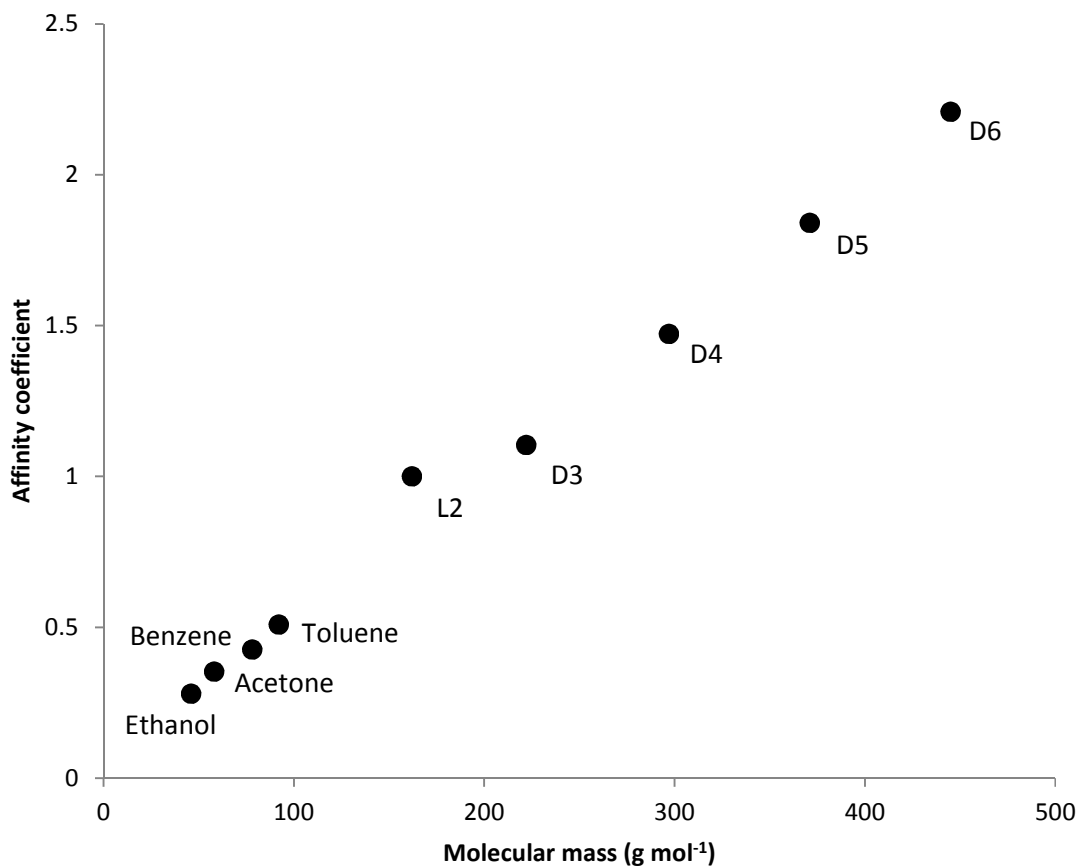


Figure 2-1. Relationship between molecular weight and Dubinin-Radushkevich affinity coefficient for selected VOCs (using L2 as reference compound).

This finding correlates with that of Guar et al. (2010), that smaller molecules are displaced by larger molecules. The presence of smaller molecules can, however, still have a negative effect on the adsorption capacity for larger molecules. For example Ricaurte Ortega and Subrenat (2009a) found using batch experiments that adding 10 mg m^{-3} of toluene to the model biogas resulted in a 50 g kg^{-1} reduction in the adsorption capacity of activated carbon cloth for L2. However, competition between siloxanes and other VOCs has not yet been demonstrated in a dynamic setting.

Physical properties of the adsorbate (Table 2-5) also influence the effect of humidity on adsorption capacity. Cal et al. (1996) compared the effect of humidity on the adsorption of a soluble VOC (acetone) and an insoluble VOC (benzene) onto activated carbon cloth. They found the adsorption capacity for benzene decreased sharply at humidities greater than 65% but humidities up to 90% had little effect on the adsorption of acetone. Similarly, Vizhemehr et al. (2011) found humidity of 50% had no effect on the adsorption of n-hexane (insoluble) but humidity of 55% led to a small reduction in removal efficiency. Lee et al. (2005) found that increasing humidity up to 80% had a minimal effect on trichloroethene (trichloroethylene, soluble) adsorption. The positive influence of decreased hydrophobicity can outweigh the influence of molecular weight, as shown by Schwegkofler and Niessner (2001), who demonstrated that silica gel had a greater adsorption capacity for L2 ($\log K_{ow} = 4.76$) than D5 ($\log K_{ow} = 5.71$) at all humidities tested (0 – 50%) (D5 and L2 were tested separately). At higher humidities, it is easier for L2 to pass through any water absorbed onto the silica gel. In general, adsorbates with stronger dipoles (such as L2 compared to D5) are more strongly attracted to hydrophilic adsorbents (Perry and Green, 1998).

Table 2-2. Parameters of VOC column experiments from the literature

Adsorbate	Carrier gas	Adsorbate concentration	Temperature	Humidity	Contactor volume	Contactor / bed height	Contactor i.d.	Contactor aspect ratio	Volumetric flowrate	Linear velocity	EBCT	Mass of adsorbent	Re	Contactor material	Analyser	References
		g m^{-3}	$^{\circ}\text{C}$	%	mm^3	mm	mm	[L/W]	ml min^{-1}	m min^{-1}	s	g	-			
Benzene	Air nitrogen, landfill gas	0.029 – 2.4	20 - 30	0 - 90	196 - 2827	36 - 200	4.6 - 10		60 - 10000	20.4- 59.53	0.1 – 0.25	0.765 - 250	190 - 555	Stainless steel, glass	GC-FID, UV spectroscopy	[3,4,5,6,9,12,13,14]
Toluene	Air, landfill gas	0.038 - 15	15 - 33	0 - 90	154 - 2827	0.85 - 40	7.5 - 36		20 - 7000	0.2 – 59.53	0.1 – 2.7	0.765 - 2	1.1 - 555	Stainless steel, glass	GC-FID	[1,2,3,4,6,7,8,10,12]
Ethyl benzene	Air, landfill gas	0.031 – 1.9	24 - 30	0 - 90	2827	36	10		674 - 16000	20.4 – 59.53	0.1 – 0.25	1 - 2	190 - 555	Stainless steel	GC	[6,12]
o-xylene	Air, landfill gas	0.015 - 16	24-25	0	100 - 2827	36	7.5 - 10		60 - 674	23.83	0.25	0.765 - 1	222	Stainless steel, quartz, glass	GC-FID	[3,4,12,15]
m-xylene	Air	3.2	25	0	nd	nd	7.5		60	nd	nd	0.765 - 1	nd	Glass	GC-FID	[3]
Chloroform, trichloromethane	Landfill gas	0.30	24 - 30	0	2827	36	10		674 - 1600	20.4 – 23.83	0.1 – 0.25	1 – 1.2	190 - 222	Stainless steel	GC	[6,12]
Carbon tetrachloride, tetrachloromethane	Landfill gas	0.20	24 - 30	0	2827	36	10		674 - 1600	20.4 – 23.83	0.1 – 0.25	1 – 1.2	190 - 222	Stainless steel	GC	6,12]
Trichloroethylene, trichloroethene	Landfill gas	0.0065	24 - 30	0	2827	36	10		674 - 1600	20.4 – 23.83	0.1 – 0.25	1 – 1.2	190 - 222	Stainless steel	GC	[6,12]
Tetrachloroethylene, tetrachloroethene	Landfill gas	0.0040	24 - 30	0	2827	36	10		674 - 1600	20.4 – 23.83	0.1 – 0.25	1 – 1.2	190 - 222	Stainless steel	GC	[6,12]
n-butane	Air, N ₂	0.005 - 0.19	15 - 33	50 - 90	nd	0.85	nd		60	0.2	nd	nd	1.1	nd	nd	[5,10]
Ethanol	Air	0.47	25	nd	1963 - 3927	100 - 200	5		1000	50.9	2.0 – 4.0	500	283	nd	nd	[13]
Acetone, propan-2-one	Air, nitrogen	1.2 – 2.4	20 - 25	nd	nd	nd	nd		60 - 200	nd	nd	nd	nd	nd	nd	[5,9,11]
Methylethylketone, butan-2-one	Air	0.30	20	20	154 - 693	4 - 18	7		250	6.5	0.6 – 2.7	250	36.4	nd	nd	[1]
Limonene, 1-methyl-4-(1-methylethenyl)-cyclohexane	Air	0.36	20	20	154 - 693	4 - 18	7		250	6.5	0.6 – 2.7	250	36.4	nd	nd	[1]

All experiments carried out at atmospheric pressure.

References: [1] (Anfruns et al., 2011) [2] (Balalay et al., 2011) [3] (Carrasco-Marín et al., 2009) [4] (Fairén-Jiménez et al., 2007) [5] (Foster et al., 1992) [6] (Gaur et al., 2010) [7] (Lorimier et al., 2005) [8] (Mohan et al., 2009) [9] (Ramirez et al., 2005) [10] (Sager and Schmidt, 2010) [11] (Shih and Li, 2008) [12] (Shin et al., 2002) [13] (Silvestre-Albero et al., 2010) [14] (Štandeker et al., 2009) [15] (Zaitan et al., 2008)

Table 2-3. Bench-scale siloxane adsorption experiments from the literature

Experiment type	Carrier gas	Siloxanes investigated	Siloxane concentration	Temperature	Humidity	Contactor volume	Contactor / bed height	Contactor i.d.	Contactor aspect ratio	Volumetric flow rate	Linear velocity	EBCT	Re ^a	Mass of adsorbent	Contactor material	Analyser	Ref
			mg m ⁻³	°C	%	mm ³	mm	mm	[L/W]	L min ⁻¹	m min ⁻¹			g			
Batch	Synthetic biogas	D4	30 – 11	25	nd	nd	nd	nd	nd	n/a	n/a	n/a	n/a	nd	nd	GC-FID	[1]
Batch	Synthetic biogas	D4	nd	25	<10	2 x 10 ⁶	nd	nd	nd	n/a	n/a	n/a	n/a	nd	Glass	GC-FID	[2]
Batch	Nitrogen	L2, D4, D5 (1:1:1 mixture)	L2 – 5710 D4 – 7140 D5 – 7150	30	nd	2.5 x 10 ⁶	nd	nd	nd	n/a	n/a	n/a	n/a	0.01 – 0.1	Serum bottle with Teflon septum	GC-MSD	[3]
Batch	Real biogas	Total siloxanes	nd	nd	nd	nd	nd	nd	nd	n/a	n/a	n/a	n/a	nd	nd	nd	[4]
Batch	Air	L2, D4	nd	25 / 60	0 / 70	nd	nd	nd	nd	n/a	n/a	n/a	n/a	0.5	nd	GC-FID	[5]
Dynamic	Nitrogen / synthetic biogas / air	D4	18; 490-2200; 12000	20	0; 20; 80	192 - 346	5 - 9	7	0.7 – 1.3	0.2	5.2	0.06 – 0.1	5.3 ^b	0.25	nd	GC-FID	[6]
Dynamic	Synthetic biogas	D3	83000	25	100	8480	300	6	50	0.06	2.12	2	1.4 ^c	1.3	Quartz and glass wool	IR spectroscopy	[7]
Dynamic	Nitrogen	L2	200 - 3000	30	nd	nd	nd	6	nd	0.1	3.5	nd	3.4 ^b	0.15 / 0.30	Quartz	MS	[8]
Dynamic	Real biogas?	Total siloxanes	nd	nd	nd	nd	nd	nd	nd	nd	nd	nd	nd	nd	nd	nd	[9]
Dynamic	CO ₂	D4	nd	20	nd	3040 / 29200	155 / 190	5 / 14	31 / 14	0.5	25.4 / 3.2	0.3 / 3.5	16.4 / 2.1 ^c	nd	Glass	GC	[10]
Dynamic	Real biogas	D4, D5, D6	3.5 – 20	nd	nd	908000 / 721	190 / 102	39 / 3	4.8 / 34	0.07 / 0.04	0.06 / 5.65	192 / 1.2	0.2 / 16.4 ^b	295 / 0.2	Stainless steel	GC-MS	[11]
Dynamic	Synthetic biogas	D4	360	nd	nd	nd	nd	nd	nd	0.1	nd	nd	nd	0.5	Glass	GC-MS	[12]
Dynamic	Nitrogen	D4	4500	35	nd	nd	nd	60	nd	15	5.31	nd	3.4 ^c	150	Teflon	GC-FID	[13]
Dynamic	Nitrogen	D4, D5	550 D4, 250 D5	27	nd	56700	250	17	15	1	4.41	3	2.8 ^c	0.5	Glass and Teflon	Siloxane continuous analyser	[14]
Dynamic	Nitrogen	L2, D5	1000 - 4000	nd	0 - 50	2360	120	5	24	0.2	10.2	0.7	6.6 ^c	0.5	Glass	GC-FID	[15]
Dynamic	Nitrogen	D4	400	20 ^d	0 / 70	123000	250	25	10	4	8.4	1.8	5.4	5-20	Stainless steel	GC-FID	[16]
Dynamic	Synthetic biogas	D4	1440	30	nd (0)	1767	40	7.5	5.3	0.55	12.4	0.19	10.2 ^b	1.0	nd	GC-FID	[17]
Dynamic (pilot scale)	Real biogas	Total siloxane	nd	21 - 29	nd	0.22 x 10 ^d	3200	260	12	2800	53	0.001	125	96000	nd	nd	[18]

nd = no data. ^aEstimated median values where multiple data available. ^bEstimated using void fraction = 0.5. ^cEstimated using particle diameter = 200 m and void fraction = 0.5. ^dEstimated: study says ambient room temperature. ^eEstimated using media density of 27.5 lb cu ft⁻¹ (Applied Filter Technology, 2011) and aspect ratio of 1:12 based on photograph. All experiments carried out at atmospheric pressure except Liang et al. (2001) which was run at 406-448 kPa. References: [1] (Boulinguez and Cloirec, 2009) [2] (Boulinguez and Le Cloirec, 2010) [3] (Nam et al., 2013) [4] (Prabucki et al., 2001) [5] (Ricaurte Ortega and Subrenat, 2009b; Ricaurte Ortega and Subrenat, 2009a) [6] (Cabrera-Codony et al., 2014) [7] (Finocchio et al., 2009; Montanari et al., 2010) [8] (Gislon et al., 2013) [9] (Hagmann et al., 2001) [10] (Huppman et al., 1996) [11] (Khandaker and Seto, 2010) [12] (Lee et al., 2001) [13] (Matsui and Imamura, 2010) [14] (Oshita et al., 2010) [15] (Schweiggkofler and Niessner, 2001) [16] (Sigot et al., 2014) [17] (Yu et al., 2013) [18] (Liang et al., 2001)

Table 2-4. Physical properties of adsorbents

Adsorbent	Porous volume	BET surface area	Microporous volume	Micropore surface area	External surface area	Average pore diameter	Bed density	Particle density	Grain diameter	Fibre cloth thickness	Ash content	Total carbon	References
	cm ³ g ⁻¹	m ² g ⁻¹	cm ³ g ⁻¹	m ² g ⁻¹	m ² g ⁻¹	nm	g cm ⁻³	g cm ⁻³	mm	mm	wt%	wt%	
Minworth carbon	0.13950	205.7447	nd	nd	nd	2.2022		nd		n/a	nd	nd	
PpTek media	0.488406	276.5495	nd	nd	nd	6.4824		nd		n/a	nd	nd	
Granular activated carbon	0.346 – 1.36	650 - 1930	0.32 – 0.7	334 - 1149	118 - 1040	1.6 – 3.04	0.4 – 1.54	0.85	1.16 – 1.22	n/a	3.59 – 12.6	66 – 97.1	[1,2,5,7,8,9,12,13,14,15,16,17,18,20,21,22]
Activated carbon fibre	nd	900 - 2420	nd	nd	nd	nd	nd	nd	nd	nd	nd	92.8 – 95.4	[6]
Activated carbon fibre cloth	0.305 – 0.79	663 - 2059	0.278 – 0.6918	835.1 – 1742.6	1000 - 2000	1.69 - 2	0.222 - 0.347	n/a	n/a	0.4 – 0.5	nd	95.4	[2,11,16]
Activated carbon fibre felt	0.603 - 0.748	999.4 - 1853	0.3649 – 0.597	899.1 – 1288	1000 - 1800	1.67 – 1.82	0.0533 – 0.0789	n/a	n/a	1.8 – 2.57	nd	nd	[2,11]
Carbon aerogel	nd	907 - 1537	nd	nd	nd	nd	0.64 – 0.79	nd	nd	n/a	nd	nd	[3,4]
Multiwalled carbon nanotube	nd	108 - 114	0.00222 – 0.00614	nd	nd	10.2 – 10.9	nd	nd	nd	nd	nd	nd	[19]
Sewage sludge	nd	188 - 990	0.09 – 0.45	nd	nd	nd	nd	nd	nd	n/a	nd	nd	[1]
Silica gel	0.2431 – 0.376	550 - 717	0.227	233	484	2.1	0.72 - 2.11	nd	0.85 – 2.0	n/a	92.1 (???)	0.6	[5,12,14,15,18,22]
Silica aerogel	0.005 – 3.67	112 - 812	nd	nd	nd	4.8 – 18.1	nd	nd	0.25	n/a	nd	nd	[22]
Zeolite	0.328 – 0.506	607 - 712	0.227	596	143	2.85	0.69 – 2.17	nd	0.85 – 2.0	n/a	99.1	nd	[10,12,14,15,18]
Alumina	nd	107	0.011	12.85	94.64	7.47	nd	nd	nd	n/a	nd	nd	[5,10,23]
Natural clays	nd	83.5	0.0005	2.4691	81.024	10.2	nd	nd	nd	n/a	nd	nd	[9,23]

References: [1] (Anfruns et al., 2011) [2] (Balanay et al., 2011) [3] (Carrasco-Marín et al., 2009) [4] (Fairén-Jiménez et al., 2007) [5] (Finocchio et al., 2009) [6] (Foster et al., 1992) [7] (Gaur et al., 2010) [8] (Huppman et al., 1996) [9] (Khandaker and Seto, 2010) [10] (Lee et al., 2001) [11] (Lorimier et al., 2005) [12] (Matsui and Imamura, 2010) [13] (Mohan et al., 2009) [14] (Montanari et al., 2010) [15] (Oshita et al., 2010) [16] (Ramirez et al., 2005) [17] (Sager and Schmidt, 2010) [18] (Schweigkofler and Niessner, 2001) [19] (Shih and Li, 2008) [20] (Shin et al., 2002) [21] (Silvestre-Albero et al., 2010) [22] (Štandeker et al., 2009) [23] (Zaitan et al., 2008)

Table 2-5. Physical properties of adsorbates

Adsorbate	Formula	Molecular mass	Boiling point	Vapour pressure		Aqueous solubility		log Henry's Law constant	log K_{oc}	log K_{ow}	Concentration range tested	Example concentrations in landfill gas ^a	Example concentrations in sewage sludge derived gas
				mm Hg	at °C	mg l ⁻¹	at °C						
Hexamethyldisiloxane, L2, MM, HDMS	(CH ₃) ₃ SiOSi(CH ₃) ₃	162	100.5	42.2	25	0.93	25	1.98	3.75	4.76	1.0 – 4.0	0.22	0.001 – 0.008
Hexamethylcyclotrisiloxane, D3	((CH ₃) ₂ SiO) ₃	222	135.1	8.6	25	1.56	25	1.86	3.55	4.47	83	2.29	<0.04
Octamethylcyclotetrasiloxane, D4, OMCTS	((CH ₃) ₂ SiO) ₄	297	175.6	0.99	25	0.056	25	2.69	4.17	5.09	0.0029 – 4.5	0.93	0.03 – 0.87
Decamethylcyclopentasiloxane, D5	((CH ₃) ₂ SiO) ₅	371	211.1	0.174	25	0.017	25	2.43	4.60	5.71	0.014 – 4.0	1.31	0.1 – 1.27
Dodecamethylcyclohexasiloxane, D6	((CH ₃) ₂ SiO) ₆	445	518.1	0.03	25	0.005	15		5.08	6.33	0.0035	nd	nd
Benzene	C ₆ H ₆	78.11	80.1	76	20	1780	20	-0.65		2.13	0.029 – 2.4	2.8	0.1 – 0.3
Toluene	C ₆ H ₅ -CH ₃	92.1	110.8	22	20	515	20			2.69	0.038 - 15	42	2.8 – 11.8
Ethyl benzene	C ₆ H ₅ -C ₂ H ₅	106.17	136.2	7	20	152	20	-0.45		3.15	0.031 – 1.9	15	nd ^d
o-xylene	C ₆ H ₅ -(CH ₃) ₂	106.17	144	5	20	175	20			2.77	0.015 - 16	7.9	nd ^d
m-xylene	C ₆ H ₅ -(CH ₃) ₂	106.17	139	6	20					3.20	3.2	25 ^c	nd ^d
Chloroform, trichloromethane	CHCl ₃	119.3	62	160	20	8000	20			1.97	0.30	nd	nd ^d
Carbon tetrachloride, tetrachloromethane	CCl ₄	153.82	76.7	90	20	1160	20			2.64	0.20	nd	nd ^d
Trichloroethylene, trichloroethene	CCl ₂ =CHCl	131.5	87	60	20	1100	25			2.42	0.0065	nd	nd ^d
Tetrachloroethylene, tetrachloroethene	CCl ₂ =CCl ₂	165.83	121	14	20	150	25			2.53	0.0040	nd	nd ^d
n-butane	C ₄ H ₁₀	58.14	-1	1823	25	61	20	1.58			0.005 - 0.19	6.2	nd ^d
Ethanol	CH ₃ CH ₂ OH	46.07	78.4	43.9	20			-3.59		-	0.47	0.0	nd ^d
Acetone, propan -2-one	CH ₃ -CO-CH ₃	58.08	56.2	270	30					0.32	1.2 – 2.4	5.3	nd ^d
Methylethylketone, butan-2-one	CH ₃ COCH ₂ CH ₃	72.1	79.6	7.5	20	35300	10			0.24	0.30	nd	nd ^d
Limonene, 1-methyl-4-(1-methylethenyl)-cyclohexane	CH ₃ -C ₆ H ₈ -C ₃ H ₅	136.25	175.18							0.26	0.36	240	nd ^d

^aSiloxane data from Arnold and Kajolinna, (Arnold and Kajolinna, 2010)2010 and VOC data from Eklund et al, (Eklund et al., 1998)1998. ^bSiloxane data from (Rasi et al., 2010) and VOC data from (Rasi et al., 2007). ^cCombined figure for o- and p-xylene. ^dNo data for individual VOC species, but total VOCs 20 – 270 mg m⁻³ (Rasi et al., 2007).

2.5 Conclusions

There has been relatively little research into the adsorption of trace gases for environmental applications, especially siloxanes, compared to industrial adsorption processes. In particular, the current understanding of the effects of humidity on VOC adsorption, such as the differentiation between capillary condensation and water film formation, is limited and sometimes contradictory (e.g. when does a threshold effect occur?). Nevertheless, it is possible to draw some conclusions about how to match an adsorbent to an adsorbate.

In general, large molecules adsorb more strongly but can access less of an adsorbent's porous surface area. Matching the size of the adsorbate with the pore size distribution of the adsorbent is important when looking at single species adsorption. Smaller pores make more surface area available for adsorption but pores must not be so small the adsorbate molecules cannot enter or move along the pores. Based on Fairen-Jimenez's (2007) findings, the ideal pore diameter may be two to three times the adsorbate molecule's diameter. Interspecies competition for adsorption sites should also be taken into account. Larger molecules tend to adsorb more strongly than smaller molecules of a similar chemistry, potentially displacing smaller molecules when adsorption sites are scarce. It would therefore be beneficial, if possible, to exclude molecules larger than the target molecule in a large portion of the pore space when considering the pore size distribution of a potential adsorbent.

The octanol-water partition coefficient and solubility of the adsorbate affect the choice of adsorbent as hydrophilic adsorbates have greater affinity for hydrophilic adsorbents. The adsorbability of highly soluble adsorbates is also much less affected by the presence of humidity in the gas. When the adsorbate is hydrophobic, using a hydrophobic adsorbent can reduce the effect of humidity. Humidity is less of a problem at high adsorbate concentrations. Reducing humidity to below the level at which capillary condensation occurs in a significant proportion of the adsorbent pore space was effective for BTEX

adsorption but siloxane adsorption was still hindered by the water film surrounding the adsorbent particles.

3 On-line siloxane detection for adsorption vessel characterisation using FTIR spectroscopy

C.A. Hepburn^a, A. Brown^b, N.J. Simms^c, and E.J. McAdam^a

^aCranfield Water Science Institute, Cranfield University, Cranfield, Bedfordshire, MK43 0AL, UK

^bNational Physical Laboratory, Hampton Road, Teddington, Middlesex, TW11 0LW, UK

^cCentre for Power Engineering, Cranfield University, Cranfield, Bedfordshire, MK43 0AL, UK

Abstract

Siloxane damage to combined heat and power (CHP) engines accounts for up to 16% of water utilities' revenue from using biogas to generate electricity, so it is common to pre-treat biogas by adsorbing siloxanes onto activated carbon. In this study, on-line Fourier transform infrared (FTIR) spectroscopy was used to measure siloxane concentrations in real biogas both upstream (siloxane range 86.1 – 157.5 mg m⁻³) and downstream (siloxane range 2.2 – 4.3 mg m⁻³ (as measured by GC-MS)) of activated carbon vessels and in synthetic biogas, to assess the suitability of this method for monitoring the adsorption process. With laboratory gas chromatography – mass spectrometry used for verification, the FTIR spectrometer provided accurate readings upstream of the carbon vessel with a root mean square error (RMSE) of 15.8 mg m⁻³ (16%), which was improved to 9.8 mg m⁻³ (10%) when partial least squares analysis was used to process the spectral data. Interference from volatile organic carbons limited the precision in the siloxane outlet concentrations from the vessel even after PLS analysis was used (RMSE = 1.5 mg m⁻³). However the limit of detection (3.2 mg m⁻³) is lower than most engine manufacturer's recommended siloxane limits, which evidences the applicability of on-line FTIR for use by water utilities. This was illustrated through application of on-line analysis to full scale activated carbon vessels in which on-line siloxane analysis is estimated to reduce costs by up to £0.007 kWh⁻¹ (50% of estimated associated cost) by providing enhanced engine protection.

Keywords: *Anaerobic digestion; Biogas; CHP; Landfill; Interference; VOCs*

3.1 Introduction

A significant proportion (1%, or 6.34 GWh per day) of electricity generated in England and Wales, is used to treat wastewater (Parliamentary Office of Science and Technology, 2007). Producing electricity onsite at sewage treatment works can therefore produce significant cost savings for water utilities. To illustrate, UK water utilities currently have an installed capacity of 198 MW in combined heat and power (CHP) engines which generated 761 GWh in 2013 from biogas arising from the anaerobic digestion of sewage sludge (DECC, 2013). The UK government's Anaerobic Digestion Strategy and Action Plan sets out a desire for a "significant increase" in energy generation from anaerobic digestion (AD) and the Department for the Environment, Food and Rural Affairs (DEFRA) forecasts the potential for electricity generation from AD in the UK to be 3-5 TWh per annum by 2020 (DEFRA, 2011).

To ensure the biogas is utilised economically, some trace gases must be removed (Arnold, 2009). One group of contaminants, volatile methyl siloxanes (VMSs), is of particular concern due to the potential for damage to CHP engines. When combusted, siloxanes form silicon dioxide. Some of this silicon dioxide is deposited in the engine as microcrystalline silica, where it abrades the inner surfaces of the combustion chamber (Schweigkofler and Niessner, 2001), clogs valves (Accettola et al., 2008) and reduces engine efficiency (Ohannessian et al., 2008). Damage caused by siloxanes is estimated to cost around £0.015 kWh⁻¹ (Lemar, 2005), or 16% of the current UK feed-in tariff for electricity from CHP engines (£0.094 kWh⁻¹, Read and Hofmann, 2011).

Current best practice for removal of siloxanes from biogas is pre-treatment using carbon vessels filled with granular activated carbon (GAC) (Ajhar et al., 2010a). Whilst many GAC vessels have been installed at sewage treatment works, there remains relatively little data relating to the effectiveness of these systems. This can, in part, be attributed to the difficulties in measuring siloxanes as until recently the most common methods involve discrete sampling using gas bags (Ajhar et al., 2010b) or canisters (Schweigkofler and Niessner,

1999), followed by analysis using gas chromatography-mass spectrometry (GC-MS) at an external laboratory. Not only is this expensive, at up to £100 per sample, but the data density provided is insufficient to fully characterise either the siloxane profile of the biogas or the performance of the carbon vessels. To illustrate, it is rare for biogas sampling to be carried out more than once per day, but at the point of siloxane breakthrough, the outlet concentration from the carbon contactor rises from the leakage concentration ($\approx 7 \text{ mg m}^{-3}$) to equal the inlet concentration ($\approx 100 \text{ mg m}^{-3}$) in less than four hours (Hepburn et al., 2014). This steep breakthrough curve is characteristic of gas adsorption processes, as gases are characterized by a low Schmidt number which facilitates high mass transfer rates (Wakao and Funazkri, 1978; Cooney, 1999). Frequent measurement of siloxane concentrations in the outlet gas and timely receipt of results is therefore required for effective vessel management.

Arnold and Kajolinna (2010) and Bramston-Cook and Bramston-Cook (2012) were amongst the first to develop online siloxane detection. The authors used portable gas chromatography (GC) to characterize siloxane concentrations in untreated biogas at sewage treatment works and landfill sites. Both calibrated their instruments using synthetic gases and demonstrated the ability of field GC to measure siloxanes in the complex matrix of biogas, although Arnold and Kajolinna (2010) noted that the gas chromatograms were difficult to interpret due to the presence of other volatile organic carbons (VOCs) in addition to siloxanes and found that results obtained using their field GC were higher than those obtained in the laboratory using GC-MS. Although portable gas chromatography is an effective tool and is capable of individual speciation of siloxanes, it requires regular use of standard gases for calibration and specialist training to operate, making running a field GC costly and impractical for a water utility.

Oshita et al. (2010) used a Fourier transform infrared (FTIR) spectrometer to measure siloxane concentrations in biogas from a sewage treatment plant in Japan. The authors achieved a close correlation between the results from on-line FTIR and laboratory GC-MS in both synthetic and real biogas, despite the

size of the siloxane peaks, which are approximately 1/50th of the height of the peaks caused by the bulk gases (Figure 3-1). Like Arnold and Kajolinna (2010), Oshita et al. (2010) found that in real biogas the on-line results were higher than the results from laboratory GC-MS: The authors propose positive interference from VOCs as the cause.

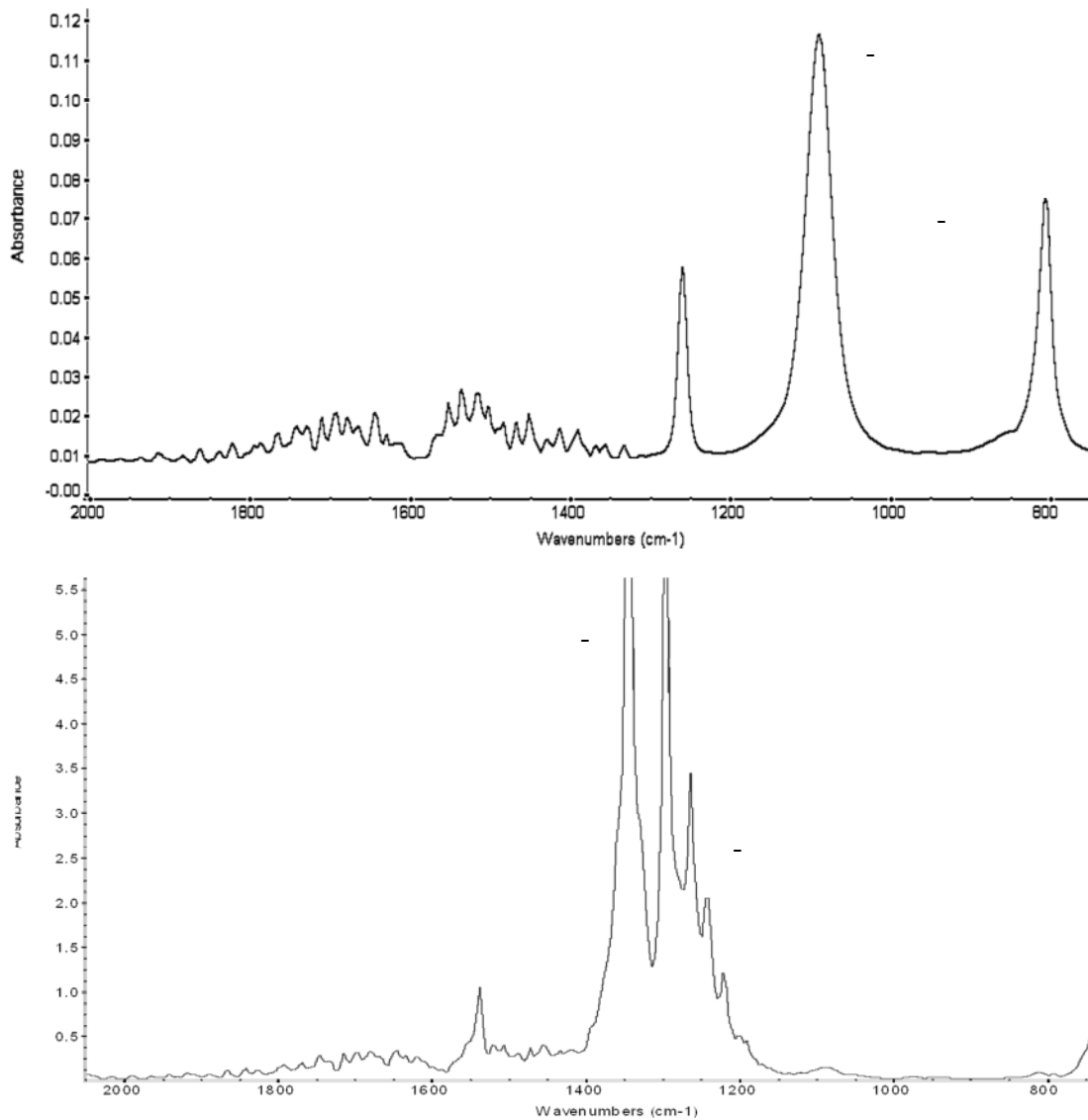


Figure 3-1. Infrared absorbance spectra for (a) D5 in nitrogen and (b) biogas. The main peaks are labelled with the corresponding chemical bonds (Stuart, 2004). Note the difference in y-axis scale – the peaks caused by D5 are 1/50th of the height of the large peaks caused by the bulk gases (CH₄ and CO₂).

An FTIR spectrometer only needs to be calibrated once and subsequent use is fast and straightforward, taking around eight minutes to acquire background and sample spectrums, as demonstrated by Bendini et al. (2007), who used FTIR spectroscopy to identify the geographical origin of olive oils. FTIR is therefore a more practical option for a water utility to install to monitor carbon contactors.

All of the above mentioned studies have measured siloxane concentrations in raw biogas, i.e. biogas before treatment by activated carbon. The aim of this study is to investigate the applicability of on-line Fourier transform infrared spectroscopy to providing enhancement of carbon vessel management and as an aid to economic utilisation of biogas as a fuel. The objectives of this study are: (i) to develop a calibration curve in for siloxanes in synthetic reference gases using an industry-ready FTIR spectrometer; (ii) to investigate interferences in FTIR spectra when applied to real biogases due to biogas composition by comparing FTIR readings to laboratory GC-MS measurements real biogas samples from both upstream and downstream of an activated carbon vessel; (iii) to refine calibration for use in real biogases whilst validating the results using a certified primary reference gas mixture; and (iv) to develop some of the first seen breakthrough curves for full scale siloxane removal carbon vessels and illustrate the benefits of on-line siloxane measurement.

3.2 Materials and Methods

3.2.1 Instrument and set up

The Fourier Transform Infrared spectrometer was an Antaris Industrial Gas System (Thermo Fisher Scientific Inc, Waltham, MA). The gas cell had a 2 m path length and was operated at 80°C to minimise the probability of condensation within the cell. The mirrors within the gas cell were coated with gold to limit deposition of carbon fines introduced in the biogas. Background spectra (found by scanning with the gas cell evacuated) were subtracted from the sample spectrum and the reported value was ascertained from the average value of the scans, with cyclic siloxanes discriminated at 817 – 798 cm^{-1} . This

region corresponds to the infrared (IR) absorbance caused by the Si-(CH₃)₂ group (Figure 3-1a, Table 3-1).

3.2.2 Calibration and verification

Reference gas was generated by spiking a carrier gas (carbon dioxide or nitrogen) with D5 using the apparatus described by Hepburn et al. (in preparation). The test rig was connected directly to the inlet of the spectrometer gas cell, so that gas constantly flowed through the gas cell.

Table 3-1. Infrared absorbance peaks for siloxanes.

Bond	Molecules	Peak position	Reference
Si-O	All siloxanes	1150 – 1000 cm ⁻¹ 1035 cm ⁻¹	(Oshita et al., 2010) (Montanari et al., 2010)
Si-O-Si	All siloxanes	near 1050 cm ⁻¹ (antisymmetric stretch) 1090 cm ⁻¹ (cyclotrisiloxanes) 1020 cm ⁻¹ (cyclotetrasiloxanes) Broad doublet with maxima at 1020 and 1090 cm ⁻¹ for more than twenty coupled siloxane units 1095 – 1075 cm ⁻¹ and 1055 – 1020 cm ⁻¹ 1300 – 1000 cm ⁻¹ (asymmetric stretching)	(Lipp and Smith, 1991) (Coates, 2000) (Stuart, 2004)
Si-O-C	All volatile methyl siloxanes	1110 – 1080 cm ⁻¹ 1110 – 1050 cm ⁻¹ (stretching)	(Coates, 2000) (Stuart, 2004)
Si-CH ₃	Linear siloxanes	850 - 770 cm ⁻¹ 818 cm ⁻¹ Near 775 cm ⁻¹ 1280 – 1250 cm ⁻¹ (symmetric bending)	(Oshita et al., 2010) (Montanari et al., 2010) (Lipp and Smith, 1991) (Stuart, 2004)
Si-(CH ₃) ₂	Cyclic siloxanes	Near 805 cm ⁻¹	(Lipp and Smith, 1991)
Si-(CH ₃) ₃	Linear siloxanes	760 and 845 cm ⁻¹	(Lipp and Smith, 1991)
CH ₃	Siloxanes Many other organic compounds	1262 ± 5 cm ⁻¹ and around 800-900 cm ⁻¹	(Lipp and Smith, 1991)

To validate the FTIR results, gas samples (ten CO₂ and eight N₂) were collected downstream of the FTIR gas cell into Type 232 SKC gas bags (Tedlar body and polypropylene fitting), to be subject to GC-MS analysis. Ajhar et al. (2010b) have shown that this type of gas bag provides high and stable recovery of siloxane samples in biogas up to eight days after sampling. The samples were analysed at a UKAS (United Kingdom Accreditation Service) accredited laboratory to give complete siloxane speciation. At the laboratory 100-250 ml of gas is passed through a Tenax adsorption tube at 30-50 ml min⁻¹. A stock standard containing eight siloxane species and toluene is used to prepare at least four calibration tubes. The samples, calibration standards, QC standards, drift checks and blanks are all analysed using a Markes Unity ATD system connected to an Agilent 5890/5973 GC-MS system (CERAM, 2012). This procedure is compliant with ISO17025 (International Organisation for Standardisation, 2005). The limit of detection is equivalent to 1 mg m⁻³ in the original sample.

To verify the spectrometer's readings, a certified primary reference gas mixture (PRGM) was supplied by the National Physical Laboratory (NPL, Teddington, UK). The concentration of D5 in methane was 6.9 μmol_{D5} mol⁻¹_{CH4} (110 mg_{D5} m⁻³_{CH4} at standard temperature and pressure).

To evaluate the performance of the FTIR spectrometer on a real biogas, the FTIR was moved to a large sewage treatment works and connected to gas sampling points upstream and downstream of the activated carbon contactor (6.76 m³, 3000 kg_{carbon}). The sampling lines were purged for two minutes (greater than three line volumes) before FTIR readings were taken. During measurement, gas was drawn through the gas cell by vacuum pump with 20 scans taken over 120 s. Nine bag samples were collected for GC-MS analysis from the gas sampling lines upstream and downstream of the activated carbon vessel by disconnecting the sampling line from the inlet of the FTIR spectrometer immediately after taking a FTIR reading. The samples were collected over three days to capture variations in gas composition. Two discrete gas samples were also taken from the sampling ports next to the

carbon vessel to capture the “same” gas entering and exiting the vessel. The ports were purged before sampling. These samples were analysed for a suite of VOCs by a UKAS accredited laboratory.

3.2.3 Data analysis

To distinguish between the trueness and precision of the FTIR readings (compared to the GC-MS results), two statistics have been used: the coefficient of determination (r^2) and the root mean square error (RMSE). The coefficient of determination is a measure of precision (Miller and Miller, 2005) where RMSE is a measure of overall accuracy, combining trueness and precision, and is commonly used for calibrating new FTIR methods (Bendini et al., 2007; Bertran et al., 1999):

$$RMSE = \sqrt{\frac{\sum_{i=1}^n (y_{i,FTIR} - y_{i,GC-MS})^2}{n}} \quad (1)$$

where $y_{i,FTIR}$ is the FTIR reading for sample i , $y_{i,GC-MS}$ is the GC-MS results for sample i and n is the number of samples. The limit of detection (LOD) is given by:

$$LOD = y_B + 3s_B \quad (2)$$

where y_B is the blank signal, considered equal to the y-intercept of the line of regression, and s_B is the standard deviation of the blank signal, considered equal to $s_{y/x}$, the standard deviation of each data point in the y-direction (Miller and Miller, 2005).

3.3 Results

3.3.1 FTIR calibration using reference gas and real biogas

Decamethylcyclopentasiloxane (D5) was the dominant siloxane in all the real biogas samples, both upstream (68.2 – 131.0 mg m⁻³) and downstream (2.2 – 4.3 mg m⁻³) of the carbon vessel (Table 3-2). This correlates with other studies which also found D5 to be the most abundant siloxane in digester gas, with D4

the next most abundant (Arnold and Kajolinna, 2010; Oshita et al., 2010; Rasi et al., 2010; Bramston-Cook and Bramston-Cook, 2012). Due to the dominance of cyclic siloxanes (85 - 95% of siloxanes in upstream samples and 100% in downstream samples) this study was focused on the calibration of the FTIR instrument for cyclic siloxanes.

To establish the response of the FTIR spectrometer to D5 in an environmentally relevant concentration range, the infrared absorbance spectra produced at 5 – 60 mg_{D5} m⁻³_{carrier gas} were analysed. The heights of the infrared absorbance peaks corresponding to the Si-O bond and Si-CH₃ bond show a strong correlation with the expected D5 concentration in the siloxane reference gas ($r^2 = 0.99$ for both correlations, Figure 3-2). Comparison of the FTIR calibration to the expected D5 concentration in the reference gas therefore similarly provides a strong correlation ($r^2 = 0.97$, Figure 3-3). For external verification of the calibration, FTIR results were compared to those produced by GC-MS (Figure 3-4). A strong linear relationship was found, with $r^2 = 0.99$ for D5-spiked nitrogen and $r^2 = 0.98$ for D5-spiked carbon dioxide. In both reference gases the FTIR readings are higher than the GC-MS results, 60 – 120% higher for D5 in nitrogen and 30 - 80% higher for D5 in carbon dioxide.

Table 3-2. Speciated siloxanes measured by GC-MS from gas bag samples from sewage treatment works (n = 9).

Siloxane species	Upstream concentration (mg m ⁻³)*			Downstream concentration (mg m ⁻³)*		
	Mean	St. dev.	Range	Mean	St. dev.	Range
L2	10.0	3.2	5.3 – 15.2	<1.0	-	-
L3	1.3	0.14	1.0 – 1.5	<1.0	-	-
L4	<1.0	-	-	<1.0	-	-
D3	<1.0	-	-	<1.0	-	-
D4	13.4	1.5	10.7 – 16.0	<1.0	-	-
D5	87.7	21.0	68.2 – 131.0	3.1	0.62	2.2 – 4.3

*Method detection limit is 1 mg m⁻³.

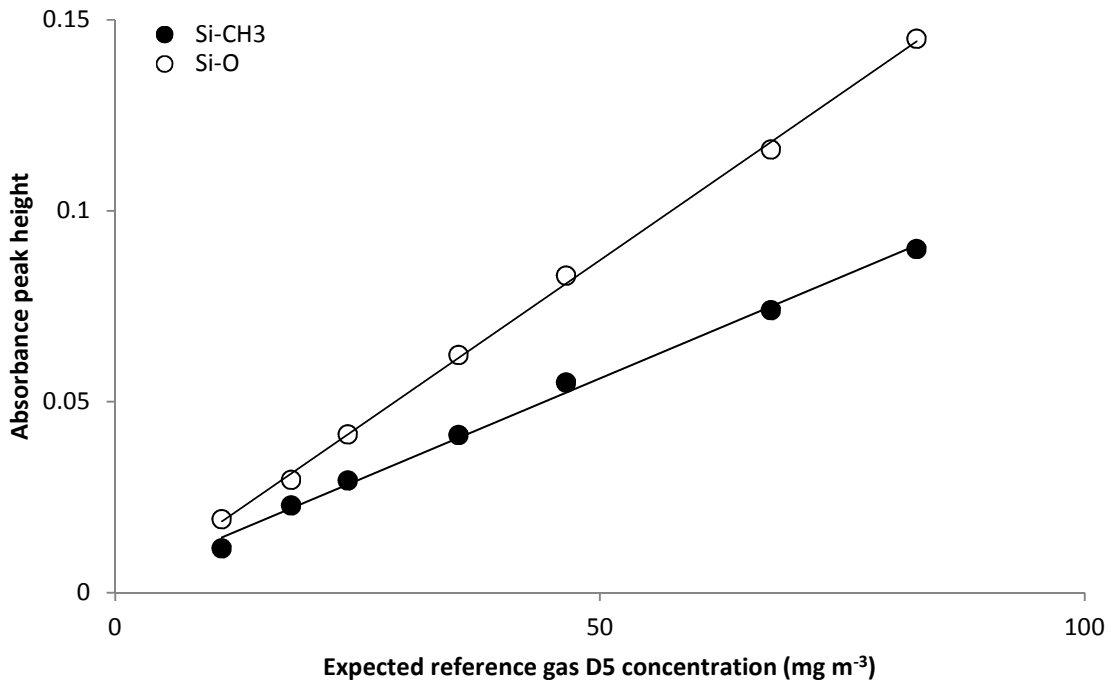


Figure 3-2. Comparison between expected D5 concentrations in reference gas (N₂) and absorbance peak heights in FTIR spectra. $r^2 = 0.99$ for both correlations.

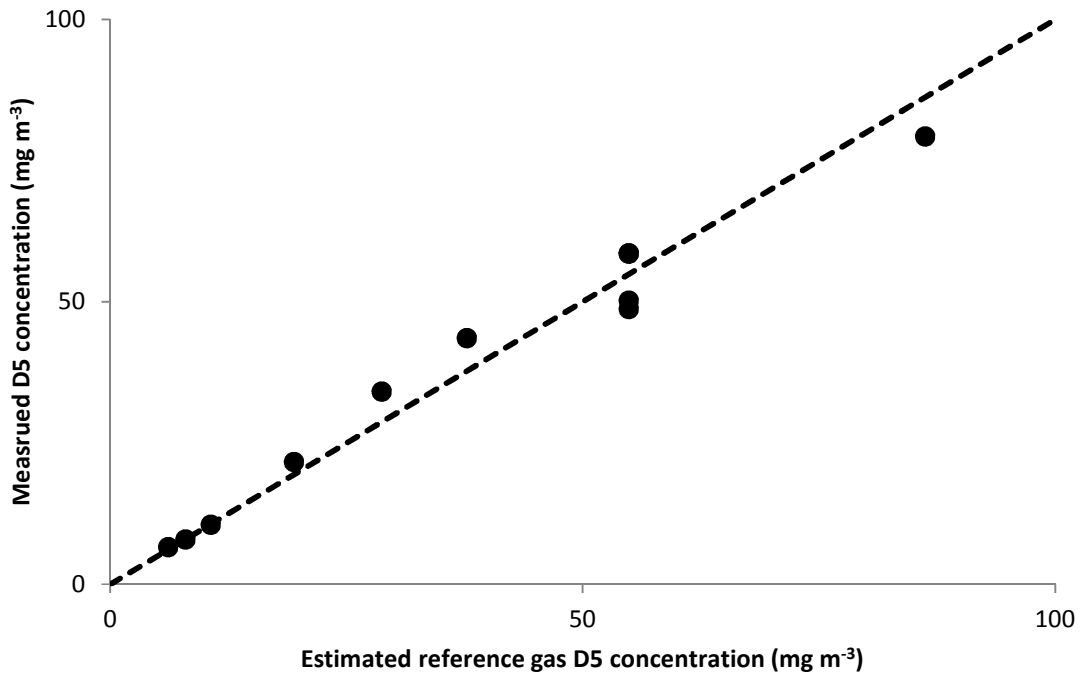


Figure 3-3. Comparison between expected D5 concentrations in reference gas (CO₂) and FTIR readings. The dashed line represents $y = x$.

When FTIR was applied to real biogas, D5 concentrations of 77 – 109 mg m⁻³ and 6.4 – 7.9 mg m⁻³ were recorded upstream and downstream of the carbon vessel. FTIR data was subsequently compared to the samples analysed by GC-MS for external verification in the complex biogas matrix. Upstream of the carbon vessel, the correlation between the FTIR and the GC-MS readings was good ($r^2 = 0.86$, Figure 3-5a) but the FTIR results were 0 - 25% lower than the GC-MS results. The RMSE was 15.8 mg m⁻³ or 15.7%. In the downstream samples, the correlation between the two methods' results was weaker ($r^2 = 0.52$, Figure 3-5b) and the FTIR results were 84 - 214% higher than the results from GC-MS. The RMSE was 4.5 mg m⁻³ or 147%. It should be noted that the RMSE is expected to be higher in the downstream samples as the siloxane concentration is lower.

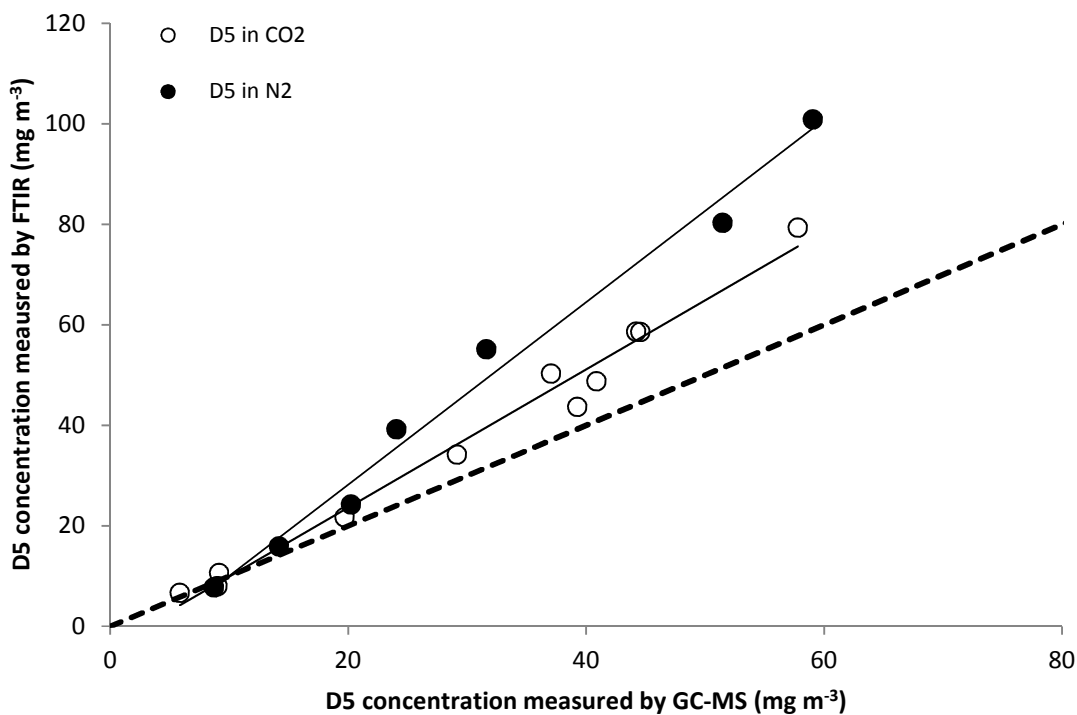


Figure 3-4. FTIR readings compared to GC-MS measurements in synthetic reference gas. $r^2 = 0.99$ for D5 in N₂ and $r^2 = 0.98$ for D5 in CO₂. The dashed line represents $y = x$.

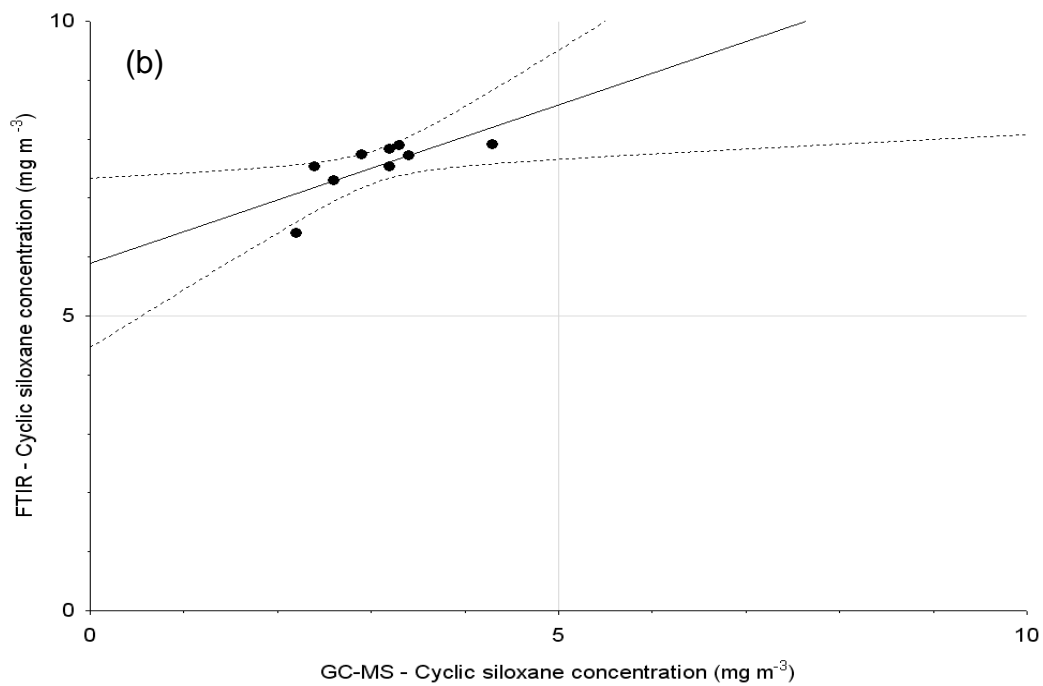
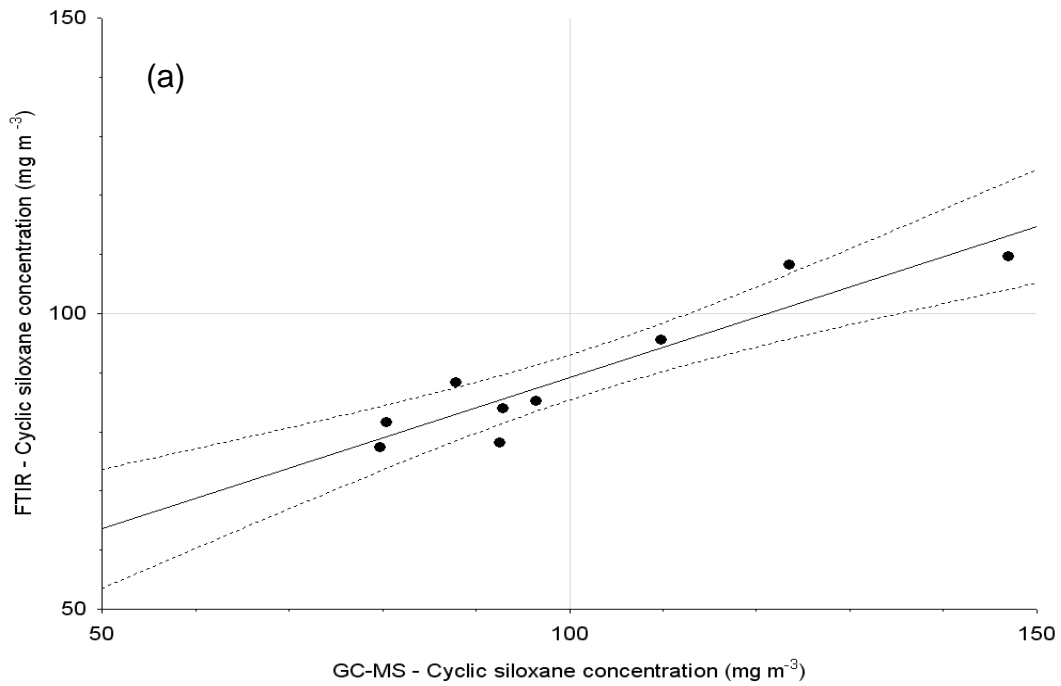


Figure 3-5. FTIR reading for cyclic siloxanes compared to total cyclic siloxanes measured from gas bag samples by GC-MS from biogas (a) upstream of carbon vessel and (b) downstream of carbon vessel. The dashed lines show the 95% confidence limits.

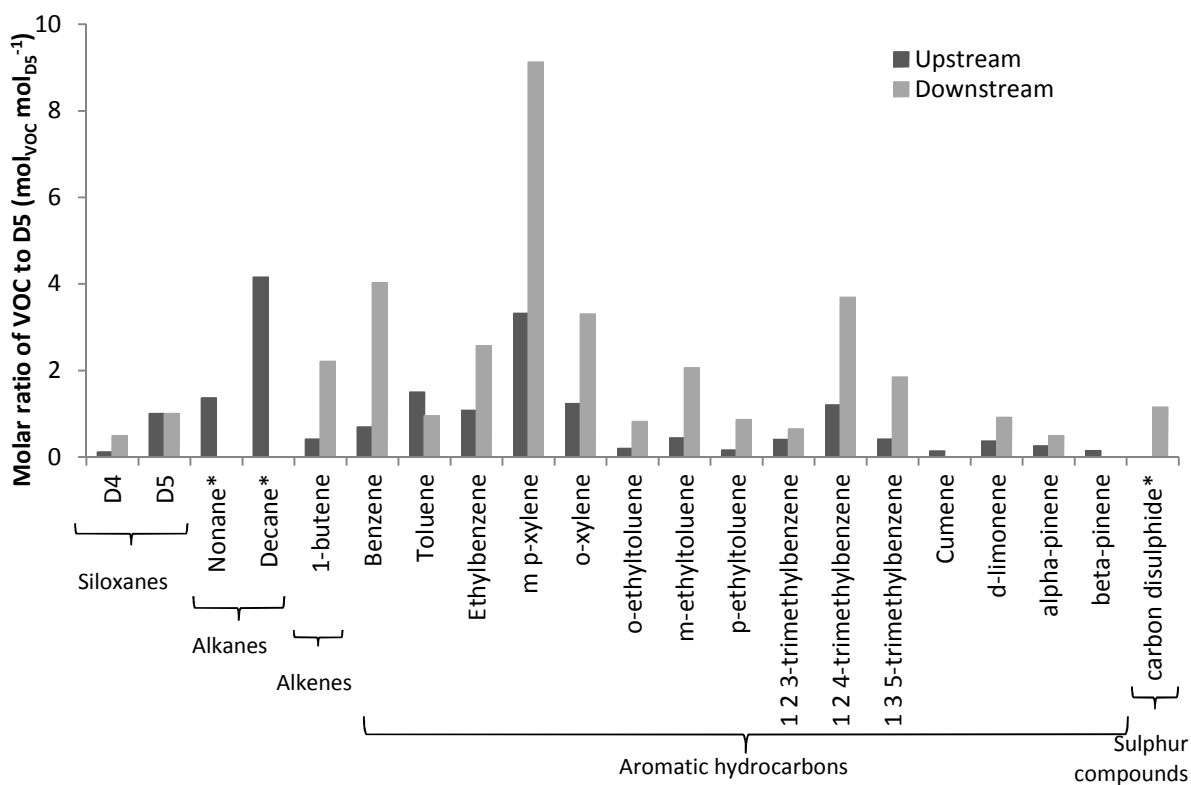
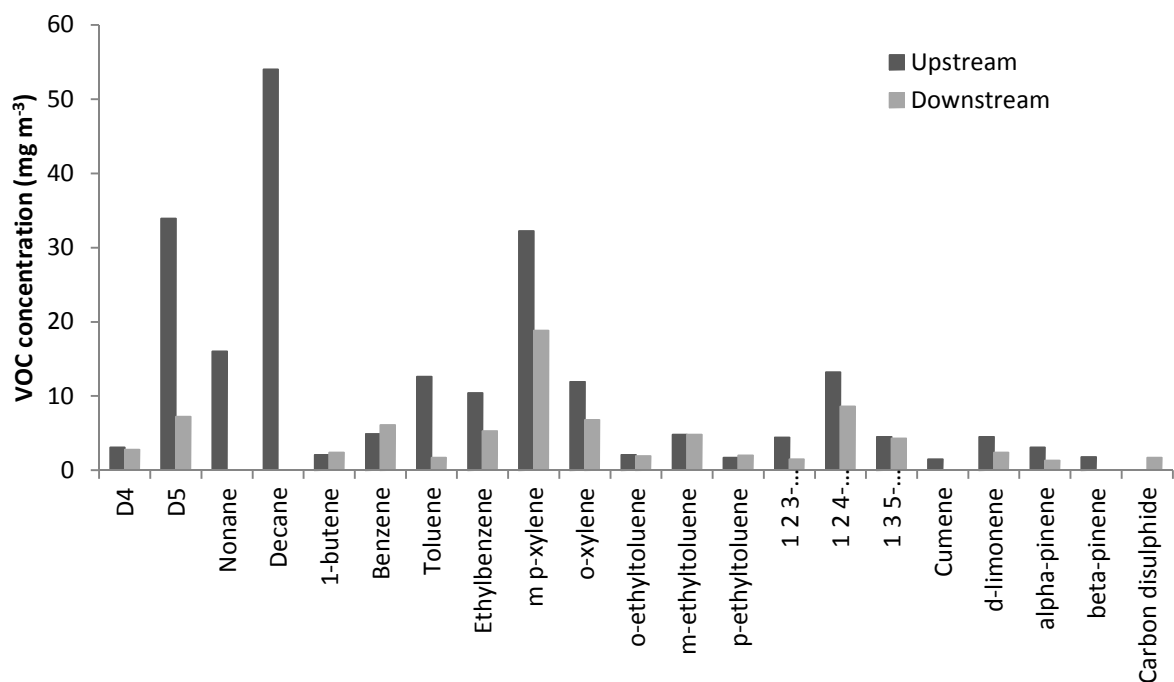


Figure 3-6: Volatile organic compounds found in the biogas samples from upstream and downstream of a carbon vessel. (a) Concentration; (b) molar ratio to D5. *Nonane, decane and carbon disulphide, do not contain bonds which are thought to contribute to interference in the FTIR readings.

3.3.2 Volatile organic carbons in biogas samples

A range of volatile organic carbons (VOCs) were found in the real biogas at concentrations ranging from 1.5 mg m^{-3} (cumene) to 54 mg m^{-3} (decane). The concentrations of VOCs were generally lower downstream of the carbon vessel, ranging from 1.3 mg m^{-3} (alpha-pinene) to 18.8 mg m^{-3} (m,p-xylene) (Figure 3-6a), with the exception of benzene which rose from 4.9 mg m^{-3} to 6.1 mg m^{-3} and carbon disulphide which went from below the detection limit to 1.7 mg m^{-3} . This indicates that the activated carbon also adsorbs the VOCs in addition to the target siloxanes. However, the molar ratio with respect to D5 of most species was higher downstream of the carbon vessel (Figure 3-6b). For example, the molar ratio of benzene to D5 upstream of the vessel was 0.69 and downstream of the vessel was 4.02. The upstream and downstream molar ratios of m,p-xylene to D5 were 3.32 and 9.12 respectively. Many of the VOC species found absorb infrared radiation at frequencies which coincide with the target region of the spectrum targeted by the FTIR spectrometer for siloxane quantification (Table 3-3).

3.3.3 Finalised calibration using partial least squares analysis and verification using external reference gas

A new analysis method was developed for the FTIR spectrometer using the collated spectra from real and synthetic biogas. The new analysis used a Partial Least Squares to analyse the peaks in the infrared absorbance spectrum. The original analysis used a Classical Least Squares (CLS) technique. In addition, a new region of the infrared absorbance spectrum was included, $1114.65 - 991.23 \text{ cm}^{-1}$, to utilise the absorbance peak caused by the stretching of the Si-O-C bond (Table 3-1). The region of the spectrum analysed to detect the Si-CH₃ bond was expanded from $817.67 - 798.39 \text{ cm}^{-1}$ to $879.38 - 798.39 \text{ cm}^{-1}$. The spectra generated by the original FTIR readings were reanalysed using the new PLS method. The accuracy of the real biogas readings was improved: the RMSEs were 9.8 mg m^{-3} (9.7%) and 1.5 mg m^{-3} (47.8%) for upstream and downstream results respectively. The limit of detection (LOD) was also improved, from 6.9 mg m^{-3} to 3.2 mg m^{-3} (Table 3-4).

Table 3-3. VOC species present in biogas samples and associated infrared absorbance peaks (Stuart, 2004). The italicised peaks may fall into the zones monitored by the FTIR spectrometer and cause positive interference.

Species	Concentration (mg m ⁻³)	Bonds ^a	Peaks
Alkanes			
Nonane	6	-CH ₂ -	2930; 2850; 1465; 1305; 1300; 720
Decane	9		
Alkenes			
1-butene	3.4	=C-H C=C	3100-3000; 1400; <i>1000-600</i> 1680-1600
Aromatic hydrocarbons			
Benzene	3.6	C-H	3100-3000; 1275-1000; <i>900-690</i>
Toluene	25.3	C=C	1650-1430
Ethyl benzene	15.1	Substituted aromatic compounds will also have peaks similar to the aliphatic compounds above	
m,p-xylene	32.9		
o-xylene	11.		
o-ethyltoluene	16.2		
m-ethyltoluene	47.7		
p-ethyltoluene	21.0		
1,2,3-trimethylbenzene	5.7		
1,2,4-trimethylbenzene	44.5		
1,3,5-trimethylbenzene	22.2		
Cumene	10.9		
d-limonene	8.8		
Alpha-pinene	9.3		
Beta-pinene	3.1		
Sulphur compounds			
Carbon disulphide	2.2	C-S	700-600

^aBonds shown are representative of chemical groups

To verify the new calibration, the cylinder containing primary reference gas mixture ($110 \text{ mg}_{\text{D}_5} \text{ m}^{-3} \text{ CH}_4$) was connected to the test rig so that gas flowed directly through the spectrometer's gas cell. The original CLS method provided readings in the range 83.22 mg m^{-3} to 91.15 mg m^{-3} (mean 87.6 mg m^{-3}), 20.4% lower than the expected value. The new PLS method provided readings in the range 109.83 mg m^{-3} to 119.37 mg m^{-3} (mean 114.2 mg m^{-3}), 3.8% higher than the expected value.

3.3.4 Application to full scale contactors

The FTIR spectrometer was used to construct a breakthrough curve for the carbon vessel at the sewage treatment works (Figure 3-7). The mass of siloxane passing into the engine can be calculated by integrating under the outlet concentration graph – 0.94 kg of siloxane was found to have entered the engine before breakthrough (over a period of 18 days). When breakthrough begins, the cyclic siloxane concentration in the outlet gas rises from 18 mg m^{-3} to 101 mg m^{-3} in four hours. A further 0.94 kg of siloxane entered the engine during the three days after breakthrough (equivalent to the time required for external analysis of a grab sample). The potential for siloxane-induced damage is therefore doubled if breakthrough is not captured in a timely manner using on-line analysis. At the case study sewage treatment works, on-line analysis is not currently used to inform when the carbon beds should be changed, as a result the carbon vessel was run for 29 days between carbon changes, during which a total of 4.60 kg of siloxane entered the engine.

3.4 Discussion

This study has shown that FTIR spectrometry is capable of measuring siloxanes in biogas both upstream and downstream of activated carbon vessels. In the initial analysis of biogas using FTIR, data produced were predominantly within the 95% confidence limits (Figure 3-5). The spectrometer demonstrated excellent linearity ($r^2 = 0.98 - 0.99$) for the reference gases (Figure 3-4) and good linearity for the upstream real biogas ($r^2 = 0.86$). This is equivalent to the results of Oshita et al. (2010) who achieved $r^2 = 0.98 - 0.99$ for synthetic

biogas and $r^2 = 0.90$ for real biogas using FTIR spectroscopy (Table 3-4). The RSME of 9.7% in upstream gas is comparable to the 10% error estimated by Arnold and Kajolinnä (2010) using field GC (Table 3-4), but was achieved using a simpler analytical method (FTIR). Biogas composition, including bulk gases, has an effect on the FTIR spectra, as demonstrated when real biogas and the two reference gases are compared: synthetic biogas with nitrogen as a carrier provided the highest siloxane readings, and real biogas provided the lowest, and closest to the GC-MS results, indicating a negative bias when in the presence of carbon dioxide.

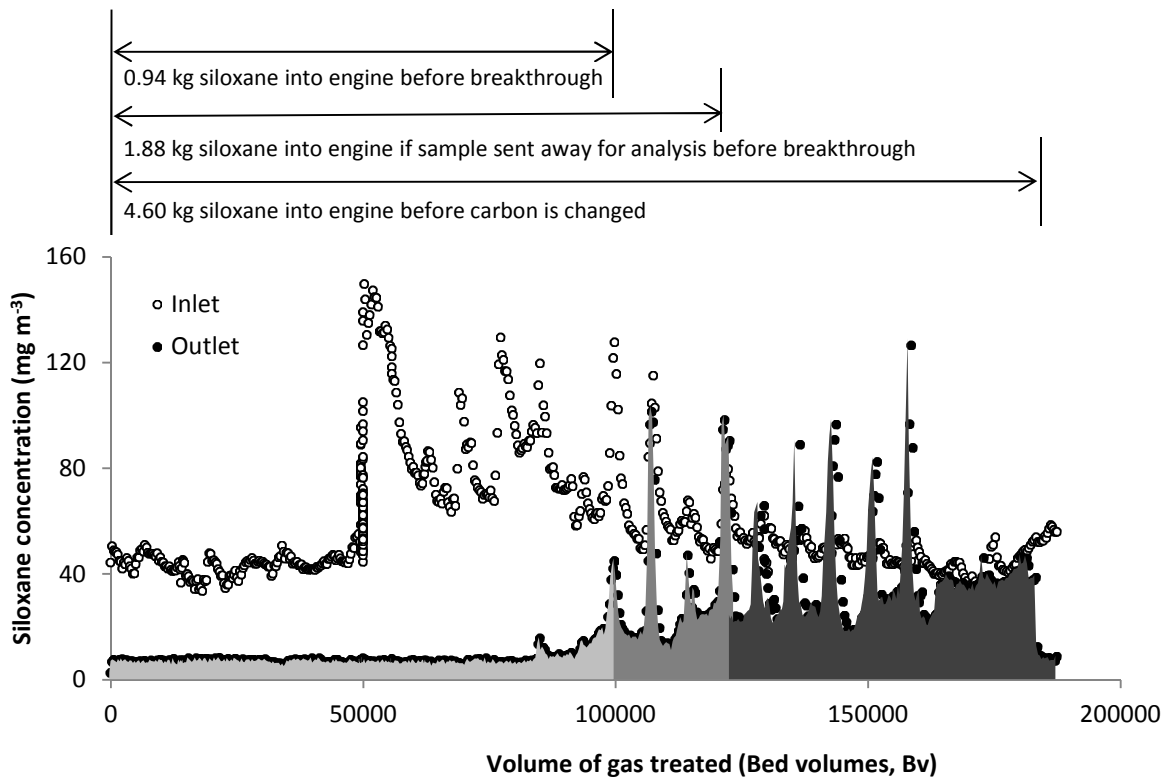


Figure 3-7. An example breakthrough curve for a carbon vessel (1.21 m³, 450 kg_{carbon}). The area under the outlet concentration graph can be used to calculate the mass of siloxane entering the engine as follows: light grey - 0.94 kg over 18 days before breakthrough; mid grey - 0.94 kg over three days after breakthrough; dark grey - a further 2.72 kg over eight days before the carbon is changed.

Carbon dioxide is known to cause interference in FTIR spectra, for example Lechner et al. (2001) found that carbon dioxide caused interference when measuring benzene in air near a paper mill. The proportions of the bulk gases in biogas are relatively stable (Rasi et al., 2010), so it is straightforward to carry out a correction to account for the gas matrix (Marshik and Perez, 2013). This is evidenced by the good correlation between FTIR and GC-MS results in real biogas (RSME = 15.7%, Figure 3-5a) which indicates that the bulk gases caused a linear interference which can be compensated for by adjusting the calibration. To find the absorbance spectrum of D5, nitrogen was used as a carrier in the reference gas. Nitrogen is a homonuclear diatomic molecule and therefore does not absorb infrared radiation (Stuart, 2004). When carbon dioxide was used as the carrier gas, the FTIR siloxane concentration readings were lower (Figure 3-4). The effect of bulk gases depends on the temperature and pressure in the gas cell and on the relative sizes of the target and matrix molecules (Marshik and Perez, 2013), so finding a negative bias is not uncommon (e.g. (Lorberau, 1990; Williams et al., 2014)). Methane will also affect the FTIR readings, and so the spectrometer has been calibrated assuming a mixture of methane and carbon dioxide as the gas matrix (resulting in the reference gas readings appearing high).

The presence of other trace gases also hinders siloxane quantification. Non-target VOC species containing aliphatic =C-H bonds and/or aromatic C-H bonds (which absorb infrared radiation in the region $1000-600\text{ cm}^{-1}$ and $900-690\text{ cm}^{-1}$ respectively, Table 3-3) cause positive interference as these absorbance regions overlap with the regions analysed by the FTIR spectrometer to quantify siloxanes. Positive interference from similar species is common in FTIR analysis, for example Lechner et al (2001) could not differentiate between different alcohols, acetates and methyl-alkanes in air from the production hall of a recycling centre and Li et al. (2002) showed that the characteristic peaks of chloroform, methylene chloride and acetone overlapped, requiring a more complex analysis to separate the species.

Table 3-4. Comparison of total siloxanes measured in real biogas samples using a variety of sampling and analytical procedures.

Gas	Total Siloxanes (mg m ⁻³)	On-line analysis	Calibration	Verification	Reference
Landfill Digester	1.6-7.9 ^a 0.1-1.3 ^b 0.2-4.3 ^c 2.5-29.6 ^a 4.5-27.1 ^b	Portable GC-PID Perkin Elmer Photovac Voyager (Speciated Siloxanes)	Reference gases from liquid standards (L2,L3,L4,D3,D4,D5) injected via syringe pump into a nitrogen flow using a Gasmet™ calibrator. LOD = 0.01 ppm.	ATD-GC-MS (Perkin Elmer ATD400, HP5890/HP5972) Range (L2,L3,L4,D3,D4,D5) Standards prepared in methanol and preloaded onto Tenax TA adsorbent tubes Results obtained by direct GC measurement (GC-PID) higher than ATD-GC-MS. Some conformity noted. D4 around 10% difference; D5 comparable for concentrations >1-2 mg m ⁻³	Arnold and Kajolinna, 2010
Landfill Digester	4.9 ^{a,d} 4.6 ^{c,d} 20.2 ^{a,d} 8.4 ^{c,d} 11.5 ^{b,d}	GC-MS Bruker 451 GC/Scion SQ MS used with multi stream selector valve for automated switching between sample, standard, blank (hydrophobic mixed bed adsorbent trap) (Speciated Siloxanes)	Standards generated on demand with Dynacal® permeation tubes and a Dynacalibrator® calibration gas generator with N ₂ as dilution gas. LOD = 0.08 ppbv for D5.	None stated	Bramston-Cook and Bramston-Cook, 2012
Digester	32.2±13.3 ^a 25.5±11.4 ^b	FTIR VA-3001S, Osaka Gas Engineering (Total siloxanes)	Use of D4 Standard Gas 42.5ppmv/N ₂ prepared by Sumitomo Seika Chemicals Co. Level of determination = 0.6 mg m ⁻³ .	GC-MS (HP6890/HP5973) Range (L2,L3,L4,D3,D4,D5,D6) Close correlation identified between FTIR and GC-MS in both model biogas and real biogas	Oshita et al., 2010
Digester	87.7 ^{b,e} 13.4 ^{c,e}	FTIR Thermofisher Antaris IGS (Cyclic/linear siloxanes)	Reference gas from liquid standard (D5) produced from controlled volatilisation into CO ₂ / N ₂ flow. LOD = 3.2 mg m ⁻³ .	Tedlar bag samples loaded onto Tenax tubes and measured used GC-MS. Close correlation identified between FTIR and GC-MS. RMSE = 9.8 mg m ⁻³ (9.7%) and 1.5 mg m ⁻³ (48%) respectively for real biogas from upstream and downstream of a carbon vessel. Primary reference gas (110 mg _{D5} m ⁻³ _{CH4}). 4% error.	This study

^aTotal siloxanes; ^bD5 concentration. ^cD4 concentration. ^dUnits are ppmV. ^eMean based on initial speciation by GC-MS.

In this study sixteen potentially interfering species were identified in biogas at the case study site (Figure 3-6). The VOC concentrations relative to the concentration of D5 were higher in the sample taken from downstream of a carbon vessel ($9.7 \text{ mg}_{\text{VOC}} \text{ mg}_{\text{D5}}^{-1}$ downstream compared to $5.5 \text{ mg}_{\text{VOC}} \text{ mg}_{\text{D5}}^{-1}$ upstream, Figure 3-6), and it is postulated that is the interference caused by this higher VOC/siloxane molar ratio that leads to high FTIR readings downstream (Figure 3-5b) and a greater RSME (147%) downstream than upstream. Whilst analysis of VOCs was not undertaken in their study, Oshita et al. (2010) also suggested positive interference from VOCs to explain the high readings their on-line FTIR gave when used on real biogas. The strength of the correlation between the GC-MS results and FTIR readings for the synthetic gas (which does not contain VOCs) (Figure 3-4) is further evidence that VOCs are responsible for the higher error relative to that observed in the reference gas. It is possible to carry out spectral corrections to allow for interference (Li et al., 2002), but it is necessary to identify all the interfering species (Ruyken et al., 1995), making this a potentially formidable task when applied to biogas, so instead, in this study, the analysis method was changed. The infrared spectra generated from real biogas were reanalysed using a partial least squares (PLS) regression method instead of classical least squares (CLS), as PLS is considered to be more effective for complex mixtures (Stuart, 2004). The PLS method also incorporated a new region of the infrared absorbance spectrum: $1114.65 - 991.23 \text{ cm}^{-1}$ which includes the resonance frequency of the Si-O-C bond stretching. The Si-O bond absorbs infrared radiation strongly (Stuart, 2004; Coates, 2000) resulting in a tall absorbance peak (Figure 3-1a), making quantification easier. The systematic error in readings from real biogas both upstream and downstream of the carbon vessels was reduced by more than 50%. The PLS method is therefore able to achieve a limit of detection of 3.2 mg m^{-3} . This is below the siloxane limits set by CHP engine manufacturers: 6 mg m^{-3} (Deutz), 12 mg m^{-3} (Jenbacher, Caterpillar) and 30 mg m^{-3} (Waukesha). FTIR is therefore capable of demonstrating compliance with these limits, evidencing the industry relevance of this method. There may be potential for

further improvement of the LOD: using standard dilutions of siloxanes in methane and diluted digester biogas Marshik and Zemek (2012) achieved a LOD of 300 – 500 ppbv using an FTIR spectrometer. Since they used diluted biogas, the interferences from VOCs were reduced compared to the biogas used in this study, but this indicates the potential limit of the precision that may be achieved using FTIR spectrometry. Further improvement of the LOD of the spectrometer used in this study, could be achieved through analysis of further gas samples across a greater concentration range and refinement of the PLS method.

At £50,000 (including multi-sampling-point installation), an FTIR spectrometer is a large capital investment for a water utility, but it can provide great cost savings (Table 3-5). By replacing daily bag sampling, £36,500 per year can be saved (giving a payback period of 16 months). However the most significant savings are due to improvements in engine protection and carbon bed management. At the case study sewage treatment works, carbon bed replacement frequency is independent of siloxane data, and the beds are currently replaced every four weeks. Using on-line siloxane analysis to capture siloxane breakthrough, it was observed that whilst the carbon bed was operated for 29 days, breakthrough occurs after two weeks, and the siloxane concentrations subsequently exceed the engine manufacturer's limit, so carbon replacement is required. Replacing the carbon every two weeks instead of every four weeks could reduce the mass of siloxane which enters the CHP engines by up to 80% (Figure 3-7). By reducing the damage caused by siloxanes to the engines, extra maintenance requirements (beyond the normal maintenance schedule) can be reduced or eliminated. The savings in maintenance costs (£307,000) are greater than the cost of the extra carbon required (£70,000 per year) leading to a net saving of £328,000 per year for the case study sewage treatment works compared to the current scenario (Table 3-5). This leads to a payback period of two months for the FTIR spectrometer.

Table 3-5. Costs of siloxane monitoring and removal and CHP engine maintenance (estimated considering a carbon vessel containing 3000 kg of carbon protecting five 1MW CHP engines).

Scenario	No gas treatment		Carbon beds changed every four weeks		Carbon beds changed after breakthrough using FTIR		
	Cost	Frequency	Annual cost	Frequency	Annual cost	Frequency	Annual cost
Siloxane monitoring^a							
Bag sampling	£100	Daily	£36,500	Daily	£36,500	-	-
FTIR service	£1,500	-	-	-	-	Annual	£1,500
Siloxane removal system^a							
Replace GAC (3000 kg virgin GAC)	£5,052	-	-	700 hours	£63,000	400 hours	£110,000
Replace GAC (delivery/labour)	£3,000	-	-	700 hours	£39,000	400 hours	£62,000
Engine maintenance^b							
Service	£225,000	5000 hours	£390,000	9000 hours	£220,000	20000 hours	£100,000
Decoke	£50,000	nd	nd ^c	3000 hours	£150,000	9000 hours	£50,000
Oil change	£7,500	250 hours	£260,000	500 hours	£130,000	1500 hours	£44,000
Spark plugs	-	500 hours	£15,000	1200 hours	£6,000	1500 hours	£5,000
Engine operation^b							
Downtime	£80,000 per week	5 weeks per year	£400,000	1 week per year	£80,000	0.3 weeks per year	£24,000
Total			£1,251,500		£724,500		£396,500
Annual saving (compared to no treatment)			-		£527,000		£855,000
Annual saving (compared to bag sampling)			-		-		£328,000
Payback period for FTIR spectrometer	£50,000		-		-		2 months

nd = no data. ^aCosts based on case study sewage treatment works (Griffiths, 2012). ^bCosts estimated using data for Santa Cruz case study from Tower and Wetzel (2006) – pre-treatment cost, post-treatment low estimate and post-treatment high estimate. ^c£150,000 per annum used in total cost calculation. Biogas revenue is £0.19 m⁻³ (Read and Hofmann, 2011).

3.5 Conclusions

This study presents the first use of on-line Fourier transform infrared spectrometry to measure siloxanes in biogas both upstream and downstream of an activated carbon vessel at a full scale sewage treatment works. Excellent linearity was found when on-line FTIR spectroscopy and laboratory GC-MS results in synthetic reference gas were compared and good linearity was found for real biogas samples upstream of the carbon vessel. Positive interference from VOCs limited precision in downstream gas samples, but introducing a partial least squares methodology to analyse the infrared spectra led to a limit of detection of 3.2 mg m^{-3} being achieved. It is anticipated that the RMSE can be improved through greater data density to help refine the PLS analysis. Importantly, the limit of detection is below the siloxane target set by engines manufacturers, which evidences that FTIR is industry relevant. Whilst savings are provided over classical sampling and analysis routes, it is the improved carbon management that FTIR analysis can facilitate which leads to the greatest economic return. This is estimated to be $\text{£}0.007 \text{ kWh}^{-1}$, or 50% of the estimated associated cost of siloxane damage.

3.6 Acknowledgements

The authors would like to thank Thermo Scientific (Madison, WI), in particular J. Roberts, S. Halsey and M. Arrowsmith, for their assistance with the calibration of the FTIR spectrometer.

4 On-line management of siloxane breakthrough in carbon contactors using changepoint detection

C.A. Hepburn^a, A. Daneshkhah^a, N.J. Simms^b, E.J. McAdam^a

^aCranfield Water Science Institute, Cranfield University, Cranfield, Bedfordshire, MK43 0AL, UK

^bCentre for Power Engineering, Cranfield University, Cranfield, Bedfordshire, MK43 0AL, UK

Abstract

Siloxanes cause around £70,000 of damage per annum per MW of engine capacity installed for producing electricity from biogas. Pre-treatment of biogas to remove siloxanes using activated carbon is therefore typically practiced to ensure economic utilisation. Carbon vessel performance is currently determined by discrete sampling followed by siloxane analysis at an external laboratory, making refined process control difficult to achieve. This paper introduces the use of on-line siloxane detection to enhance the rate and intensity of data acquisition. Importantly siloxane breakthrough curves within this paper identified that upon approaching carbon media exhaustion, a set-point breakthrough concentration of 30 mg m^{-3} was reached within a short time frame. Consequently, changepoint analysis was evaluated as a method to predict the onset of breakthrough through probabilistic analysis. Baseline breakthrough data was collated from carbon vessels that exhibited both broad-fronted and sharp-fronted breakthrough profiles. When applied to broad-fronted profiles, changepoint analysis identified breakthrough between 25 and 45 hours before the set-point. However, for carbon vessels characterised by sharp fronts, discrimination was difficult to ascertain. At full scale, it is recommended that carbon vessels should be designed for higher Reynold's numbers which enable broad-fronted breakthrough profiles. In this case, probabilistic changepoint detection methods facilitated by on-line analysis provide sufficient process lag time to enable duty/standby switchover before the critical set-point is reached.

Keywords: *Adsorption; CHP; FTIR spectroscopy; GAC; Landfill; Silicon*

4.1 Introduction

Biogas produced through anaerobic digestion of sewage sludge (47-65% methane, Rasi et al., 2007) is a valuable energy resource and potential revenue stream for water utilities. To illustrate, in 2013 Severn Trent Water had 40 MW capacity in combined heat and power (CHP) engines installed over 35 sites (Severn Trent Water, 2013a) which were used to generate 23% of their annual electricity demand (Severn Trent Water, 2013b). In addition to methane and carbon dioxide, biogas contains a number of trace gases (0-200 ppmv), some of which are detrimental to the economic utilisation of this resource. Volatile methyl siloxanes are one such group of contaminants which, when combusted in CHP engines, form hard microcrystalline silica, causing damage to the engines which contributes up to 80% of maintenance costs (Lemar, 2005). Consequentially, some engine manufacturers have introduced siloxane concentration limits for biogas entering engines.

To achieve the proposed warranty limits imposed by engine manufacturers, pre-treatment of the biogas is required. At present, best practice is considered to be adsorption of siloxanes onto activated carbon (Ajhar et al., 2010a). There is currently no preferred configuration for activated carbon vessels, thus the simplest systems comprise a single carbon vessel. Once the carbon is saturated with siloxanes, the gas flow is stopped (or bypassed to enable continuous engine operation) and the spent carbon is replaced. Duty-standby systems have also been installed at larger scale plants (Tower and Tower, 2007; Tower, 2003) which enable continuous gas treatment (and hence continuous engine operation) through switching between vessels once the carbon in the duty vessel is saturated. To establish the carbon replacement frequency in both configurations, the outlet must be monitored for siloxanes to determine breakthrough. Grab sampling followed by gas chromatography – mass spectrometry (GC–MS) analysis at an external laboratory is the most commonly used method of siloxane measurement (Ajhar et al., 2010b; Tower and Tower, 2007). However breakthrough occurs over reasonably short timescales in gas phase carbon vessels owing to high mass transfer rates and a short mass transfer zone (Cooney, 1999). Consequentially, grab sampling does not give satisfactory data density (Hepburn et al., in preparation). In addition, there

is a lag time between sampling and receiving the results (Hepburn et al., in preparation), thus siloxanes are currently observed to breach the GAC bed and enter the CHP engine. Arnold and Kajolinna (2010), Bramston-Cook and Bramston-Cook (2012) and Oshita et al. (2010) introduced on-line analysis to ascertain to first complete characterisation of siloxanes in biogas. More recently, Hepburn et al. (in preparation) demonstrated the use of on-line Fourier transform infrared spectrometry to evaluate activated carbon vessels for siloxane removal. On-line analysis provides multiple readings per hour and allows siloxane breakthrough curves to be constructed with sufficient data density to pinpoint the onset of breakthrough which often occurs within an hour. With high data densities now attainable, statistical methods, such as changepoint detection, can be used to provide process control by not only determining breakthrough in a timely manner but also predicting the onset of breakthrough and providing time for an operational response before breakthrough is reached. Early changepoint detection methods originated from analysing quality control data, where the goal was to monitor the output of manufacturing processes and detect faults as quickly as possible (Lai, 1995). Since then, changepoint detection techniques have been used in a wide range of fields including genetics, medicine, computer science, reliability analysis, economics and finance. Other researchers have applied changepoint detection algorithms to processes in the water industry. For example, Jeison and van Lier (2006) used Cao and Rhinehart's R statistic (1995) to detect cake-layer formation in anaerobic membrane bioreactors by monitoring trans-membrane pressure. The aim of this study is to evaluate the value of changepoint detection as a real-time analytical method that can provide early detection of breakthrough to allow effective carbon vessel management in siloxane removal from biogas. The objectives are to: (i) use purpose built on-line Fourier transform infrared (FTIR) spectrometry to establish breakthrough profiles for carbon vessels; and, (ii) design and test a changepoint detection algorithm to establish its suitability for process control optimisation.

4.2 Materials and Methods

4.2.1 The FTIR spectrometer and case study site

The FTIR spectrometer used was an Antaris Industrial Gas System (ThermoFisher, Waltham, MA) with a 2 m path length. The spectrometer was installed at a large UK sewage treatment works which treats sewage sludge from 2.5 million population equivalents, producing around $3400 \text{ m}^3 \text{ h}^{-1}$ of biogas. The biogas is utilised in CHP (combined heat and power) engines onsite giving a total electrical power of approximately 8 MW. Seven GAC (granular activated carbon) vessels of four different designs are used to remove siloxanes in a pre-treatment step. Gas sampling ports are located upstream and downstream of each GAC vessel and the FTIR spectrometer was set to give one reading per port per hour. The limit of detection and accuracy provided by the manufacturer are 7 mg m^{-3} and 10%. Cyclic siloxane data measured in real biogas using the FTIR were compared to data provided using a UKAS accredited GC-MS method on comparable samples. The method comparison presented a linear response within 95% confidence limits (Hepburn et al., in preparation).

4.2.2 The changepoint detection algorithm and calculations

To maximise the time available for a process action to take place, breakthrough of a carbon bed should be identified as early as possible. This type of changepoint detection problem is known as a sequential problem, as the observations (siloxane concentrations) are received and processed over time. After receiving each observation, a decision needs to be made about whether a change has occurred based only on the observed data which have been received so far. The following setting for the observed data is assumed:

$$X_i \sim \begin{cases} F_0 & \text{if } i \leq \tau_1 \\ F_1 & \text{if } \tau_1 < i \leq \tau_2 \\ F_2 & \text{if } \tau_2 < i \leq \tau_3 \\ \dots & \dots \end{cases} \quad (4-1)$$

where X_i is the variable of interest, F_0 is the probability distribution function on the first segment, F_1 is the probability distribution function on the second segment and

so on; and τ_1, τ_2 , etc denote the unknown change points. It is usually assumed that the observations are independent between every pair of change points so that the distribution of the sequence can be written as above.

We first present the methodology for the problem of testing whether a change occurs immediately after some specific observation k . This problem is reduced to choosing between the following two hypotheses:

$$H_0 : X_1, \dots, X_n \stackrel{iid}{\sim} F_0(x; \theta_0) \text{ vs. } H_1 : X_i \sim \begin{cases} F_0(x; \theta_0) & i = 1, 2, \dots, k \\ F_1(x; \theta_1) & i = k + 1, \dots, n \end{cases} \quad (4-2)$$

where θ_0 is the unknown parameters of the distribution chosen based on the first k observations (or the distribution on the first segment) and θ_1 represents the unknown parameters of the distribution on the second segment after a change point has been identified, n is the total number of observations, and k indicates the change point index.

To choose between these two hypotheses, a suitable statistic or criterion (denoted by $D_{k,n}$) must be selected, and after computing its value if $D_{k,n} > h_{k,n}$ for some appropriately selected threshold $h_{k,n}$ then it can be concluded that a change point has occurred following the k^{th} observation. This threshold is normally selected to bound the Type 1 error value which is a standard method in statistical hypothesis testing. In this framework, α is a fixed value (e.g. $\alpha = 0.05$) and known as an acceptable level for the proportion of false positives. In other words, α can be considered as the probability of falsely declaring that a change has occurred if in fact no change has occurred. Then, $h_{k,n}$ will be determined as the upper quartile of the distribution of $D_{k,n}$ under the null hypothesis. Since the location of change point is not known in advance, $D_{k,n}$ is assessed for every value of $k=1,2,\dots,n$, and the best estimate of the change point location is obtained by maximising the chosen statistic (Ross et al., 2011), that is:

$$\hat{\tau} = \arg \max_k D_{k,n} \quad (4-3)$$

The test statistic $D_{k,n}$ should be chosen depending on distribution of the observed data. For instance, if the observations are normally distributed, a two sample Student

t-test would be a suitable statistic. Non-parametric test statistics, such as the Mann-Whitney, Kolmogorov-Smirnov, or Cramer-von-Mises, may also be used to avoid making or checking any distributional assumptions (Ross et al., 2011). In this paper, the Mann-Whitney U-test is used.

The method described above can be simply extended to sequential change point identification where new observations are received over time. When a new observation x_t is received, the method described above can be applied to the following sequence of data, x_1, x_2, \dots, x_t by computing an appropriate test statistic D_t , and check whether a change has been occurred. If no change is detected, the next observation x_{t+1} is received, and similarly checked to see whether a change has occurred following receiving the new observation. The threshold, h_t should be chosen so that the probability of incurring a Type I error is constant over time (Ross et al., 2011; Ross, 2013).

4.3 Results and discussion

4.3.1 Changepoint detection for broad-fronted breakthrough curves

Breakthrough curves were found to conform to two profiles: broad-fronted and sharp-fronted. For the first 200 – 400 hours of bed operation (before breakthrough), the siloxane concentration is in a pseudo-steady state around 7 mg m^{-3} . As breakthrough occurs, broad-fronted curves exhibit a gradual rise (over around 300 hours) of the baseline siloxane concentration until it equals the inlet concentration. This is overlaid by a series of sharp concentration spikes, corresponding to spikes in the inlet concentration (Figure 4-1a), which occur at the outlet because there is no longer sufficient adsorption capacity to cope with high siloxane concentrations as the mass transfer zone reaches the end of the bed (Crittenden and Thomas, 1998). After breakthrough, the outlet concentration tracks the inlet concentration and the exhausted carbon bed provides no engine protection. Broad-fronted curves were presented by carbon vessels operated in the transitional regime ($Re > 40$ (Chilton and Colburn, 1931)).

In an example broad-fronted breakthrough curve (Figure 4-1a), the siloxane concentration first exceeds the set-point (30 mg m^{-3} , Wauksha siloxane warranty

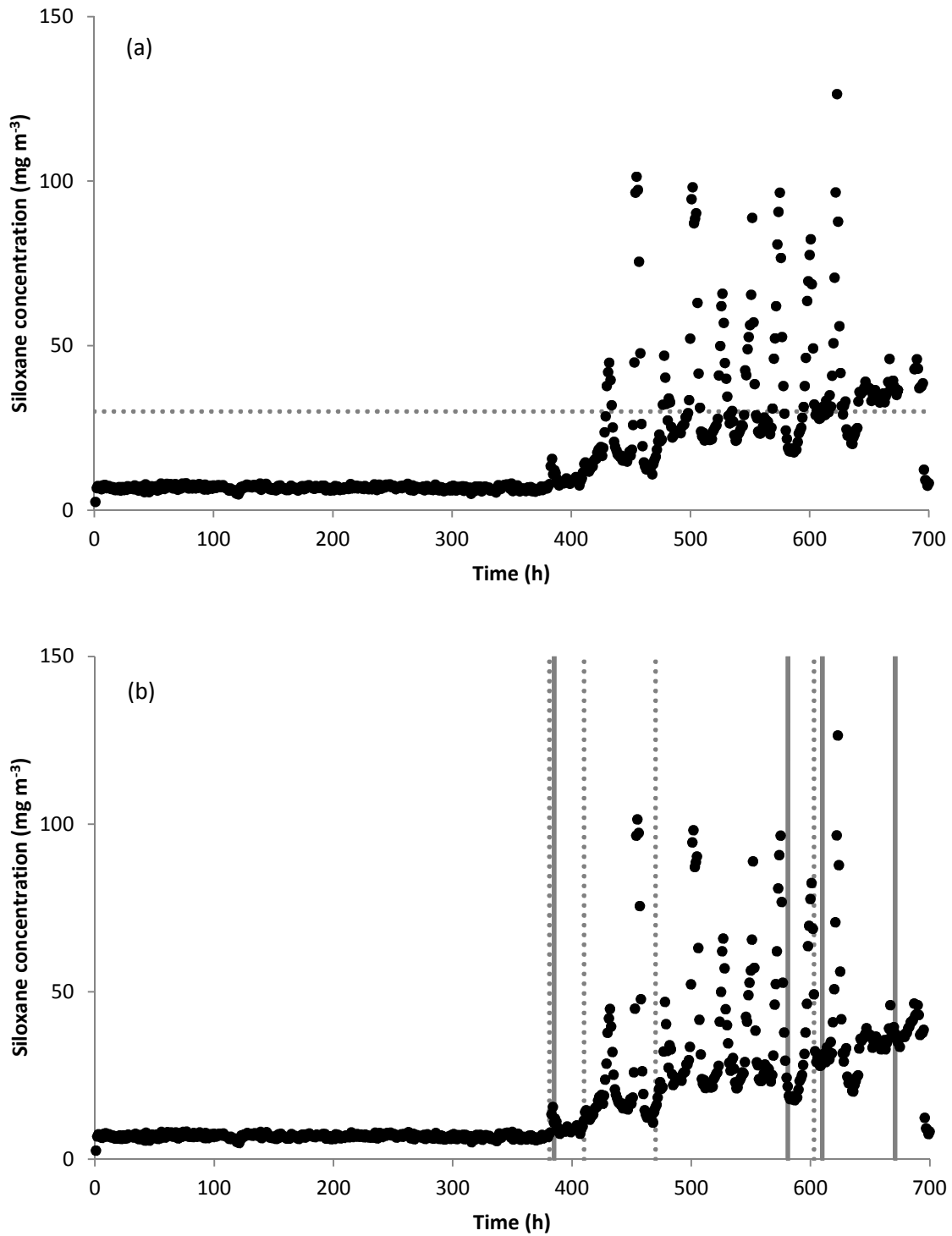


Figure 4-1. A broad-fronted breakthrough curve with (a) Waukesha siloxane limit (30 mg m⁻³) superimposed (dotted line) and (b) showing changepoints detected by changepoint detection algorithm (dotted lines) and the time at which the changepoint was detected (solid lines).

limit) after biogas has been passed through the carbon vessel for 430 hours. The changepoint detection algorithm (Figure 4-1b) shows that a changepoint occurred earlier, after 381 hours. This changepoint was detected after 385 hours, giving an early warning time of 45 hours (compared to using the set-point), ample time to switch vessels in a duty-standby system. The changepoint detection algorithm trigger time (detection time for the first changepoint) and the time at which the siloxane concentration exceeds 30 mg m^{-3} for three broad-fronted breakthrough curves are compared in Figure 4-2 and Table 4-1. In all cases the changepoint detection algorithm was triggered before the siloxane concentration exceeded 30 mg m^{-3} , giving early warning times of 45, 25, and 159 hours respectively. The particularly long early warning period of 159 hours was achieved because in this case the inlet concentration was relatively low and stable ($40 - 60 \text{ mg m}^{-3}$) during the period of breakthrough (400 – 600 hours) so initial concentration spikes did not exceed the 30 mg m^{-3} threshold.

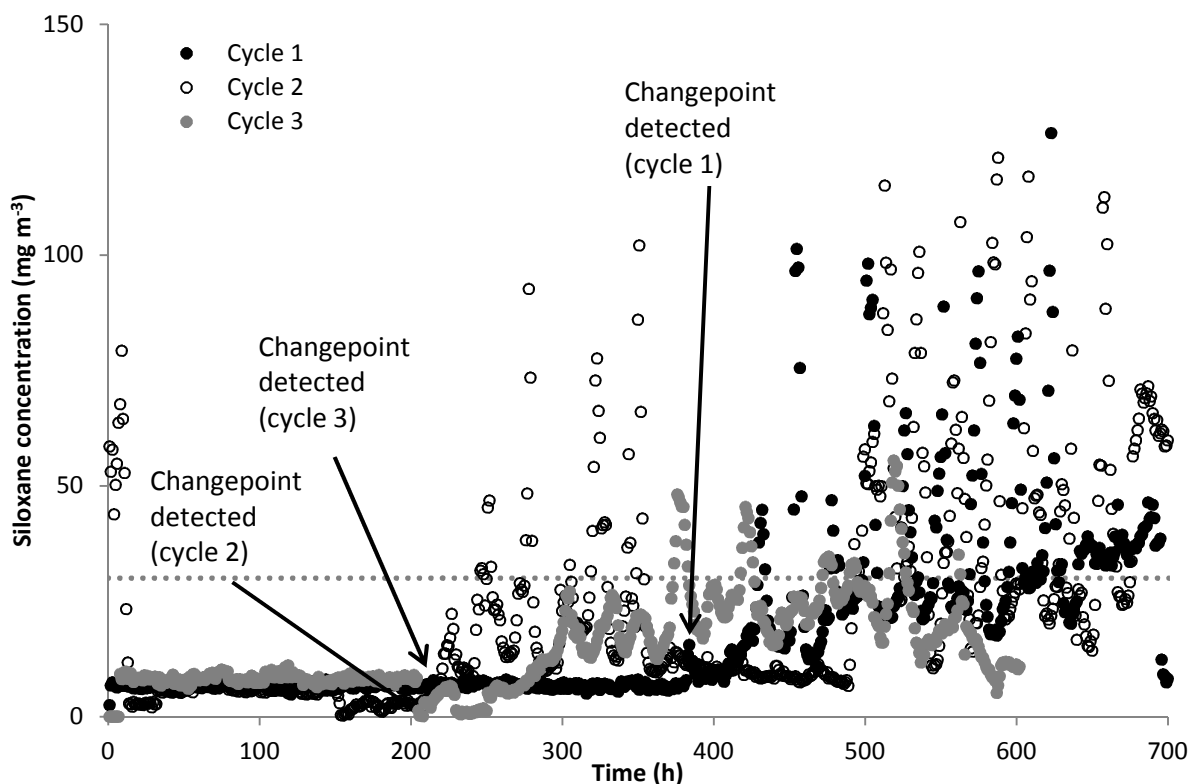


Figure 4-2. Three breakthrough curves from vessels exhibiting broad-fronted profiles. The Waukesha siloxane limit (30 mg m^{-3}) is superimposed (dotted line) and for each curve the detection time of the first changepoint is labelled.

4.3.2 Change point detection for sharp-fronted breakthrough curves

Sharp-fronted breakthrough curves exhibit a sudden, sharp rise in concentration from the baseline concentration to the inlet concentration in six hours or less (Figure 4-3a). Sharp-fronted curves were presented by carbon vessels operated in the laminar regime ($Re < 40$ (Chilton and Colburn, 1931)). In the laminar regime, Taylor-Aris axial dispersion causes self-sharpening behaviour (Cussler, 2009) resulting in a short mass transfer zone and sharp breakthrough curve.

In the example sharp-fronted breakthrough curve (Figure 4-3), the siloxane concentration exceeded the 30 mg m^{-3} set-point after 258 hours. The change point detection algorithm shows a change after 255 hours, which is detected after 259 hours – providing no early warning. (The change point at 13 hours is ignored since it occurs too early to reasonably expect breakthrough to occur.) In a comparison of three sharp-fronted breakthrough curves (Figure 4-4, Table 4-2), the change point detection algorithm is twice triggered by a change in the baseline siloxane concentration that is not related to breakthrough (giving “early warning” times of 377 and 372 hours). When such false triggers are ignored, the change points are all detected shortly after the siloxane concentration has exceeded 30 mg m^{-3} and therefore the change point algorithm does not provide early warning compared to using the set-point.

Table 4-1. Comparison of change points and detection times to the time the warranty specification is first exceeded for carbon vessels exhibiting broad-fronted breakthrough curves.

Exhaustion cycle	Change point determination			^a Time to 30 mg m^{-3} (h)	Time from onset of breakthrough to 30 mg m^{-3} (h)
	Change point (h)	Detection point (h)	Siloxane concentration (mg m^{-3})		
1	381	385	15.54	430	48
2	153	221	10.35	246	34
3	204	208	8.99	367	147

^aWaukesha warranty specification for total siloxane concentration.

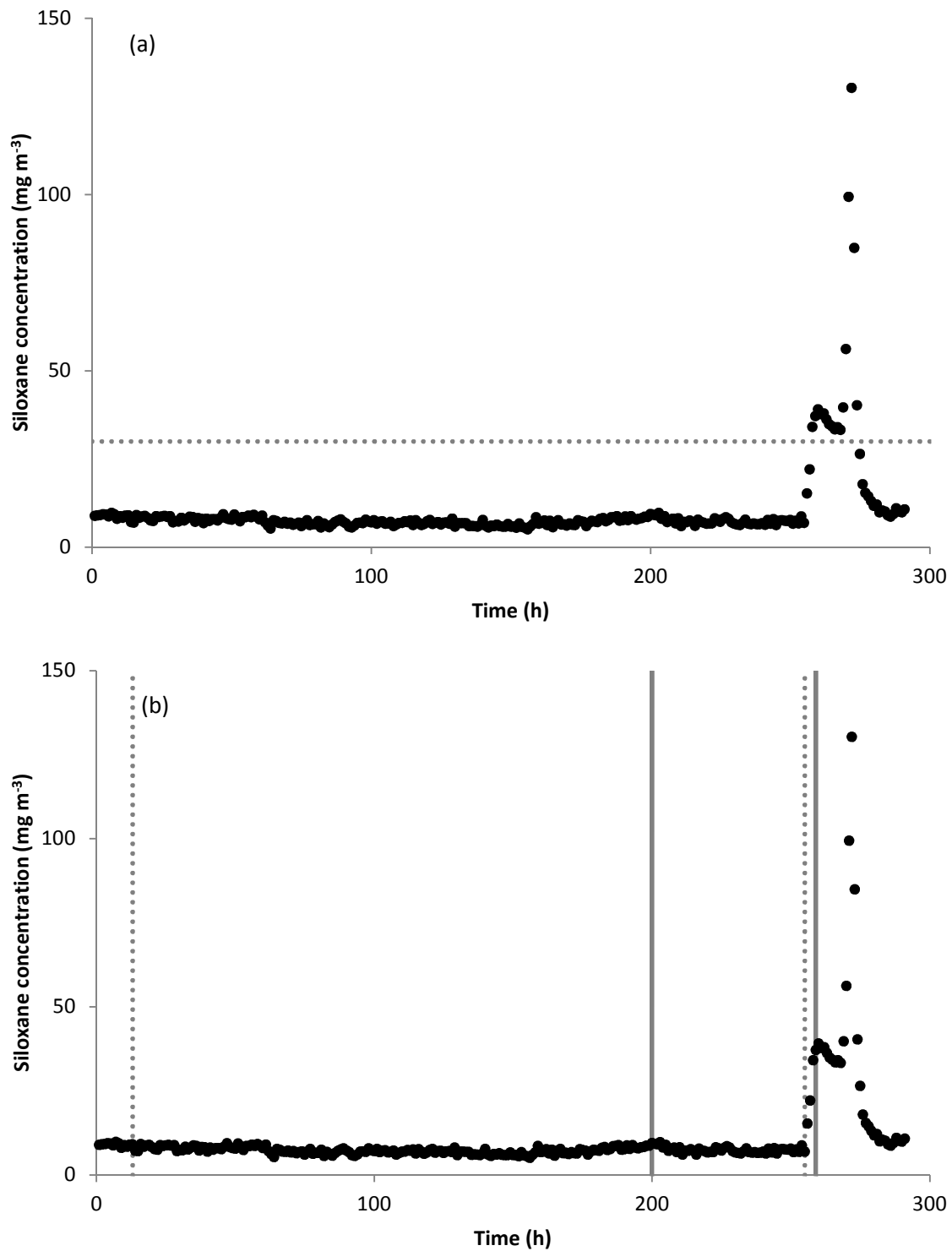


Figure 4-3. A sharp-fronted breakthrough curve with (a) Waukesha siloxane limit (30 mg m⁻³) superimposed (dotted line) and (b) showing changepoints detected by changepoint detection algorithm (dotted lines) and the time at which the changepoint was detected (solid lines).

4.3.3 Effectiveness of changepoint detection algorithm

Comparing the time at which the first changepoint is detected and the time at which the siloxane concentration limit is first exceeded for all the breakthrough curves demonstrates that the latest time the changepoint detection method is triggered is less than an hour after the set-point concentration is reached (Figure 4-5; Table 4-1; Table 4-2). This indicates that Type I errors, in which the changepoint detection method detects a change in the baseline siloxane concentration which is not related to the onset of breakthrough, dominate over Type II errors, in which the changepoint detection algorithm fails to detect the onset of breakthrough (Miller and Miller, 2005; Cao and Rhinehart, 1995). No Type II errors occurred in this study. Changing the threshold, h_t , to reduce Type I errors will result in an increase in Type II errors (Miller and Miller, 2005; Cao and Rhinehart, 1995). The cost of a Type II error, which would lead to siloxanes entering the CHP engine and causing damage, is higher than the cost of a Type I error, results in the carbon in a vessel being replaced earlier than required. Therefore the balance achieved between Type I and Type II errors is good, although further optimisation of the threshold, h_t , should result in fewer Type I errors.

A more refined approach would be to use Bayesian statistics. This method would assign a probability to each changepoint and so lower probability changepoints could be ignored. The assumption is that false positives would carry a lower probability and the changepoint at breakthrough would carry a high probability.

Table 4-2. Comparison of change points and detection times to the time the warranty specification is first exceeded for carbon vessels exhibiting sharp-fronted breakthrough curves.

Exhaustion cycle	Change point determination			^a Time to 30 mg m ⁻³ (h)	Time from onset of breakthrough to 30 mg m ⁻³ (h)
	Change point (h)	Detection point (h)	Siloxane concentration (mg m ⁻³)		
1	255	259	37.12	258	3
2	201	206	1.19	583	1
3	222	254	4.95	626	1

^aWaukesha warranty specification for total siloxane concentration.

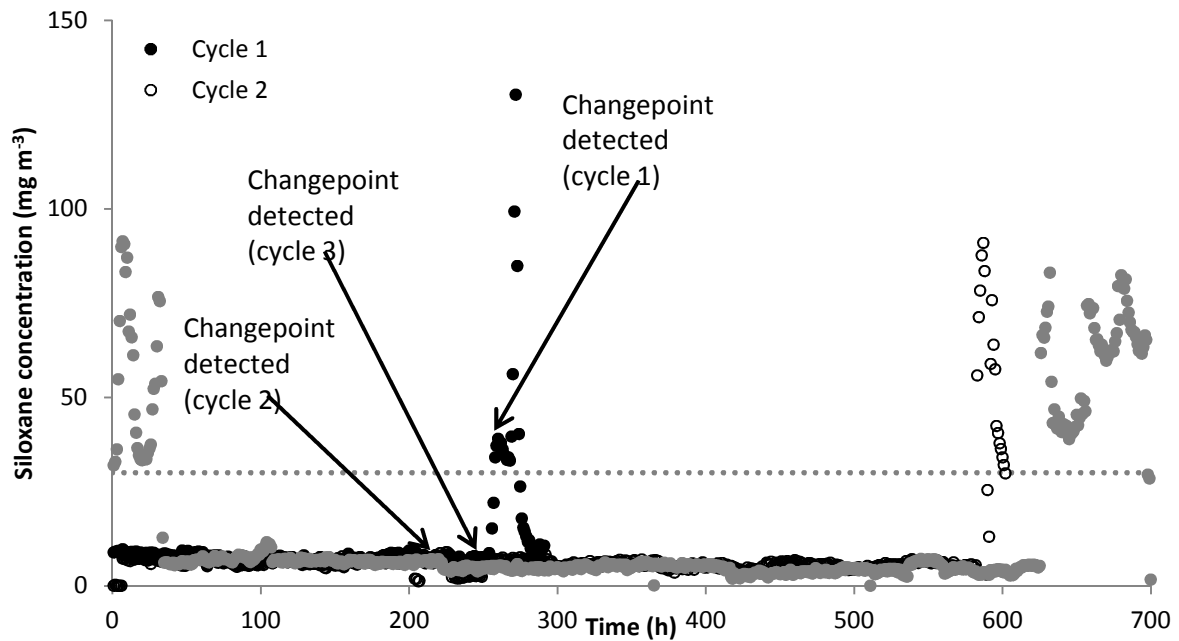


Figure 4-4. Two breakthrough curves from vessels exhibiting sharp-fronted profiles. The Waukesha siloxane limit (30 mg m^{-3}) is superimposed (dotted line) and for each curve the detection time of the first changepoint is labelled.

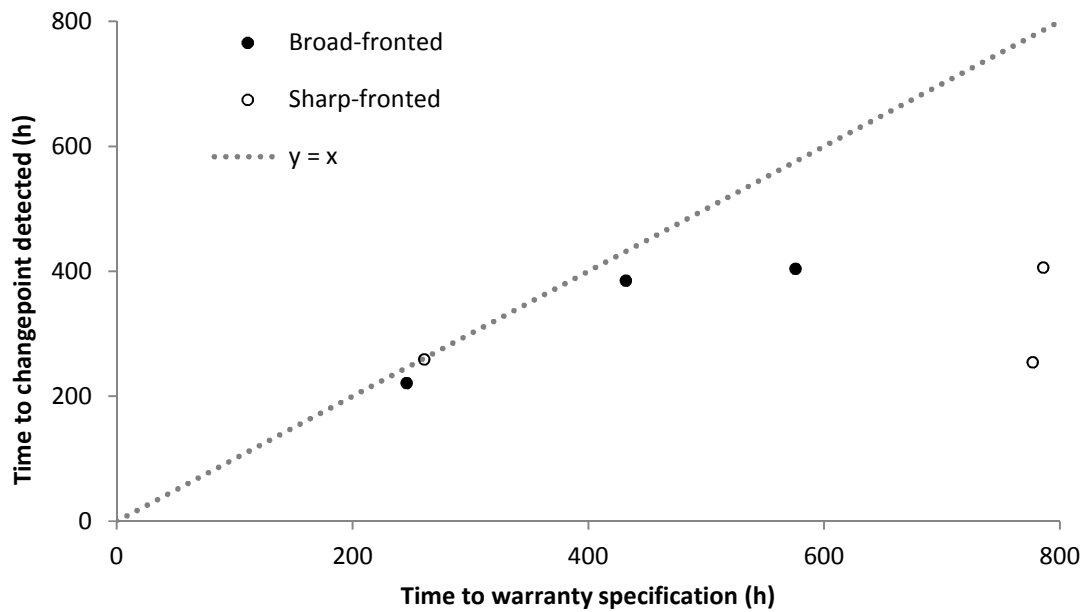


Figure 4-5. Comparison of the time taken to exceed the siloxane limit imposed by Waukesha and the time that the first changepoint was detected by the changepoint detection algorithm. $Y = x$ is shown (dotted line) to demonstrate the “early warning” potential of the change point detection algorithm.

Adams and MacKay (2007) developed a methodology for sequential changepoint detection which was successfully applied by Turner (2010) to weather satellite fault logs.

In order to apply a Bayesian method or the method used in this paper, independence between the segments of the data sets is assumed. A degree of autocorrelation exists in the data used in this study as a siloxane concentration is most likely to be similar to the previous siloxane concentration, which violates this assumption, so better results may be achieved if the data was transformed using a transformation such as Equation (4-4), or in some cases using a simpler transformation as given in Equation (4-5):

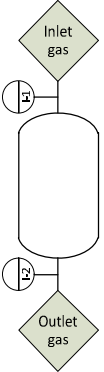
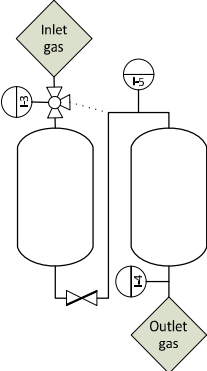
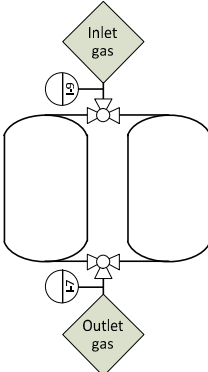
$$y_1(t) = \log(x_t) - \log(x_{t-1}) \quad (4-4)$$

$$y_2(t) = x_t - x_{t-1} \quad (4-5)$$

4.4 Implementing changepoint detection for broad-fronted breakthrough profiles

In comparison to vessels characterised by sharp fronted breakthrough profiles, a broad-fronted breakthrough profile allows more time for process intervention (such as switching between duty and standby carbon beds) before the full siloxane load passes through the exhausted carbon bed into the CHP engine. Nevertheless, the transition from pseudo-steady state to breakthrough can still occur rapidly (Figure 4-2). Deployment of changepoint detection has demonstrated that prediction of breakthrough events is possible through probabilistic analysis which provides a further lead time to prepare for process intervention. The significance of this lag time is, however, dependent upon the vessel configuration employed (Table 4-3). When comprised of a single activated carbon vessel, as installed by the Orange County Sanitation District (Pirnie, 2011) and in this study, the lag time between sampling using existing methods and receiving results (four days) coupled with the infrequency of sampling (often only once every four days) leads to a delay of 4-8 days between the onset of breakthrough and its detection.

Table 4-3. Benefits of using on-line analysis and the changepoint detection algorithm or warranty specification for different vessel layouts.

Vessel Configuration	Characterisation Method	Comment
<p>Single pass</p> 	Grab sampling and laboratory	Extensive lag time between sampling and results means breakthrough may not be detected for up to eight days, increasing siloxane load onto engine
	FTIR (set-point)	No allowance for carbon order lead time (up to a week required), leading to siloxanes passing into engine or engine downtime after breakthrough
	FTIR (changepoint)	Provides lead time (up to a week) to order replacement carbon
<p>In series</p> 	Grab sampling and laboratory	Second vessel provides buffering to cover lag time between sampling and results
	FTIR (set-point)	Second vessel provides capacity to cover lead time for carbon ordering
	FTIR (changepoint)	Algorithm provides limited benefit if siloxane concentration is measured between vessels
<p>In parallel (duty-standby)</p> 	Grab sampling and laboratory	Lag time between sampling and results means vessels switched only after siloxane breakthrough, increasing siloxane load onto engine
	FTIR (set-point)	Can be used to actuate duty-standby valve assembly. Valve actuation is slow (~ 30 minutes) to avoid pressure surges, leading to some short term siloxane loading on engine whilst switchover is completed
	FTIR (changepoint)	Provides early warning of breakthrough so valves can be actuated before siloxane warranty limit is met

Hepburn et al. (in preparation) estimated that the mass of siloxane passing into a CHP engine is doubled by operating a carbon vessel for three days after breakthrough. On-line measurement coupled with changepoint detection provides sufficient lead time (generally greater than 24 h) to procure and replace carbon before the set-point (Waukesha warranty limit) is reached which therefore maximises engine availability. When two vessels are employed in series, as described by Liang et al (2001), Wheless and Gary (2002) and in this study, siloxane concentration is best monitored between the two vessels, and following breakthrough of the first vessel, the adsorption capacity of the second vessel provides buffering capacity for procurement and delivery of fresh carbon. Consequently, changepoint detection provides little additional advantage. When two carbon vessels are connected in parallel (duty-standby setup, (Tower and Tower, 2007; Tower, 2003), on-line measurement coupled with changepoint detection enables the transition between vessels to be initiated before breakthrough which is significant as the ATEX rated valves employed to switch flow between vessels can take over 30 minutes to fully actuate to minimise pressure surge.

4.5 Conclusions

This study has demonstrated that statistical methods (coupled with on-line siloxane analysis) can be used for process control of siloxane adsorption from biogas. The changepoint detection algorithm successfully identified the onset of breakthrough in all the datasets from siloxane adsorption vessels. For broad-fronted breakthrough curves, a 25 – 45 hour early-warning of breakthrough was achieved, which is sufficient time to initiate valve actuation in a duty-standby vessel setup or shut off gas flow in a single vessel system before the siloxane warranty limit is exceeded, providing enhanced engine protection compared to grab sampling or on-line analysis alone. The application of such statistical tools is expected to be improved using a Bayesian approach to reduce the rate of false positives.

5 Characterisation of Full Scale Carbon Contactors for Siloxane Removal from Biogas using On-line Fourier Transform Infrared Spectroscopy

C.A. Hepburn^a, B.D. Martin^a, N. Simms^b, E.J. McAdam^{a*}

^aCranfield Water Sciences Institute, Cranfield University, Bedford MK43 0AL, UK

^bCentre for Energy & Resource Technology, Cranfield University, Bedfordshire MK43 0AL, UK

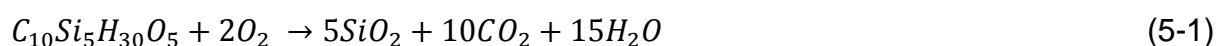
Abstract

In this study, on-line Fourier transform infrared (FTIR) spectroscopy has been used to generate the first comprehensive characterisation of full scale carbon contactors for siloxane removal from biogas. Using FTIR, two clear operational regions within the exhaustion cycle were evidenced: an initial period of pseudo steady state where the outlet siloxane concentration was consistently below the proposed siloxane limits; and a second period characterised by a progressive rise in outlet siloxane concentration during and after breakthrough. Due to the sharp breakthrough front identified, existing detection methods (which comprise field sampling coupled with laboratory based chromatographic determination) are insufficiently responsive to define breakthrough, thus carbon contactors currently remain in service whilst providing limited protection to the CHP engine. Integration of the exhaustion cycle to breakthrough identified average specific media capacities of 8.5 to 21.5 g_{siloxane} kg_{GAC}⁻¹ which are lower than has been reported for vapour phase GAC. Further speciation of the biogas phase identified co-separation of alkanes and aromatics which will inevitably reduce siloxane capacity. However, comparison of five full scale contactors identified that greater media capacity was accessible through operating contactors at velocities sufficient to diminish axial dispersion effects. In addition to enabling significant insight into gas phase GAC contactors, the use of FTIR for on-line control of GAC for siloxane removal is also presented.

Keywords: *GAC; adsorption; anaerobic digestion; landfill; CHP*

5.1 Introduction

In the UK approximately 1% of electricity produced is used to process municipal wastewater (Parliamentary Office of Science and Technology, 2007). Under pressure to reduce costs to customers, water utilities are increasingly focused on using combined heat and power (CHP) systems to generate electricity from anaerobic digester biogas to offset consumption. Currently an estimated 549 GWh_e is generated annually (DECC, 2013). However, a group of trace compounds collectively known as siloxanes are detrimental to the economic utilisation of biogas. Decamethylcyclopentasiloxane (D5) is generally regarded as the most prevalent cyclic siloxane within biogas produced from anaerobic digestion (Arnold and Kajolinna, 2010; Oshita et al., 2010) and when passed into the CHP engine it undergoes oxidation during combustion to form silicon dioxide:



Some of this SiO₂ formed is deposited within the engine (Ricaurte Ortega and Subrenat, 2009b) which causes abrasion to the engine (Schweigkofler and Niessner, 2001; Ghorbel et al., 2014), valve clogging (Accettola et al., 2008), and a reduction in conversion efficiency (Ohannessian et al., 2008). The estimated cost to industry is around 1.5p kWh⁻¹ of electricity produced or 16% of product value (Lemar, 2005). Consequently several CHP engine manufacturers have proposed limiting siloxane concentrations of between 12 and 30 mg_{siloxane} m⁻³ within the engine warranty specification. This leads to the need for siloxane removal technology to clean the biogas before injection into the CHP engine (Table 5-1).

Siloxane removal from biogas is primarily undertaken by adsorption which is presently regarded as the most viable solution (Doczyck, 2003). Granular activated carbon (GAC) is generally favoured for siloxane removal (Ajhar et al., 2010a). However, the media is non-regenerable for this application and so requires periodic

Table 5-1. Maximum silicon levels recommended by gas engine manufacturers

Company	Jenbacher	Waukesha
Silicon Specification [†] (mg/Nm ³ CH ₄)	<20	<50
Silicon Specification ^{††} mg/m ³ biogas	<12	<30

[†]as stated. ^{††}assume 60% CH₄.

media exchanges at a cost of around €2000 per change per contactor and on some biogas sites media exchange frequencies of one per week have been reported (Dewil et al., 2006). At the example site used in this study, 230,000 m³ of gas was treated by one contactor between bed changes. Consequently, the operation of siloxane removal technology is also a costly undertaking. Despite the significance of GAC contactor operation in determining the economic viability of biogas use, there remains a paucity of data in the literature on the operation of full scale GAC processes. This can be attributed to current analytical limitations where indirect methods are currently used which combine grab sampling (Ajhar et al., 2010b; Schweigkofler and Niessner, 1999) with subsequent laboratory analysis by gas chromatography. These techniques introduce a significant lag time and, due to the limited number of samples analysed, provide an incomplete description of the GAC adsorption breakthrough cycle and only a very approximate guide to the media adsorption capacity. Innovative work by Arnold and Kajolinna (2010) and Oshita et al. (2010) introduced on-line analytical methods to quantify siloxane concentration in real biogas in real-time. The authors identified that D5 was the dominant siloxane compound in biogas produced from municipal sewage sludge and also demonstrated that biogas siloxane concentration was highly transient. This has not been quantified previously due to limited data resolution. However, to date on-line siloxane analysis has not been used to characterise GAC contactor performance for siloxane removal. In this present study, we therefore use on-line Fourier transform infrared (FTIR) analysis to establish the dynamics of full scale GAC contactor operation in real time. Specifically, we seek to: (i) determine whether existing full scale GAC contactors can consistently achieve the proposed siloxane limits set out in the warranty specification; (ii) characterise breakthrough curves and determine GAC media utilisation; and (iii) compare the five full-scale GAC contactor designs to ascertain whether differences in design can improve operational performance.

5.2 Materials and Methods

5.2.1 Site description

The sewage treatment works serves 1.75 million population equivalents and also imports sewage sludge from satellite works increasing the total to 2.5 million

population equivalents. A total of sixteen anaerobic digesters produce around 3,400 m³ h⁻¹ of biogas from the sludge which is directly utilised in a CHP plant. The siloxane removal technology installed comprises seven granular activated carbon contactors of four different designs. The contactors are divided into five contactor arrangements (GAC1-5, Table 5-2) with GAC4 and GAC5 comprising contactor pairs which are operated in series to effectively double contactor length. Biogas flow is split upstream of the five contactor arrangements. As such all contactors are subject to the same feed gas composition allowing direct comparison to be made. Gas flow rates for each contactor vary by no more than 10%. Operational conditions for the contactors are shown in Table 5-3. Gas flow is upwards for all contactors with gas distribution achieved using a perforated plate. The contactors are cylindrical with heights and diameters ranging 1.6 to 2.0 m and 0.9 to 1.6 m respectively and contain between 450 and 3000 kg of carbon. The GAC media in each vessel is identical and is characterised by an approximate diameter of 4 mm and BET (Brunauer-Emmett - Teller) surface area of 782.3 m² g⁻¹ (Table 5-2). The media in each vessel is exchanged periodically with all vessels undergoing media exchange simultaneously.

5.2.2 On-line Fourier transform infrared (FTIR) analysis

The FTIR spectrometer comprised a 2 m path length (Antaris IGS, Thermo Fisher Scientific Inc, Waltham, MA). The gas cell was operated at 80°C to reduce the likelihood for condensation. The mirrors within the gas cell were coated with gold to diminish the likelihood of deposition.

Table 5-2. Design parameters of contactors and media characterisation

		GAC1/2	GAC3	GAC4		GAC5	
				Single	Pair	Single	Pair
Height	m	1.90	2.00	1.60	3.21	1.85	3.70
Diameter	m	0.90	1.05	1.60	1.60	1.53	1.53
Aspect ratio		2.11	1.90	1.00	2.00	1.21	2.42
Cross-sectional area	m	0.64	0.87	2.01	2.01	1.83	1.83
Volume	m ³	1.21	1.73	3.22	6.44	3.38	6.76
Inlet/outlet pipe diameter	m	0.15	0.18	0.20	0.20	0.25	0.25
Media mass	kg	450	500	1000	2000	1500	3000
BET surface area	m ² g ⁻¹	782.3430					
Total pore volume	cm ³ g ⁻¹	0.13950					
Total pore area	m ² g ⁻¹	205.7447					
Average pore diameter	nm	2.2022					
Particle diameter	mm	4					

Cyclic and linear siloxanes were discriminated at 798 to 817 cm^{-1} and 837 to 867 cm^{-1} respectively. Gas samples were subject to twenty scans over 120 seconds where the reported value comprised an average value from the scan. Background spectra (found by scanning with the gas cell evacuated) were subtracted from the sample spectrum. Siloxane concentrations are reported as mg m^{-3} for cyclic siloxanes, linear siloxanes and total siloxanes. The manufacturer limit of detection was stated as 7 mg m^{-3} with an accuracy of 10%. Cyclic siloxane data measured in real biogas using the FTIR were compared to data provided using a UKAS accredited GC-MS method on comparable samples. The method comparison presented a linear response within 95% confidence limits. A coarse filter was sited upstream of the instrument to protect from free water ingress and any carbon fines. Gas samples were drawn into the cell using a vacuum pump linked to a multipoint valve assembly which enabled samples to be drawn from upstream of the contactors (biogas feed) and from downstream of each contactor (six actuating ports in total). Data was therefore simultaneously collected from all contactors. Before drawing a sample into the gas cell, gas lines were purged for two minutes which was equivalent to greater than three retention times.

Table 5-3. Operational conditions used in studies contactors (mean reported, n = 5-17)

Contactor		GAC1	GAC2	GAC3	GAC4	GAC5
Media mass (kg)		450	450	500	2000	3000
Gas flowrate	($\text{m}^3 \text{h}^{-1}$)	323	258	396	408	1968
Linear velocity	(m h^{-1})	505	403	455	203	1075
EBCT	(s)	13.5	16.9	15.7	56.8	12.4
Siloxane inlet concentration (mg m^{-3})	mean	77.3	77.3	77.3	77.3	77.3
	median	64.5	64.5	64.5	64.5	64.5
	max	313.8	313.8	313.8	313.8	313.8
	min	22.9	22.9	22.9	22.9	22.9

5.2.3 Data analysis

Time to breakthrough (tb) was defined as the time at which the outlet siloxane concentration exceeded 30 mg m⁻³ for the third consecutive measurement. This concentration corresponds to the upper limit proposed within the engine warranty specifications (Table 5-1). The volume of gas treated before breakthrough V(tb) is calculated by integrating the gas flow over time:

$$V(tb) = \frac{1}{BV} \int_0^{tb} F(t) dt = \frac{1}{BV} \sum_0^{tb} F(t)(h(t) - h(t - 1)) \quad (5-2)$$

where V(t) is the cumulative gas volume (measured in bed volumes), F(t) is the flow in m³ h⁻¹ and h(t) is the hours elapsed since the previous bed change, and BV is the volume of the contactor (m³). The mass of siloxane adsorbed before breakthrough (M_{SX,ad}[tb]) was calculated by integrating the product of the siloxane concentration and the gas flow rate over time:

$$M_{SX,ad}(tb) = 10^{-6} \left[\int_0^{tb} C_{SX,in}(t) * V(t)dt - \int_0^t C_{SX,out}(t) * V(t)dt \right] \quad (5-3)$$

where M_{SX,in}(t) and M_{SX,out}(t) are cumulative masses of siloxane in kg having entered and exited the contactor at time t and C_{SX,in}(t) and C_{SX,out}(t) are the inlet and outlet concentrations of siloxane in mg m⁻³ at time t. The height of the mass transfer zone (MTZ, the zone in which adsorption takes place) in the contactors was also calculated from the breakthrough curve (Metcalf & Eddy Inc et al., 2004):

$$H_{MTZ} = Z \left(\frac{V(te) - V(tb)}{V(te) - 0.5(V(te) - V(tb))} \right) \quad (5-4)$$

where Z is the height of the contactor in meters and te is the time of exhaustion.

5.3 Results

5.3.1 Evaluation of siloxane concentration in the treated biogas

A median biogas inlet siloxane concentration of 64.5 mg m⁻³ was recorded (Table 5-3), although the inlet siloxane concentration was characterised by sharp fluctuations in concentration (Figure 5-1) with a maximum inlet siloxane concentration of 314 mg m⁻³. Whilst siloxane concentration in the feed gas

presented significant instability, a consistent outlet concentration was maintained in the early stages of the media exhaustion cycle (GAC1, Figure 5-1). The siloxane concentration in the GAC treated biogas (or leakage concentration) corresponding to the early period of the exhaustion cycle was between 7 mg m⁻³ (the limit of detection (LOD) for the FTIR) and 8.9 mg m⁻³ for all five full scale GAC contactors studied. This is below the siloxane limits proposed by several CHP engine manufacturers (Table 5-1). During this period, mean removal efficiency for all five GAC contactors was between 84.6% and 98.8%. However, in the latter stages of the exhaustion cycle, siloxane concentration increased in the treated biogas and the proposed siloxane limit was exceeded before the GAC contactors were stopped for media replacement.

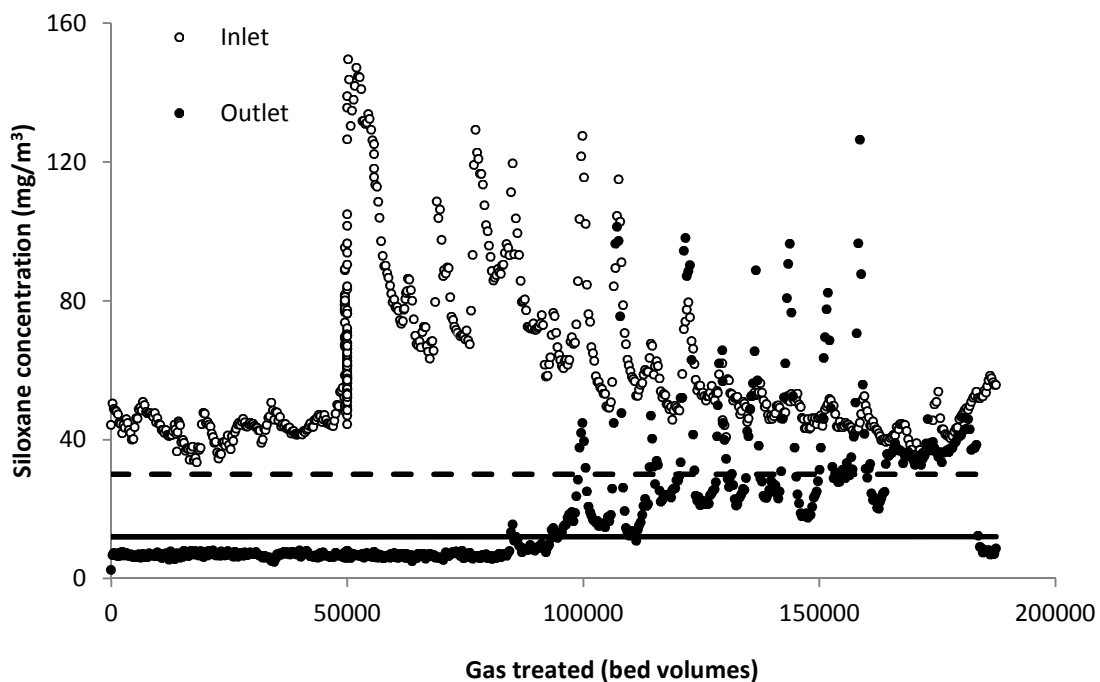


Figure 5-1. Inlet and outlet siloxane concentrations for one of the carbon contactors during a single exhaustion cycle (run time, 706 h between media changes). The solid and dashed lines represent the Jenbacher and Waukesha siloxane limits.

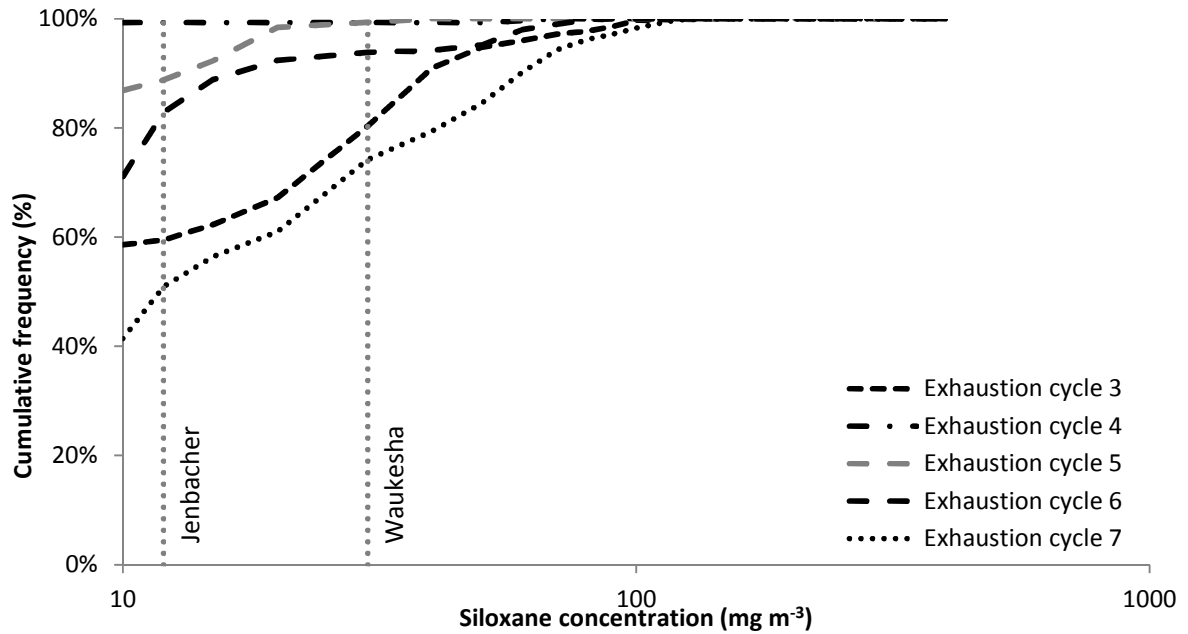


Figure 5-2. Cumulative frequency curves developed using outlet siloxane data from GAC 1 to ascertain conformity to proposed warranty specification (Table 5-1). Data is provided from five consecutive exhaustion cycles.

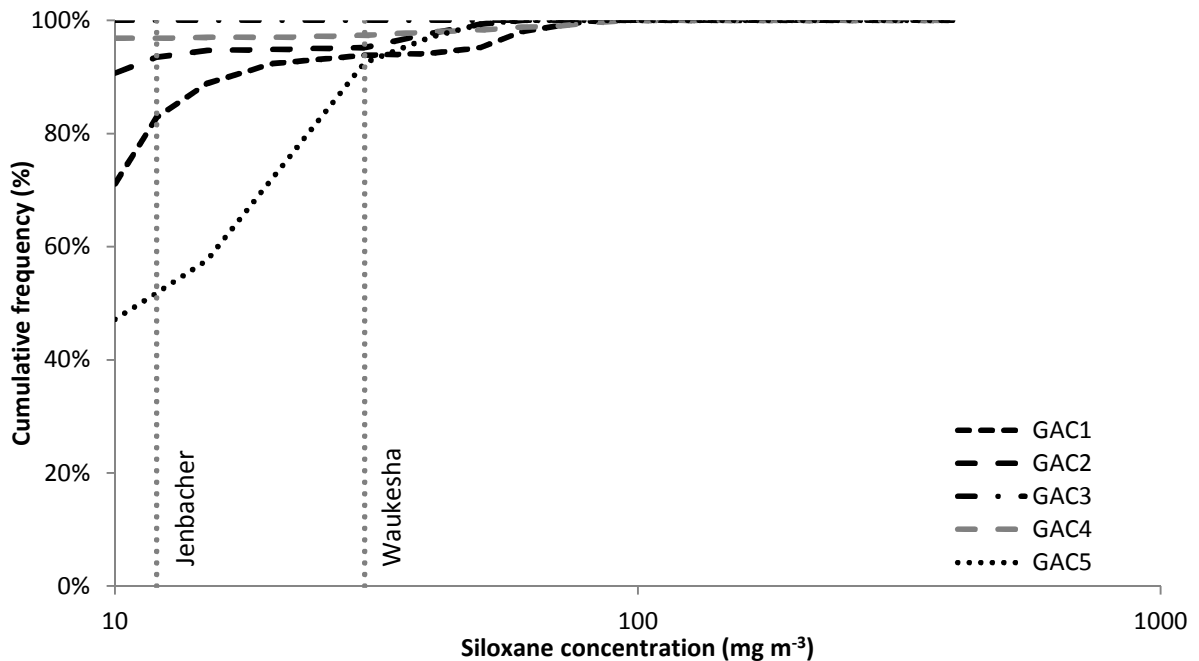


Figure 5-3. Cumulative frequency curves developed using outlet siloxane data from all five GAC contactors to ascertain conformity to proposed warranty specifications (Table 5-1). Data is from a single exhaustion cycle in which all five contactors are assessed simultaneously.

Whilst the early stage of the exhaustion cycle is characterised by a period of steady state operation and the treated biogas is below the proposed siloxane limits, statistical analysis of several consecutive exhaustion cycles (defined as operation between media exchanges) of one of the GAC contactors (GAC1) illustrates that these limits of 12 and 30 mg m⁻³ are met in only 50% and 74% of samples analysed over the full exhaustion cycle up to contactor media exchange (Figure 5-2). Cycle times ranged from 313 hours to 851 hours and one siloxane reading was taken per contactor per hour (n = 313-851). Outlet siloxane concentrations from all five GAC contactors were subsequently compared using data collected during simultaneous contactor operation in the same media exhaustion cycle (Figure 5-3). Sample conformity of 52% and 92% were recorded for the proposed limits of 12 and 30 mg m⁻³. However, in this single cycle comparison, the lower limit of 12 mg m⁻³ was met in >82% of samples in the breakthrough cycle from all contactors except GAC5.

5.3.2 Analysis of siloxane uptake in the GAC contactors

Breakthrough was identified for four of the five GAC contactors following analysis of the exhaustion cycle data (Figure 5-4). Although this GAC contactor data was collected during simultaneous exhaustion cycles (so each contactor was subject to the same biogas phase), breakthrough occurred for each contactor following a different number of bed volumes of biogas treated, with GAC4 breaking through earliest. The breakthrough curves could be differentiated into two shapes, a sharp fronted curve which characterised GAC contactors with early breakthrough (GAC2 and GAC4), and a broad fronted curve which more adequately described those with longer breakthrough cycles (Figure 5-4). Over the seven exhaustion cycles monitored, the mean number of bed volumes (Bv) passed before breakthrough ranged 34587 Bv (GAC4) to 119040 Bv. This corresponded to mean specific GAC media capacities at breakthrough ranging between 8.5 (GAC4) and 21.5 g_{siloxane} kg_{GAC}⁻¹ (GAC1). Exhausted media was collected from GAC1 and GAC4 after the contactors were shut down at the end of an exhaustion cycle for media exchange. The exhausted media were radially cross sectioned to semi-quantitatively evaluate Si media uptake and indicated that media collected from GAC1 comprised higher Si content than that sampled from GAC4 (Figure 5-5).

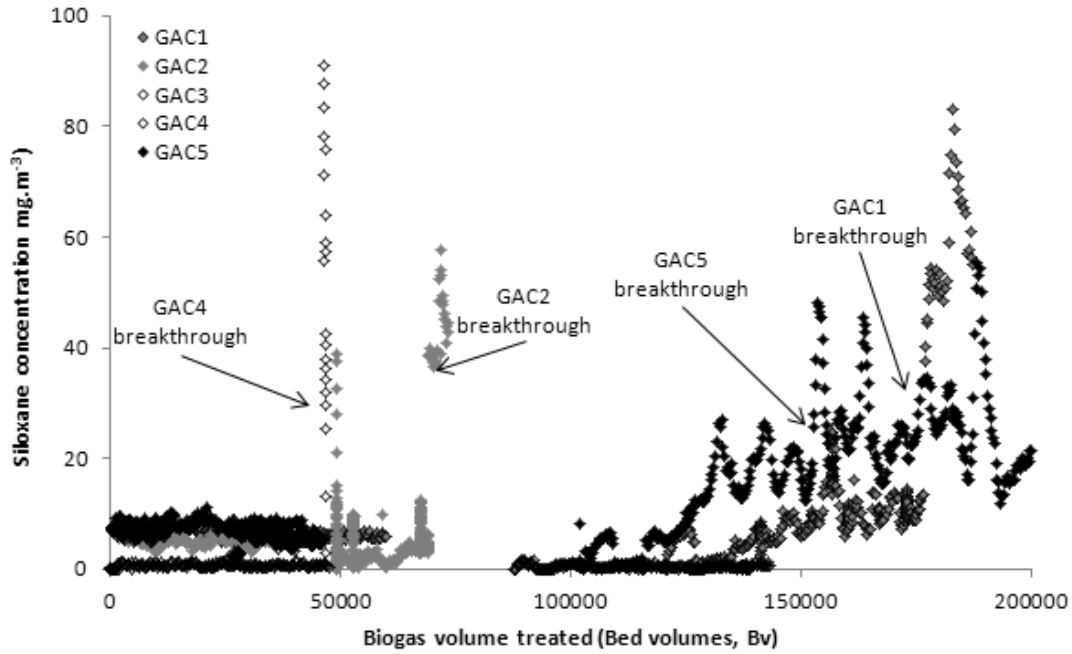


Figure 5-4. Breakthrough curves for four of the GAC contactors which experienced breakthrough. Breakthrough is defined as the outlet concentration exceeding 30 mg m⁻³ for the third consecutive reading (equivalent to the Waukesha warranty limit, Table 5-1).

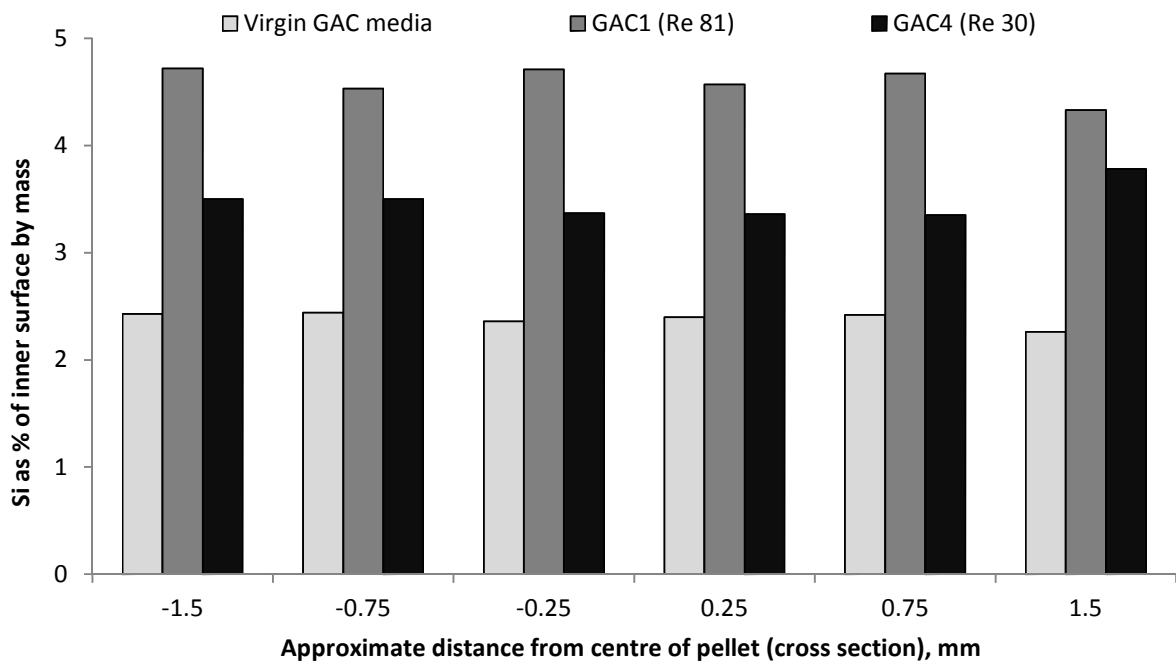


Figure 5-5. Media sampled at breakthrough, cross-sectioned (at centre) and analysed for Si to determine Si deposition in media operated at low Re_p (GAC4, $Re = 30$) and high Re_p (GAC1, $Re = 81$).

Onsite biogas samples were collected for wider speciation of trace biogas components (Table 5-4). Biogas sampled upstream comprised cyclic siloxanes D4 and D5 and also notable concentrations of both alkanes (nonane, decane) and aromatics (toluene, ethyl benzene, o,m,p - xylene). Mass balances across one of the contactors indicated considerable co-separation of these trace components with the cyclic siloxanes and suggests that siloxanes only represent around 20% (by weight) of the total mass of trace biogas components absorbed during the exhaustion cycle.

5.3.3 Analysis of GAC contactor operational conditions

Mean total biogas flow rate was $3353 \text{ m}^3 \text{ h}^{-1}$ and was consistent during contactor characterisation (median $3342 \text{ m}^3 \text{ h}^{-1}$), providing stable empty bed contact times (EBCTs). However, the EBCT (defined by contactor length/superficial velocity) used in each contactor was different, yielding EBCTs ranging 12s to 57s (Table 5-3). A general positive trend in the number of bed volumes of biogas treated before breakthrough (BvBB) was illustrated when using EBCT as the dependent variable (Figure 5-6). The difference in EBCT also provided differences in superficial velocity for each contactor which was evaluated through conversion to the modified Reynolds number (Re_p) for packed beds (Figure 5-7). The general trend indicates that an increase in the number of BvBB is achieved through increasing the Re_p up to a limiting value of between Re_p 81 and 162.

5.4 Discussion

In this study, on-line FTIR has been used to generate the first comprehensive siloxane breakthrough curves from full scale carbon contactors used for biogas preconditioning. A key finding was that the mean outlet siloxane concentrations of <LOD to 8.9 mg m^{-3} determined during the early stages of the exhaustion cycle were consistently below the siloxane limits cited in the engine manufacturers warranty specifications (12 to 30 mg m^{-3} , Table 5-1). However, over the full operating cycle (i.e. to media change) only 50% to 80% conformity was observed due to continued contactor operation beyond breakthrough.

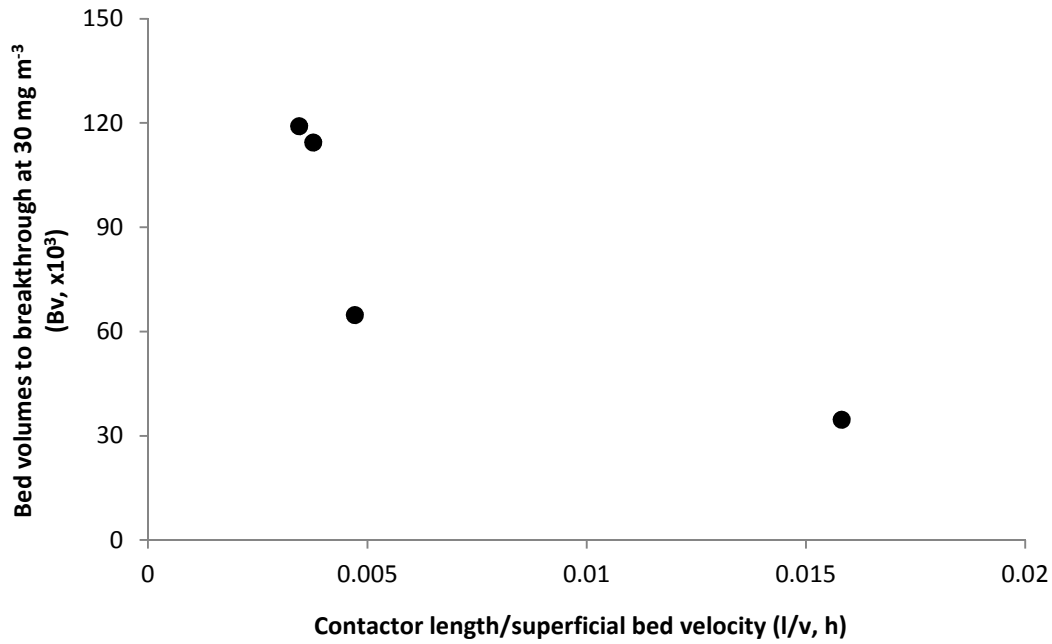


Figure 5-6. Evaluating the role of empty bed contact time (EBCT) in determining the number of bed volumes of biogas that can be treated before breakthrough. EBCT is determined by contactor length/superficial velocity.

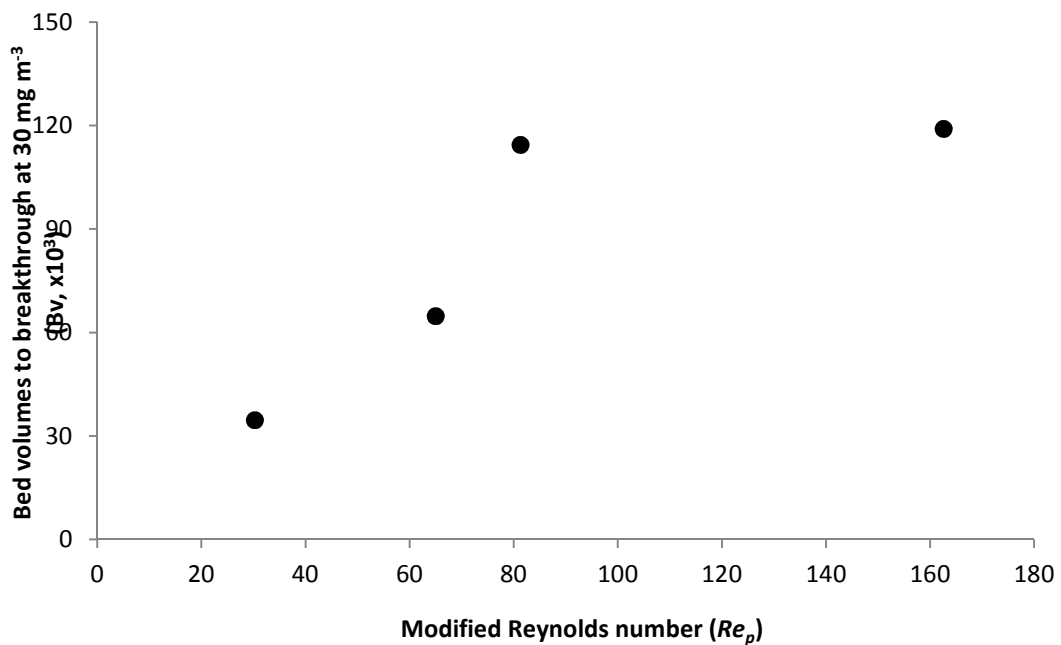


Figure 5-7. Evaluating the role of the modified Reynold's number (Re_p) in determining the number of bed volumes of biogas that can be treated before breakthrough. The modified Re_p was calculated based on specific contactor and media dimensions.

Tower and Wetzel (2004) described the economic incentive that siloxane removal provided through reducing SiO₂ deposition in the CHP engine, but noted that SiO₂ deposition still occurred during contactor operation albeit at a significantly lower rate. In this study it is suggested that the primary source of continued siloxane deposition is not leakage during the initial stage of the GAC operational cycle, but is instead continuous operation of contactors beyond breakthrough. To illustrate, for each mole of D₅ oxidised during combustion five moles of SiO₂ are formed (Equation (5-1), 0.82 mg_{SiO₂} mg_{D₅}⁻¹) which in this study equates to around 860 g_{SiO₂} h⁻¹ (using the assumption that contactors are operated at saturation following breakthrough). Tower (2003) postulated that up to 0.5% of the SiO₂ formed during combustion was retained within the engine, with around 45 g_{SiO₂} deposition proving critical to trigger reactive engine maintenance intervention. This is equivalent to operating the GAC contactors in this study at saturation for only 11 h following breakthrough. Importantly, in this study on-line FTIR was used for the first time to characterise contactor operation rather than control. Consequently, implementation of on-line FTIR is recommended to enable reactive contactor shutdown prior to breakthrough which presents two advantages: (i) limiting SiO₂ deposition post-breakthrough; and, (ii) enhancing conformity with the specified siloxane limits. Importantly, the contactors were characterised by a short mass transfer zone (generally less than 1.5% of total bed length) which is common for gas adsorption applications and can result in sharp breakthrough curves (Crittenden and Thomas, 1998). This means the transition from pseudo steady-state outlet siloxane concentration to breakthrough occurred in less than one hour for GAC2 and GAC4. Current detection methods generally couple grab sampling with laboratory based determination which introduces a lag time of over 48 hours. This is insufficiently responsive to react to this type of breakthrough curve, underpinning the important role that on-line detection can have in enabling reactive contactor shutdown once breakthrough is reached.

Specific media capacities of between 8.5 and 22 g_{siloxane} kg_{GAC}⁻¹ were recorded for the five parallel full scale GAC contactors which is below the adsorption capacity typically quoted for vapour phase GAC of around 100 g kg⁻¹ (Kuo, 1999).

Table 5-4. Estimated mass balance of GAC4 for fully speciated siloxanes and competing VOCs using a UKAS accredited GCMS trace analysis suite.

Gas phase determined	Inlet gas (mg m ⁻³)	Outlet gas (mg m ⁻³)	Total adsorbed ^b (g)
<i>Siloxanes speciated</i>			
Hexamethylcyclotrisiloxane (D3)	<1.0	<1.0	N/a
Octamethylcyclotetrasiloxane (D4)	3.1	2.8	66.8
Decamethylcyclopentasiloxane (D5)	33.9	7.2	5947.2
Dodecamethylcyclohexasiloxane (D6)	<1.0	<1.0	N/a
Hexamethyldisiloxane (L2)	<1.0	<1.0	N/a
Octamethyltrisiloxane (L3)	<1.0	<1.0	N/a
Decamethyltetrasiloxane (L4)	<1.0	<1.0	N/a
Dodecamethylpentasiloxane (L5)	<1.0	<1.0	N/a
Trimethyl Silanol (toluene equivalent)	<1.0	<1.0	N/a
<i>Non-siloxane species detected</i>			
Total Organo-Sulphur Compounds as S	1.5	N/d	334.1
Nonane	15.7	<5.3	2316.5
Decane	52.4	<5.8	10379.7
Cumene	1.5	<1.0	111.4
d-Limonene	4.5	2.4	467.8
alpha-Pinene	3.1	1.3	400.9
beta-Pinene	1.8	<1.0	178.2
Toluene	12.6	1.7	2427.9
Ethyl benzene	10.4	5.3	1136.0
m,p-Xylene	32.2	18.8	2984.7
o-Xylene	11.9	6.8	1136.0
o-ethyltoluene	2.1	1.9	445.5
1,2,3 – Trimethylbenzene	4.4	1.5	646.0
1,2,4 – Trimethylbenzene	13.2	8.6	1024.6
1,3,5 – Trimethylbenzene	4.5	4.3	445.5
Total cyclic siloxane mass adsorbed			6014
Specific cyclic siloxane mass adsorbed (g kg ⁻¹)			3
Mean specific siloxane breakthrough ^a			8
Total mass adsorbed			30448
Specific total mass adsorbed (g kg ⁻¹)			15

^aBased on real-time mass balance (from Table 5-4). ^bProvides an estimate based on mass balance of GAC4 to average breakthrough (34587 Bv).

Media capacities close to this value of up to $75 \text{ g}_{\text{siloxane}} \text{ kg}_{\text{media}}^{-1}$ have been reported at full scale for siloxanes removal using a proprietary graphite based media (Table 5-5) (Tower and Wetzel, 2004). However, data from this study is comparable to Wheless and Pierce (2004) who reported media capacities of a carbon/graphite mixed bed contactor ranging 5 to $15 \text{ g}_{\text{siloxane}} \text{ kg}_{\text{GAC}}^{-1}$. In this study, the low capacity can be ascribed to co-separation of both alkane and aromatic groups with siloxanes during the exhaustion cycle (Table 5-5). Shin et al. (2002) also identified the presence of the BTEX aromatics in landfill biogas at similar concentrations to this study. The authors further identified specific capacities for pure toluene in a synthetic gas phase, for example, of up to $497 \text{ g} \text{ kg}_{\text{GAC}}^{-1}$. The mean time to breakthrough in this study was less than 26 days which is less than has been reported at full scale. For example, Tower and Wetzel (2004) evidenced an exhaustion cycle of several months during the treatment of a biogas composed of $0.58\text{-}1 \text{ mg}_{\text{D5}} \text{ m}^{-3}$ and $4.52\text{-}13.0 \text{ mg}_{\text{D4}} \text{ m}^{-3}$. The contactors that the authors described were operated using a similar EBCT to this study but due to the low inlet siloxane concentration, siloxane loading was only $1.47 \text{ g}_{\text{siloxane}} \text{ m}^3_{\text{graphite}} \text{ h}^{-1}$. In this study inlet siloxane concentration ranged from 22.9 to $313.8 \text{ mg} \text{ m}^{-3}$ which yielded siloxane loading of up to $97.5 \text{ g}_{\text{siloxane}} \text{ m}^3_{\text{GAC}} \text{ h}^{-1}$. It is therefore posited that it is the high inlet siloxane concentration which induced comparatively shorter exhaustion cycles in this study.

Cooney (1999) proposed that if the same media is used in different contactors, then provided EBCT, bed velocity and column length are consistent, the contactors should process an equivalent number of bed volumes before breakthrough. However, whilst the same media was employed in each contactor, the number of bed volumes treated before breakthrough (mean range, 34587 to 119040) varied markedly between contactors. Dimensional analysis of the contactors identified a minimum contactor diameter to particle diameter ratio (d_c/d_p) of 225, which suggests that the reduction in specific capacity noted in several contactors is not expected to arise from channelling effects at the wall (generally noted at d_c/d_p below 20) or random variations in the interstitial velocity in the bed interior (Crittenden and Thomas, 1998; Cooney, 1999).

Table 5-5. Estimation of full scale carbon vessel operation from the literature compared to this study.

		This study (GAC1)	Tower & Wetzel, 2004 ^e	Orange County Sanitation District	Liang et al., 2001	Wheless & Pierce, 2004 / Wheless & Gary, 2002
		Carbon	SAG™ (graphite based)	SAG™ (graphite based)	Carbon and graphite	Carbon and graphite
Volume	m ³	1.21	26.6	10.0	0.2	0.07
Pressure	bar	0.12	N/s	4.0	4-4.4	N/s
Gas flow	m ³ h ⁻¹	323	1700-2800	2450	177	85
EBCT	s	12.8	34-56	14.7	4.7	2.9
Inlet concentration	mg m ⁻³	65.4 ^a	0.58-1 ^b , 4.5-13.0 ^c	76	38-62	N/s
Siloxane loading	mg kg ⁻¹ h ⁻¹	46.9	3.34	41.2	88.9	N/s
Specific media capacity	g kg ⁻¹ (%w/w)	21.5 (2.1)	7.2 (0.72) ^d	75.0 (7.5)	59.5 (5.95)	10-15 (1.0-1.5)
Time to breakthrough	d	16.4	~90	77	21-28	nd
Sampling method	-	On-line	Impinger (MeOH)	Bag/ Canister	Impinger ^f	ns
Analytical method (Speciation)/	- mg m ⁻³	FTIR (Cyclic/linear)	GC-MS (Speciation)	GC-MS (Total) N/s	HPLC ^f (Total VMS)	nd
Limit of detection		7	0.3 L2, 0.29 D6		N/s	
Outlet concentration	mg m ⁻³	7.0	N/d	Bdl	Bdl	N/d

N/s – Not stated. N/d – None detected. Bdl – Below detection limit. ^aPrincipally loaded with D5; GAC1. ^bmg_{D5} m⁻³. ^cmg_{D4} m⁻³. ^dAssumes 100% retention at maximum flow. ^eAs cited in Soreanu et al. (2011). ^fVariation of USEPA method TO-5.

However, superficial velocity did vary between 203 and 1075 m h⁻¹ (Table 5-3) due to differences in contactor dimensions and gas flow rate. These are within the lower range reported for vapour phase GAC of 144 to 1829 m h⁻¹ with values up to 3660 m h⁻¹ also cited (USEPA, 2006). An increased velocity corresponded to an increase in number of bed volumes treated before breakthrough (Figure 5-6) which increased mean specific media capacity from 8.5 to 21 g_{siloxane} kg_{GAC}⁻¹. It is suggested that the lower specific media capacity can be accounted for by axial dispersion effects which cause considerable error when the fluid is a gas (Wakao and Funazkri, 1978), particularly when within the *Re* range 1 to 200 (Gunn, 1987). Data from this study falls within this *Re* range. The lower *Re* region of this range represents the upper limit of the region of creeping flow in fixed beds (Gunn, 1987) and is where limited specific siloxane capacities were observed. In this region, dispersion becomes primarily controlled by molecular diffusion due to the low Schmidt number which characterises the biogas phase (*Sc*, 0.6). Urban and Gomezplata (1969) evidenced that in practice, at low *Re* the axial dispersion coefficient describes both diffusive axial dispersion and uneven convection. The latter term describes behaviour when molecular diffusion dominates. In this case radial diffusion within the velocity profile effectively inhibits dispersion caused by axial convection and leads to self-sharpening behaviour (Cussler, 2009; Urban and Gomezplata, 1969). The production of sharp fronts was evidenced in this study for GAC2 and GAC4 following breakthrough (Figure 5-2) and is coincident with their operation at the lower *Re* range (*Re* < 65).

An increase in bed volumes treated before breakthrough was achieved by increasing *Re* (Figure 5-7). Gunn (1987) identified that in packed beds the onset of turbulence was around *Re* = 200, at which point molecular diffusion is no longer the dominant mechanism of dispersion (Urban and Gomezplata, 1969). Whilst there is limited data in this study due to access to only five full scale contactor designs, the data would suggest that the plateau exhibited between *Re* 81 and 162 is representative of limiting conditions (Figure 5-6). There is evidence that for gas systems there is no unique value of the velocity parameter at which the enhancement in mass transfer reaches a limiting value. However, limiting conditions around *Re*_p 100 have similarly been reported (Urban and Gomezplata, 1969; Miyauchi et al., 1976). Interestingly,

at higher Re , axial dispersion is much greater than molecular diffusion due to turbulent fluctuations in both velocity and concentration, the effect of which is to create a broader more dispersed front. This was evidenced in this study from the GAC1 and GAC5 breakthrough curves (Figure 5-4) which represent operation at Re greater than 81. Comparison of Si distribution within exhausted GAC media collected from contactors operated within high and low Re conditions further suggests that greater utilisation of the media is achievable at higher Re (Figure 5-7). To illustrate the economic impact, GAC4 currently requires 14.6 media replacement cycles per annum which, based on a GAC replacement cost of €1.5 kg_{GAC}⁻¹, costs €43,800. Operation at higher Re conditions (equivalent to GAC1) would reduce the number of replacement cycles to 5.57 cycles (€16,710) which represents a saving of €27,090 (62%).

5.5 Conclusions

In this study, on-line FTIR has enabled the first comprehensive characterisation of full scale carbon contactors for siloxane removal from biogas. Within the initial stages of the exhaustion cycle, an initial period of pseudo steady state was observed where outlet siloxane concentration was consistently below the proposed siloxane limits, despite marked variation in inlet siloxane concentration. Following this period, siloxane breakthrough occurs quickly. This is exacerbated when contactors are operated at low Reynolds numbers due to axial dispersion effects. Due to the sharp breakthrough fronts identified, existing detection methods are insufficiently robust at defining siloxane breakthrough, resulting in continued contactor operation regardless of the diminished siloxane removal. Application of on-line FTIR for management of contactors therefore presents a real opportunity to enhance CHP engine protection. Lower than expected specific media capacities arise from co-separation of both alkanes and aromatics. However, greater specific media capacity is accessible through operating contactors at velocities sufficient to diminish axial dispersion effects.

6 Siloxane adsorption from biogas in the transitional regime

Caroline A. Hepburn^a, Nigel J. Simms^b, and Ewan J. McAdam^{a *}

^aCranfield Water Science Institute, Cranfield University, Cranfield, Bedfordshire, MK43 0AL, UK

^bCentre for Power Engineering, Cranfield University, Cranfield, Bedfordshire, MK43 0AL, UK

Abstract

The dominant technology for separating siloxanes from biogas prior to combustion is adsorption onto activated carbon. Whilst much research has focussed on adsorption media characteristics for this application, carbon vessel hydrodynamics remain largely unexplored. In this study, Reynold's number (Re) is used to evidence the significance of gas-phase hydrodynamics on the siloxane adsorption capacity of activated carbon. In dry gas, siloxane adsorption capacity was found to increase by 36% when Re was increased from within the laminar regime (Re 31) to firmly within the transitional regime (Re 107). When biogas humidity was increased from 0 to 80% under laminar conditions, adsorption capacity reduced from 135 to 69.3 $g_{D5} \text{ kg}^{-1}_{\text{carbon}}$ in a stepwise pattern, as previously observed by others. It is asserted that this reduction in siloxane adsorption capacity can be attributed to the resistance provided by a progressive increase in water film thickness. However, when biogas humidity was increased within the transitional regime, the effect on siloxane adsorption capacity was negligible. Furthermore, increasing Re from 31 to 73 at 80% humidity resulted in a 410% increase in capacity. Understanding the role of Re in gas-phase siloxane adsorption is therefore of practical importance since many full scale carbon vessels operate at low Re numbers.

Keywords: *Anaerobic digestion; CHP; Competition; GAC; Landfill; Re*

6.1 Introduction

Many water utilities generate extra revenue by selling electricity produced using biogas produced at their wastewater treatment facilities. To illustrate, total installed capacity for electricity from anaerobic digestion of sewage sludge (AD) in the UK has risen from 157 MW in 2009 to 198 MW in 2012 (DECC, 2013). However, biogas generated from the anaerobic digestion of sewage sludge contains trace components, such as siloxanes, which are detrimental to the economic utilisation of this resource. The current UK feed-in tariff for electricity from combined heat and power (CHP) engines is £0.094 kWh⁻¹ (Read and Hofmann, 2011). Siloxanes are estimated to cause damage to CHP engines costing up to £0.015 kWh⁻¹ (Lemar, 2005), or 16% of the revenue generated producing electricity. Pre-treatment of biogas to remove siloxanes is therefore desirable to reduce these costs.

A number of technologies have been trialled to remove siloxanes from biogas, including condensation and chemical absorption, but the technology most widely used in industry is adsorption, usually onto activated carbon (Ajhar et al., 2010a). In order to minimise the cost of siloxane removal, several research groups have carried out bench-scale adsorption tests to investigate how to maximise the life of an adsorption vessel before the media needs to be replaced. The most common avenue of investigation has been to change the adsorbent; Matsui and Imamura (2010) tested twenty-two different types of activated carbon and found adsorption capacities for octamethylcyclotetrasiloxane (D4) varied between 6 – 19 wt%, which they linked to variations in pore volume and BET (Brunauer-Emmett-Teller) surface area. Oshita et al. (2010) found the best indicator for siloxane adsorption potential was BET specific surface area. Other adsorbents have also been tested, including polymer beads, molecular sieves, and silica gel (Schweigkofler and Niessner, 2001). Schweigkofler and Niessner (2001) found activated charcoal and silica gel provided the best capacities for both decamethylcyclopentasiloxane (D5) and hexamethyldisiloxane (L2), each greater than 10 g_{siloxane} kg⁻¹_{media}. Competition for adsorption sites between

siloxane species is also worthy of investigation since biogas is a complex mixture containing over 50 trace gas species (Eklund et al., 1998). Anecdotal evidence suggests that smaller siloxanes are displaced by larger siloxane species when the adsorption media nears saturation (Griffiths, 2012) and Matsui and Imamura (2010) found that D4 was displaced by D5 when they used real biogas samples. When biogas is produced by the anaerobic digestion of sewage sludge, the humidity is usually close to 100% (Persson and Wellinger, 2006), so Schweigkofler and Niessner (2001) also investigated the effect of humidity on the L2 and D5 adsorption capacity of silica gel and found that, due to the hydrophilic nature of silica gel, increasing humidity to 30% decreased the siloxane uptake by 41 – 45% compared to values for dry gas ($50 - 62 \text{ g}_{\text{siloxane}} \text{ kg}^{-1}_{\text{silica gel}}$) and the D5 mass adsorbed before breakthrough was less than $6 \text{ g}_{\text{D5}} \text{ kg}^{-1}_{\text{silica gel}}$. Similarly, Sigot et al. (2014) investigated the effect of humidity on the adsorption of D4 onto silica gel and found a 90% reduction in capacity at a relative humidity of 70% compared to dry gas. Activated carbon is less hydrophilic than silica gel so a similar but weaker response to humidity is expected. Cabrera-Codony et al. (2014) carried out the only experiments into the effect of humidity on activated carbon for siloxane removal from biogas and found a 17% decrease in adsorption capacity for D4 when the relative humidity was increased from 0% to 80% but no effect between 0% and 20% humidity. The effect of humidity on the activated carbon adsorption of siloxane is of particular interest since various pre-treatment steps (such as gas drying, condensation or scrubbing (Arnold, 2009)) can change the water content so siloxane removal processes are carried out at a variety of humidities. In addition to external parameters such as humidity, operational parameters, such as contact time and Reynold's number, can impact on bed life. For example, Das et al.(2004) noted the importance of Reynold's number in their model of toluene adsorption onto activated carbon fibre and Knaebel (2000) states that Reynold's number influences bed size. To date, there has been little research focussing on the hydrodynamics of the siloxane removal vessels. Interestingly, bench scale siloxane adsorption studies have all been run at Reynold's

numbers of 0.2 – 16.4 (Khandaker and Seto, 2010) which lie in the laminar regime (Chilton and Colburn, 1931), whilst full-scale studies have been run at Reynold’s numbers between 30 and 163 (Hepburn et al., 2014), which is in the transitional regime (Chilton and Colburn, 1931). The aim of this study is therefore to compare the behaviour of activated carbon beds close to the laminar regime and further into the transitional regime. The objectives are to investigate the dependence of the adsorption capacity of activated carbon on Reynold’s number, humidity and siloxane chemistry.

6.2 Materials and Methods

6.2.1 Test rig

Four streams of carbon dioxide (>99.8%, BOC, Guildford), each controlled by a mass flow controller (MFC) (Cole Parmer, London) were mixed to form a model gas with specified siloxane concentrations and humidity (see supporting information, Figure S1). The first CO₂ stream (MFC WU-32907-71, flow rate 0.1 – 10.0 L min⁻¹) was kept dry. The second CO₂ stream (MFC WU-32907-71, flow rate 0.1 – 10.0 L min⁻¹) was passed through a 1 L glass water bubbler (Fisher Scientific, Loughborough). The third CO₂ stream (MFC WU-32907.69, flow rate 0.05 – 5.00 L min⁻¹) was passed through a 4 mL glass bubbler (Sigma Aldrich, Dorset) containing liquid decamethylcyclopentasiloxane (D5) (97%, Sigma Aldrich, Dorset). The fourth CO₂ stream (MFC WU-32907-57, flow rate 0.5 – 50 mL min⁻¹) was passed through another 4 mL bubbler containing hexamethyldisiloxane (L2) (98%, Sigma Aldrich, Dorset). Bubblers were sized according to the results of the single bubble regime analysis by Mayer et al. (2001), to ensure the gas phase reached equilibrium with the liquid phase within the residence time in the bubblers. This allowed the mass ratio of siloxane or water to carbon dioxide in each gas stream to be calculated according to (adapted from Perry and Green (1998)):

$$\frac{Mass_x}{Mass_{CO_2}} = \frac{M_x p_{vap,x}}{M_{CO_2}(P_{atm} - p_{vap,x})} \quad (6-1)$$

in which M_x is the molecular weight of component x (water or D5 or L2), $p_{vap,x}$ is the vapour pressure of component x at the experimental temperature, and P_{atm} is the atmospheric pressure. A linear relationship ($r^2 = 0.97$) was demonstrated between predicted siloxane concentrations in the model gas and FTIR readings.

The model gas then passed through either the bypass to the FTIR spectrometer (to determine the inlet siloxane concentration) or through a 6.6 mm i.d. glass column (Kinesis, St Neots) filled with activated carbon and then to the FTIR spectrometer. The pipework was made from stainless steel and the bubblers and column were made of glass. The rig was purged with dry CO_2 before each experiment and then allowed to come into equilibrium with the model gas before the gas flow was switched from bypass to column. To ensure uniformity and repeatability, the activated carbon (provided by Severn Trent Water, Coventry) was prepared by grinding and sieving to retain particle sizes in the range 500 – 710 μm . The ground carbon was dried for two hours at 80°C and stored in a tube with silica gel above and below to prevent moisture from the air being adsorbed onto the carbon. Experiments were run at ambient temperature and pressure. To demonstrate the repeatability of the breakthrough curves generated using the test rig, duplicate breakthrough curves were generated and compared. The difference in calculated adsorption capacities was 4% (defined as the mass of siloxane adsorbed before breakthrough divided by the mass of carbon).

Breakthrough was defined as the time at which the outlet siloxane concentration exceeds 10 $mg_{siloxane} m^{-3}_{CO_2}$. Adsorption capacity was calculated as the total mass of siloxane that entered the adsorption bed before breakthrough, divided by the mass of the adsorption bed. Empty bed contact time was defined as the volume of the adsorption bed divided by the volumetric gas flowrate.

The packed bed Reynold's number was calculated as:

$$\text{Packed bed Reynolds number} = Re = \frac{xU_s\rho}{\mu(1 - \epsilon)} \quad (6-2)$$

in which x is the carbon particle diameter (0.6 mm), U_s is the gas superficial velocity (equal to the volumetric gas flowrate divided by the cross-sectional area of the bed), ρ is the gas density (1.15 kg m⁻³ for biogas at 30°C and 1 atm (Fulford, 1996)), μ is the gas viscosity (1.71 x 10⁻⁵ kg m⁻¹ s⁻¹ for biogas at 30°C and 1 atm (Fulford, 1996)) and ϵ is the void fraction of the bed (0.50). The void fraction of the bed was calculated as the volume of void space (measured by weighing a volume of carbon particles with and without water) divided by the total volume of the carbon bed.

Initial experiments were carried out using a carbon bed 10 mm long and 6.6 mm in diameter (which ensured a negligible wall effect factor (Crittenden and Thomas, 1998)) containing 0.4 g activated carbon. The gas flowrate was varied to give different empty bed contact times (EBCTs). For an EBCT of = 0.15 s the bed height was doubled to 20 mm (0.8 g_{carbon}) as a sufficiently low flow rate could be not achieved due to back pressure in the test apparatus. For all conditions, Reynold's numbers ranged between 31 and 107. Chilton and Colburn (Chilton and Colburn, 1931) identified a Re of around 50 consistently marked the transition from viscous to turbulent flow for both gas and liquid packed bed studies; similar values have since been introduced into empirical mass transfer correlations by a number of authors to describe packed bed mass transfer in these two discrete regions, typically being differentiated at Re of between 50 and 55 (where for $Re < 50-55$, flow is ostensibly laminar) (Cooney, 1999; Lightfoot et al., 1962). The Re range in this study therefore extends across both laminar and turbulent conditions and corresponds to the Re range identified in full-scale siloxane contactors by Hepburn et al. (2014). To decouple empty bed contact time from Reynold's number, a larger column (10 mm i.d.) was used whilst maintaining a constant bed volume (0.4 g_{carbon}). The D5 concentration used in all of the above experiments was 70 mg_{D5} m⁻³_{CO2}. This corresponds to the mean siloxane concentration measured at a large

sewage treatment works by Hepburn et al. (2014). Competition between D5 and L2 was examined with higher siloxane concentrations (D5 = 1.2 g m⁻³ and L2 = 134 g m⁻³) as the high volatility of L2 made lower concentrations difficult to achieve with the test apparatus.

6.2.2 FTIR

The FTIR spectrometer was an Antaris IGS (Thermo Fisher Scientific Inc, Waltham, MA) with a 2m path length. The gas cell was heated to 80°C to prevent condensation and a coarse filter was sited upstream of the instrument to protect from free water ingress and any carbon fines. The test rig was connected directly to the gas cell, permitting continuous flow of gas through the cell. During a reading, twenty scans were taken over 120 seconds. The reported value comprised an average value from the scan. To reduce interference, background spectra (found by scanning with the gas cell evacuated) were subtracted from the sample spectrum. Cyclic and linear siloxanes were discriminated at 798 to 817 cm⁻¹ and 837 to 867 cm⁻¹ respectively. Siloxane concentrations are reported as mg m⁻³ for cyclic siloxanes, linear siloxanes and total siloxanes. Cyclic siloxane data measured in real biogas using the FTIR were compared to data provided using a UKAS accredited GC-MS method on comparable samples. The method comparison presented a positive linear response within 95% confidence limits which was validated using a certified primary reference gas mixture supplied by the National Physical Laboratory (NPL, Teddington, UK) (Hepburn et al., in preparation).

6.3 Results

6.3.1 Effect of EBCT and Reynold's number on uptake in dry gas

Breakthrough (taken as the point at which the outlet siloxane concentration first exceeded 10 mg m⁻³) for all the experiments occurred when between 1,100,000 and 1,600,000 bed volumes of gas had been treated (Figure 6-1), giving an adsorption capacity range of 138 – 191 g_{D5} kg⁻¹_{carbon}. The breakthrough curves

at EBCTs of 0.08 – 0.015 s have a similar, steep profile, rising from <LOD to 40 mg m⁻³ siloxane in 400,000 bed volumes, whilst at shorter EBCTs (0.03 s and 0.02 s) the curves are progressively gentler, rising from <LOD to 40 mg m⁻³ siloxane in 3,000,000 bed volumes for EBCT = 0.02s. In these experiments, Reynold's number was inversely related to EBCT. The rate constant (k_v) was estimated for each corresponding change in U_s with the modified Wheeler equation (Busmundrud, 1993) which yielded an approximation of $k_v = 223U_s^{0.23}$ (see supporting information) to describe the enhancement in rate provided by an increase in U_s . In these experiments, Re was inversely related to EBCT.

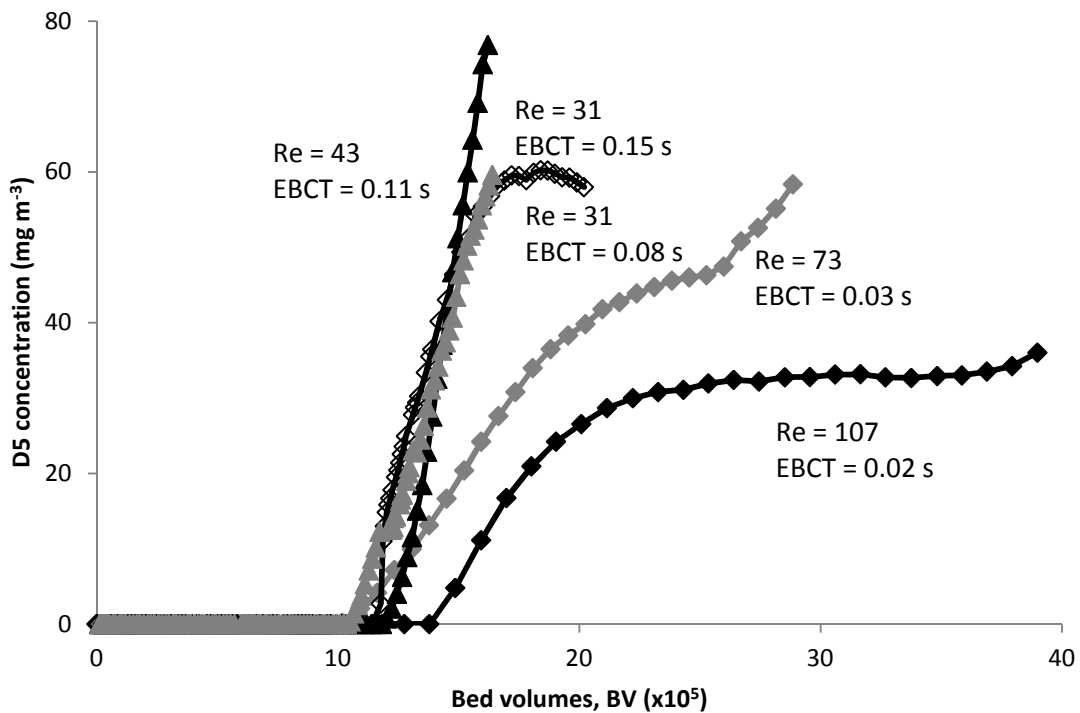


Figure 6-1. Breakthrough curves showing the effect of varying empty bed contact time (EBCT) and Reynold's number. At EBCTs above 0.05 s (and Reynold's numbers below 55) the curves are nearly identical. At lower EBCTs (higher Re), the breakthrough curves are progressively less steep. (Inlet concentration = 70 mg_{D5} m⁻³ CO₂; humidity = 0%; Re = 31 – 107; EBCT = 0.02 – 0.15 s.)

A positive correlation ($R^2 = 0.96$) was found between the packed bed Reynold's number (Re) and breakthrough time (Figure 6-2).

To decouple the effects of Reynold's number and EBCT, each was held constant whilst the other was changed. When Reynold's number was increased from 32 to 73 with EBCT held constant at 0.031s, the volume of gas treated before breakthrough increased by 790,000 bed volumes (134% increase, Figure 6-3a). When EBCT was increased from 0.014s to 0.031s with Re held constant at 73, the volume of gas treated before breakthrough increased by 740,000 bed volumes (116% increase, Figure 6-3b). This contrasts with the results when Re and EBCT are linked (Figure 6-1).

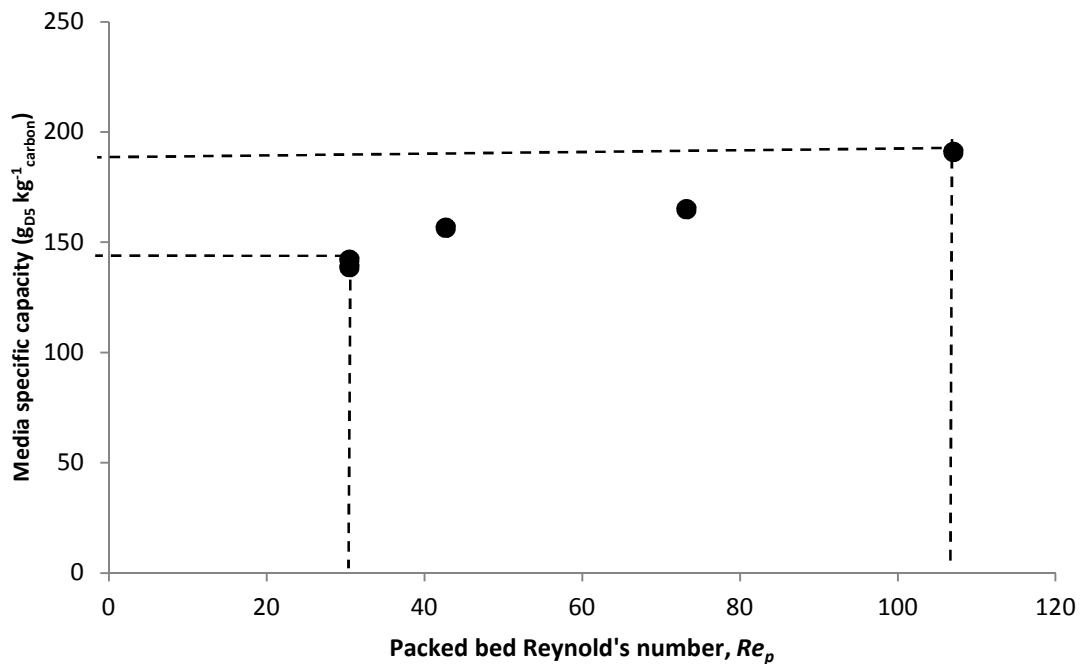


Figure 6-2. The relationship between the Reynolds number and specific media capacity. When Re is increased from 31 to 107 the media capacity increases from 138 to 191 $g_{D5} kg^{-1}_{carbon}$, an increase of 38%.

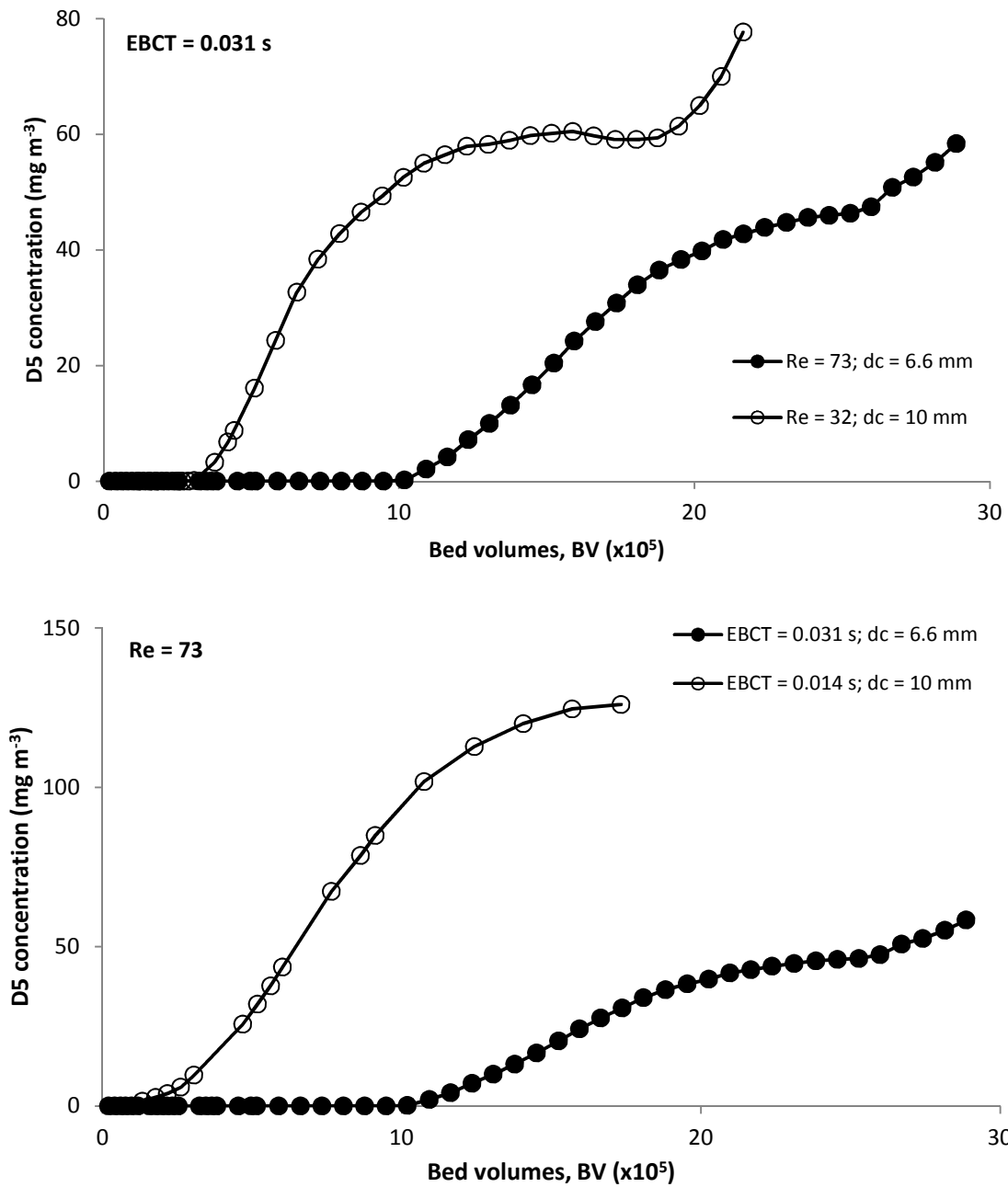


Figure 6-3. Comparison of the effects of changing EBCT and Re separately. a) EBCT is held constant whilst Re is changed from 32 to 73, resulting in an increase in media specific capacity from $70.3 \text{ g}_{D5} \text{ kg}^{-1}_{\text{carbon}}$ to $165 \text{ g}_{D5} \text{ kg}^{-1}_{\text{carbon}}$. b) Re is held constant whilst EBCT is increased from 0.014s to 0.031s, resulting in specific media capacity increasing from $76.4 \text{ g}_{D5} \text{ kg}^{-1}_{\text{carbon}}$ to $165 \text{ g}_{D5} \text{ kg}^{-1}_{\text{carbon}}$. (Inlet concentration = $70 \text{ mg}_{D5} \text{ m}^{-3}_{CO2}$; humidity = 0%.)

6.3.2 Influence of humidity

The influence of humidity was investigated at a Reynold's number of 31 (EBCT = 0.08 s, Figure 6-4) and 73 (EBCT = 0.03 s, Figure 6-5). At Re = 31, the number of bed volumes treated before breakthrough decreases stepwise as the humidity is increased, from 1,100,000 bed volumes in dry gas to 480,000 bed volumes at 80% humidity.

This corresponds to a reduction in the adsorption capacity of the carbon of 49%. At Re = 73, the breakthrough curves formed two clusters, with the curves for the 0% and 10% humidity cuts breaking through at 250,000 bed volumes and the curves for 30 - 80% humidity breaking through between 280,000 and 300,000 bed volumes. The media capacity increased by 12% from 314 g_{D5} kg⁻¹_{carbon} to 353 g_{D5} kg⁻¹_{carbon}.

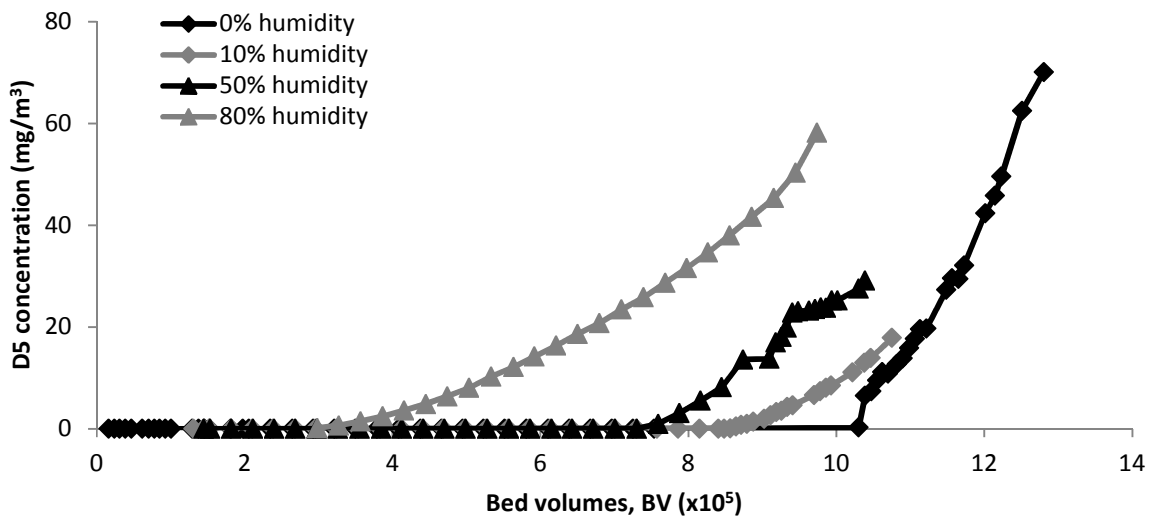


Figure 6-4. Breakthrough curves showing the effect of humidity at a Reynold's number of 31 (near-laminar flow regime). As humidity increases from 0% to 80% the media siloxane capacity decreases from 135 to 69.3 $\text{g}_{\text{D5}} \text{kg}^{-1}_{\text{carbon}}$. (Inlet concentration = $70 \text{ mg}_{\text{D5}} \text{ m}^{-3}_{\text{CO2}}$; humidity = 0 – 80%; $\text{Re} = 31$; $\text{EBCT} = 0.077 \text{ s.}$)

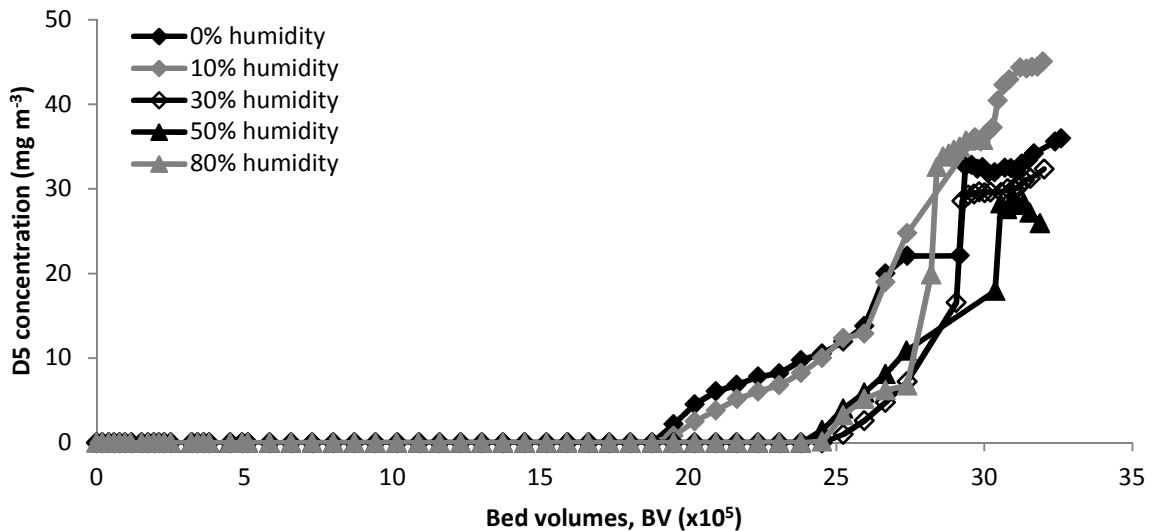


Figure 6-5. Breakthrough curves showing the effect of humidity at a Reynold's number of 73 (transitional flow regime). Adding 10% humidity has no effect on media capacity compared to dry gas. Adding 30 – 80% humidity increases the media capacity by 39 $\text{g}_{\text{D5}} \text{kg}^{-1}_{\text{carbon}}$ (12%). The differences between 30 – 80% humidity are within experimental error. (Inlet concentration = $70 \text{ mg}_{\text{D5}} \text{ m}^{-3}_{\text{CO2}}$; humidity = 0 – 80%; $\text{Re} = 73$; $\text{EBCT} = 0.031 \text{ s.}$)

6.3.3 Influence of competition between siloxane species

Competition between D5 (371 g mol^{-1} (Chandra, 1997)) and the smaller L2 (162 g mol^{-1} (Chandra, 1997)) was examined by running an experiment with both together. Breakthrough of L2 occurred first (at 4400 bed volumes, Figure 6-6) and the outlet L2 concentration increased to 1.6 times the inlet concentration, suggesting that L2 was being displaced by D5. The D5 concentration started to rise at 5900 bed volumes, corresponding to the peak L2 concentration.

Humidity has a much greater effect on D5 than on L2. Under saturated conditions, D5 broke through after 263 bed volumes of gas has been treated, compared to 1403 bed volumes under dry conditions (Figure 6-7a). Breakthrough of L2 occurs around 500 bed volumes in both dry and saturated conditions, although the breakthrough curve for L2 was less steep under high humidity than in dry conditions (Figure 6-7b).

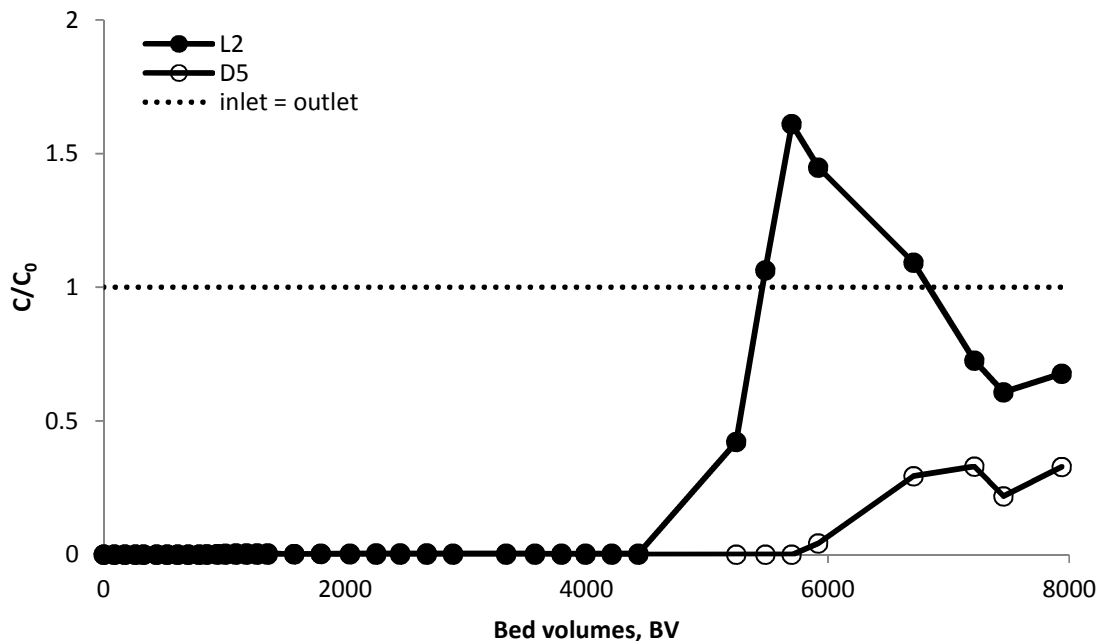


Figure 6-6. Breakthrough curves for L2 and D5 in the same gas showing competition between the two species. (Humidity = 0%; $Re = 3.6$; $EBCT = 2.7 \text{ s.}$)

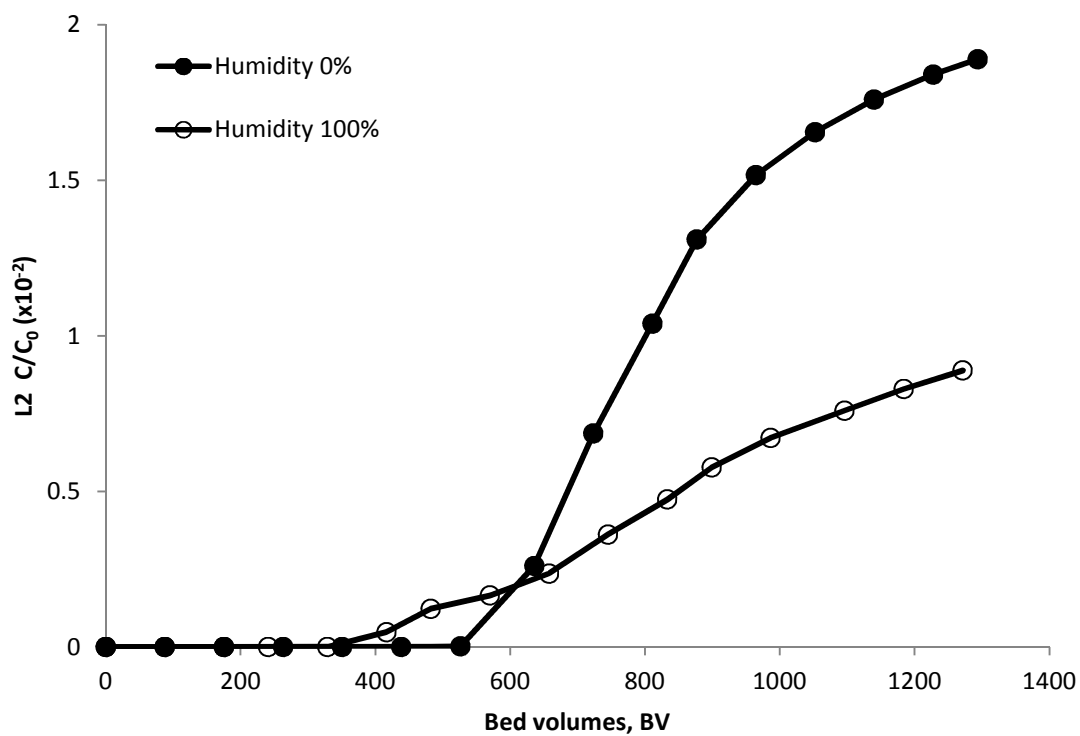
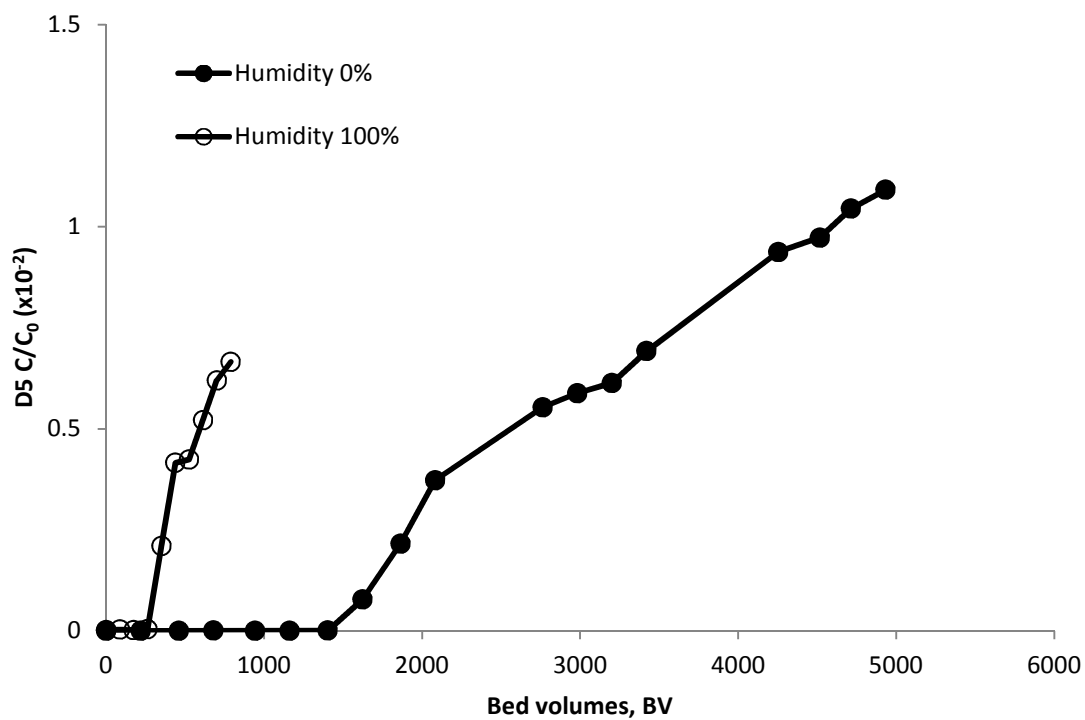


Figure 6-7. The effect of humidity on two siloxanes (a) L2 and (b) D5. (Humidity = 0 – 100%; Re = 3.6; EBCT = 2.7 s.)

6.4 Discussion

The most significant finding of this study is the contrast in siloxane adsorption behaviour when the process is moved further into the transitional regime. At 80% humidity, increasing the Reynold's number from 31 to 73 increased the adsorption capacity of the activated carbon from 69.3 to 353 $\text{g}_{\text{D5}} \text{kg}^{-1}_{\text{carbon}}$ – an increase of 410% (Figure 6-4 and Figure 6-5). Reynold's number was shown to have a significant effect on the adsorption capacity of activated carbon even in dry gas, outweighing the effect of empty bed contact time (Figure 6-1). Dynamic adsorption processes (including the majority of full-scale processes (Crittenden and Thomas, 1998)) are rate-limited as the gas does not reach equilibrium with the adsorbent (Weber Jr. and Smith, 1987; Weber Jr., 1983), so extending the contact time between the adsorbent and adsorbate is expected to increase the amount adsorbed (and hence the media capacity). However initial experiments found the opposite occurred – i.e. adsorption capacity decreased with increasing EBCT (Figure 6-1). In these experiments Reynold's number was inversely linked to EBCT and the effect of Reynold's number outweighed the effect of EBCT. At a fixed Reynold's number ($\text{Re} = 73$) increasing the EBCT by 120% led to an increase of 116% in adsorption capacity (Figure 6-3b), showing that the effect of EBCT is as expected when the two parameters are decoupled. In a bed of fixed dimensions, empty bed contact time is inversely proportional to the gas flow rate, and therefore to the Reynolds number Equation (6-2). Therefore when Reynold's number and EBCT were varied together (Figure 6-1) a positive relationship between Reynold's number and media capacity led to a negative relationship between EBCT and media capacity. The positive effect of Reynold's number on media capacity is caused by the change in thickness of the hydrodynamic boundary layer around each carbon particle. For a siloxane molecule to be adsorbed from biogas four steps must occur: transport through the bulk gas (bulk transport), transport through the hydrodynamic boundary layer (film transport), transport through the carbon pores (intraparticle transport; either along the pore walls or in the centre of the pores), and finally adsorption (Weber Jr. and Smith, 1987; Weber Jr., 1983).

Bulk transport and adsorption occur very quickly and so this process is limited by the rate of film and intraparticle transport (Weber Jr. and Smith, 1987; Weber Jr., 1983).

The increased media capacity demonstrated upon increasing Re can therefore be ascribed to the reduction in boundary layer thickness at the carbon-gas interface. When gas flow through the packed bed is laminar ($Re < 50$ (Crittenden and Thomas, 1998)), the velocity profile can be regarded as V-shaped, and molecular diffusion becomes a governing mechanism of axial dispersion (Welty et al., 2001). Urban and Gomezplata proposed that in gas phase packed beds operated at low Re , uneven convection can also contribute to axial dispersion, in which siloxanes diffuse into regions of differing velocity where the extent of build-up of siloxanes is controlled by back-diffusion of adsorbate into the bulk gas (Cussler, 2009). This summative axial dispersion effect causes the exhaustion front to sharpen (Cussler, 2009) as was evidenced in this study for breakthrough curves produced within the laminar regime (Re 31 to 43, Figure 6-1). As Re is increased into the transitional regime, dispersion is increasingly governed by a combination of concentration and velocity fluctuations which help diminish the concentration gradient within the boundary layer (Cussler, 2009). The broad exhaustion front recorded for breakthrough curves at $Re > 50$ are characteristic of greater radial dispersion within the carbon bed (Figure 6-1) and is supported by the enhancement in the rate constant observed upon increasing the superficial gas velocity. The longest period to breakthrough (3,000,000 Bv) was observed at the highest Re tested of 107 (Figure 6-1). Sherwood (1975) suggested that once Re exceeds around 100 in packed beds, mixing in the interstitial voids is rapid. It is therefore asserted that it is the enhancement in dispersion provided by an increase in Re which enhances total media siloxane capacity through: (i) limiting the boundary layer concentration gradient; and (ii) enabling greater dispersion / penetration into the carbon bed. Interestingly, in a recent full-scale survey, Hepburn et al. (Hepburn et al., 2014) evidenced sharp and broad breakthrough curves from carbon adsorbers for siloxanes operated under laminar and transitional

conditions respectively, which evidences that the phenomena outlined can be directly applied to industry for enhancement of media capacity.

Increasing biogas humidity exacerbated the contrast in adsorption behaviour noted within either laminar or transitional conditions. Within the laminar regime ($Re = 31$), the adsorption capacity of the carbon was found to decrease stepwise from 135 to 6.3 $g_{D5} \text{ kg}^{-1}_{\text{carbon}}$ as humidity was increased from 0% to 80% (Figure 4). This classical response was demonstrated by for D5 adsorbed onto silica gel by Schweigkofler and Niessner (2001) at $Re = 6.6$ and by Crittenden et al. (1988) for VOCs in air stripping off-gas adsorbed onto activated carbon (Re unknown). Acidic carbon-oxygen groups on the surface of activated carbons promote hydrophilicity (Bansal and Goyal, 2005), enabling water vapour to develop into a water film at the gas-solid interface (Habuka et al., 2013; McCoy and Rolston, 1992), which provides an additional resistance to mass transfer (water film transport). As the cyclic siloxane D5 is hydrophobic ($\log K_{ow} = 5.71$ at 25°C for D5 (Chandra, 1997)), D5 is poorly soluble, therefore the water film retarded mass transfer (Figure 6-7a). In contrast, the linear siloxane L2 is less hydrophobic ($\log K_{ow} = 4.76$ at 25°C (Chandra, 1997)) and as such the water film presents less resistance to mass transfer (Figure 6-7b) compared to the effect on D5 (81% decrease in adsorption capacity when humidity was increased from 0% to 100% at $Re = 3.6$, Figure 6-7a). This is analogous to observations made during the vapour phase adsorption of the readily soluble DMMP (solubility, $3.22 \times 10^5 \text{ mg l}^{-1}$) from humid air (Busmundrud, 1993). However, the D5 carbon adsorption capacity was found not to decrease with humidity at the higher Re tested ($Re > 73$, Figure 6-5) which can be ascribed to the velocity gradient induced under transitional conditions, which ostensibly diminishes the development of a water film. Consequently, whilst vapour phase adsorption in humid gas under low Re will favour the adsorption of more soluble adsorbates, for siloxane adsorption in humid gas at higher Re , it can be inferred that the more strongly adsorbing D5 will displace the lower molecular weight linear compounds as demonstrated in this study for dry gas (Figure 6-6) (Matsui and Imamura, 2010; Gaur et al.,

2010). This is supported by anecdotal evidence from operation of full-scale carbon contactors for siloxane removal in humid gas where L2 displacement has been observed before cyclic siloxane breakthrough (Griffiths, 2012). Unexpectedly, a 12% increase in media capacity was observed at Re 73 when humidity was increased from 10% to between 30% and 80% (Figure 6-5). Whilst the specific mechanism for this small increase in capacity is unclear, relatively little is understood about multicomponent vapour phase equilibria, with this area warranting further study (Pei and Zhang, 2012; Huang et al., 2006). Importantly, this study provides evidence for the role of Re in enhancing vapour phase adsorption which is significant as until now most laboratory analysis has been conducted under laminar conditions.

6.5 Supporting information

6.5.1 Materials and methods

Carbon dioxide is split into four streams: dry, water-saturated, D5 saturated, and L2 saturated, which are mixed to form model biogas. The model biogas is passed through a glass column containing activated carbon and the siloxane concentration is monitored using a FTIR spectrometer (**Figure S6-8**). For more detail, see main paper. To demonstrate the repeatability of the breakthrough curves generated using the test rig, duplicate breakthrough curves were generated and compared. The difference in calculated adsorption capacities was 4% (Figure S6-9). The test rig was designed to run experiments at Reynold's numbers above and below the laminar/turbulent regime boundary ($Re = 40$, (Chilton and Colburn, 1931)).

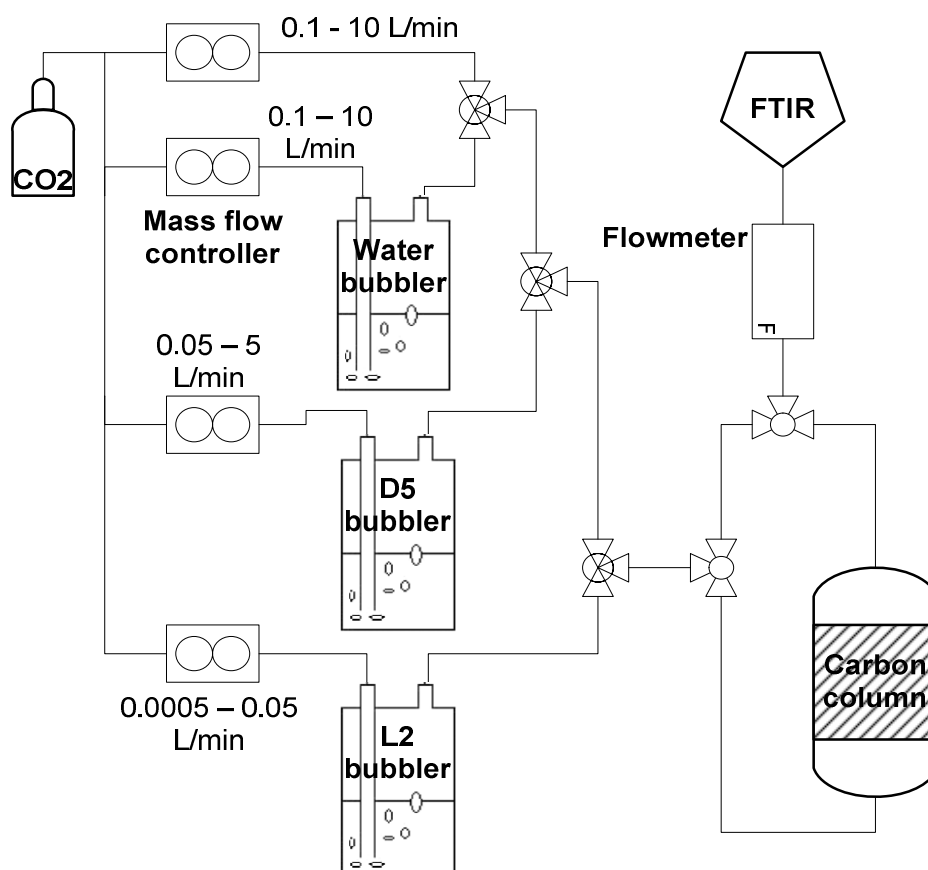


Figure S6-8. Test rig schematic

6.5.2 Capillary condensation

The pore size distribution of the activated carbon used in this study (after grinding and sieving) was measured using BJH adsorption (Figure S6-10). The average pore size is 50.3 nm. The Kelvin equation is used to describe capillary condensation (Butt et al., 2006):

$$\ln\left(\frac{P_p}{P_{sat}}\right) = -\frac{2\gamma V_m \cos\theta}{RT r_c} \quad (\text{S6-3})$$

where P_p is the partial pressure of vapour in the atmosphere (i.e. water in carrier gas); P_{sat} is the vapour pressure of the liquid (1228 Pa for water at 10°C); P_p/P_{sat} is the relative humidity of the atmosphere; V_m is the molar volume of the liquid (18.02 cm³ mol⁻¹ for water at 10°C); γ is the liquid/vapour surface tension (0.0742 N m⁻¹ for water in air at 10°C (Vargaftik et al., 1983)); R is the universal gas constant (8.314 J mol⁻¹ K⁻¹); T is the temperature (293.15 K (10°C)); r_c is the capillary radius; θ is the wetting angle of the liquid on the solid (approximately 70° for water on carbon (Tadros et al., 1974)); $r_c/\cos\theta$ is the radius of curvature of the meniscus; $2\cos\theta/r_c$ is the mean curvature of the meniscus.

The Kelvin equation may be used to calculate the relative humidity required to cause capillary condensation to occur in a pore of a given diameter. For capillary condensation to occur in a pore of the average diameter (50.3 nm) would require 99.3% humidity (Figure S6-11). At 80% humidity (the maximum used in the main experiments) capillary condensation will occur in pores with a maximum diameter of 2 nm. This accounts for less than 0.1% of the pores in the carbon used in this study, indicating that no significant capillary condensation occurred.

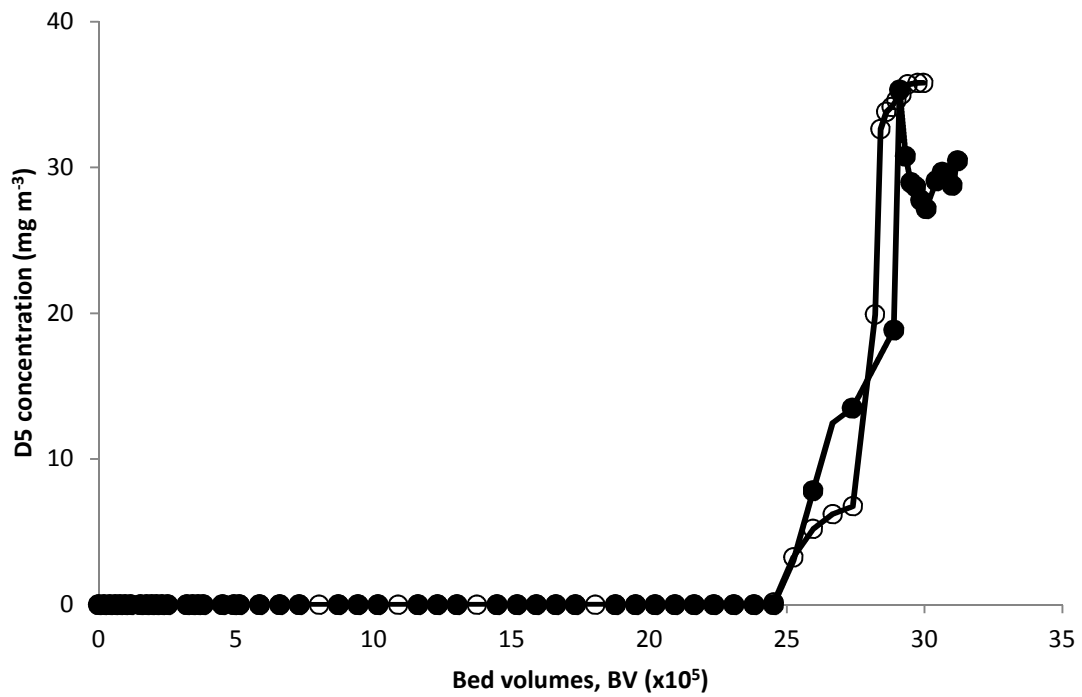


Figure S6-9. Comparison of two breakthrough curves generated using the test rig under the same conditions on different dates, demonstrating the repeatability of data generated using the test rig. The adsorption capacities calculated from these curves are $354 \text{ g}_{\text{D5}} \text{ kg}^{-1}_{\text{carbon}}$ and $342 \text{ g}_{\text{D5}} \text{ kg}^{-1}_{\text{carbon}}$ (4% error). (Inlet concentration = $70 \text{ mg}_{\text{D5}} \text{ m}^{-3}_{\text{CO2}}$; humidity = 80%; $\text{Re} = 73$; $\text{EBCT} = 0.031 \text{ s.}$)

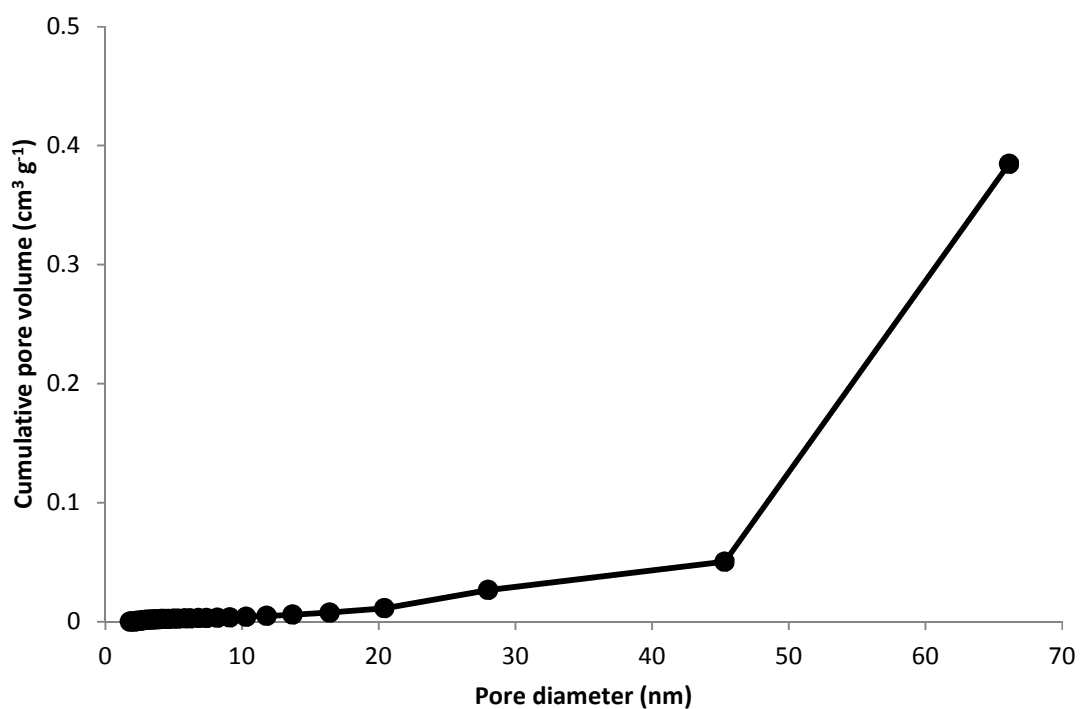


Figure S6-10. Pore size distribution of activated carbon

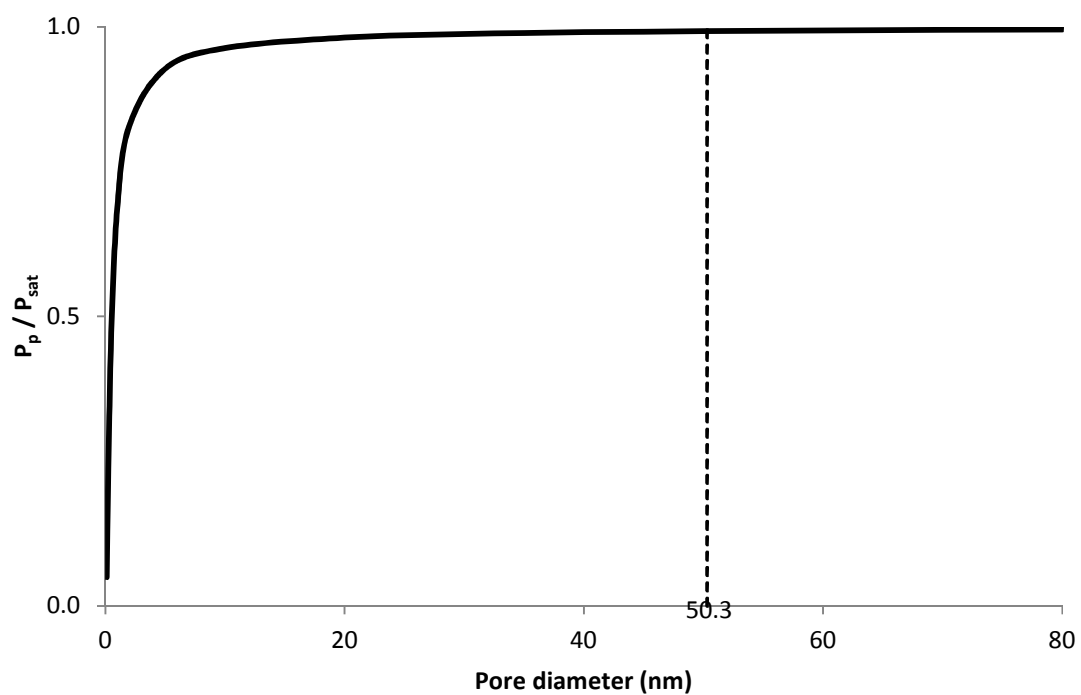


Figure S6-11. The Kelvin equation may be used to calculate the relative humidity required to cause capillary condensation in a pore of a given diameter.

6.5.3 Use of the modified Wheeler equation to calculate rate constants

A rate constant was also calculated from the breakthrough curves using the modified Wheeler equation was also used as described by Busmundrud.(1993) The modified Wheeler equation may be expressed in a linear form so that if $\ln\left(\frac{C_{out}}{C_{in}-C_{out}}\right)$ (in which C_{in} and C_{out} are the inlet and outlet adsorbate concentrations) is plotted against time, the y-intercept is equal to $-k_v L/U_s$ in which L is the bed length, U_s is the superficial gas velocity and k_v is a rate constant (Figure S6). As found by Busmundrud,(1993) the plots produced were not linear over the whole breakthrough period, so the earlier part of the curve was used, as this is equivalent to a low breakthrough concentration. In dry gas, an expression for the relationship between gas velocity and the rate constant ($k_v = 223U_s^{0.23}$) is close to the relationship found by Busmundrud (1993) for toluene in air ($k_v = 260U_s^{0.43}$) over a similar Reynold's number range (10 - 64).

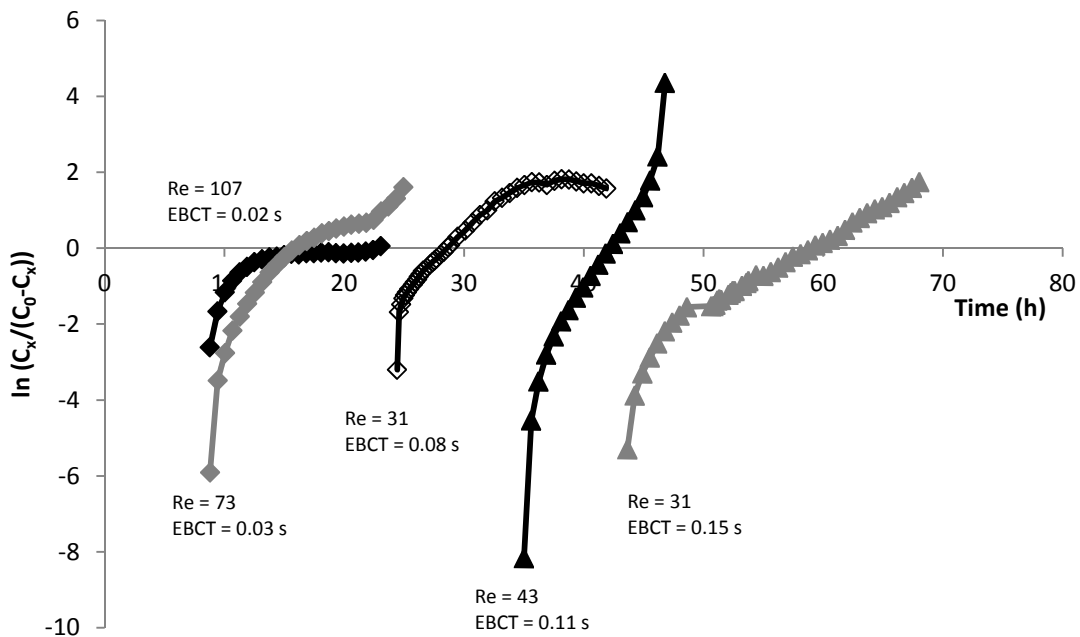


Figure S6-12. Breakthrough curves showing the effect of varying empty bed contact time (EBCT) and Reynold's number. (Inlet concentration = $70 \text{ mg}_{D5} \text{ m}^{-3} \text{ CO}_2$; humidity = 0%; Re = 31 – 107; EBCT = 0.02 – 0.15 s.)

7 Practical implementation

In this thesis, operation of activated carbon vessels for siloxane removal has been studied. The preceding literature review and technical papers have all contributed towards this aim, and benefits from this project are illustrated in Figure 7-1. In this discussion, the practical aspects of implementing the findings of the previous chapters are considered. The discussion is structured around the questions asked by the project sponsors in the final steering group meeting.

7.1 Is on-line FTIR assessment an effective tool?

Fourier transform infrared (FTIR) spectroscopy has been shown to successfully measure cyclic siloxanes in biogas from both upstream and downstream of an activated carbon vessel (chapter three). This represents the first time on-line analysis has been used to assess the performance of full scale siloxane adsorption vessels. Other technologies for siloxane measurement include gas chromatography (GC) and ion mobilisation spectroscopy (IMS) (Table 7-1).

These technologies provide a range of attributes that may be suited to different purposes. GC and IMS have higher sensitivity and lower detection limits than FTIR spectroscopy, however the FTIR's detection limit of 7 mg m^{-3} (improved to 3.2 mg m^{-3} by using the PLS analysis (chapter three)) and ppmv sensitivity is sufficient to confirm if siloxane concentrations are below engine manufacturer's limits of 12 mg m^{-3} (Jenbacher) or 30 mg m^{-3} (Waukesha) and to identify breakthrough of a carbon bed (chapter three), which is the industry requirement. All of the analytical techniques discussed have some issues with interference as biogas is a complex matrix containing over 50 trace gas species (Eklund et al., 1998). Arnold and Kajolinna (2010) described interpretation of the gas chromatograph produced for their raw biogas samples as "quite demanding". Oshita et al. (2010) and this thesis (chapter three) found positive interference in FTIR readings due to overlapping infrared absorption peaks from VOCs. However with careful analysis and calibration, a root mean square error of 10% for cyclic siloxane concentrations was achieved. This is equivalent to the accuracy achieved by Arnold and Kajolinna (2010) using field GC.

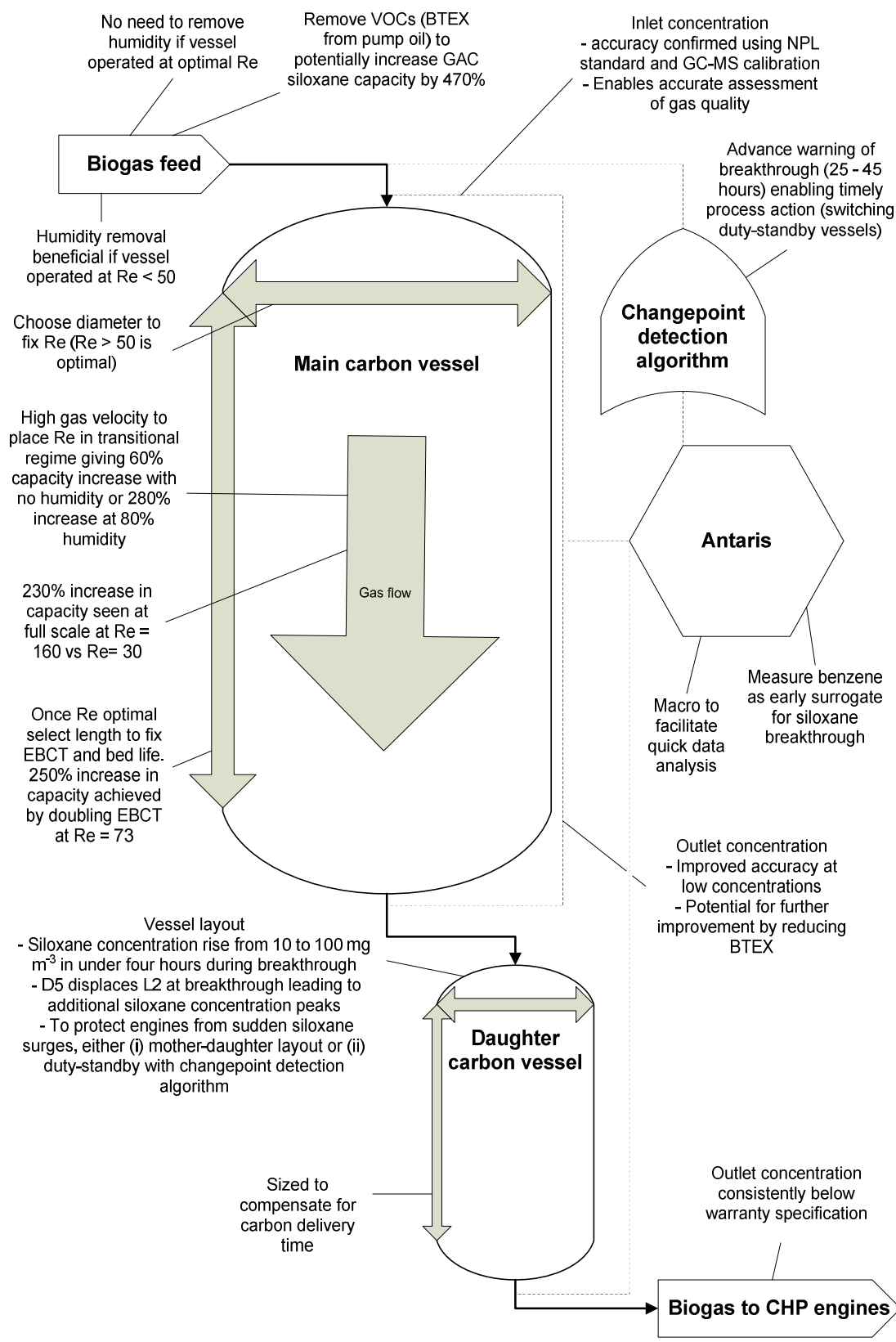


Figure 7-1. Schematic showing the outcomes of this project

However it is probable that Arnold and Kajolinna’s work has not yet penetrated the field GC industry: anecdotally, when an instrument to use in this project was being sourced, the lead GC supplier for this application, stated that they were not comfortable with using the GC on raw biogas, only downstream of carbon contactors. At the same time a supplier of A-IMS, stated that their instrument was not suitable for use with raw biogas due to the complexity of the gas matrix. In contrast this project has demonstrated that an industry-ready FTIR spectrometer is capable of measuring siloxanes in both raw and treated biogas. This capability is important because upstream siloxane concentration data is required to fully analyse adsorption vessel performance and long term trends may be monitored and linked to changes in the wastewater supply, whilst downstream siloxane concentration data inform the operator about the current performance of the adsorption vessel and whether the biogas conforms to engine manufacturer’s specifications.

Table 7-1. Instruments available for on-line measurement of siloxanes in biogas

Technique	Fourier transform infrared spectroscopy	Gas chromatography	Ion mobilisation spectroscopy
Speciation	Linear/cyclic siloxanes	Individual siloxanes	Total siloxanes
Location	Upstream & downstream	Upstream ^a & downstream	Downstream only ^b
Sensitivity	ppmv	ppmv	ppbv
LOD	7 mg m ⁻³ (460 ppbv) ^c / 3.2 mg m ⁻³ (210 ppbv) ^d	50 ppbv	ppbv
Accuracy	10% ^c / 9.7% ^d	nd	nd
Weight	60 kg	6 kg	13 kg
Run time	2 mins	30 mins	< 1 min
Cost	£35,000 ^e - £50,000 ^f	£60,000 - £70,000 ^e	£30,000 ^e
Calibration gas usage	n/a (calibration only required once during set-up)	0.30 L calibration ⁻¹	nd
Carrier gas usage	n/a	1.25 L h ⁻¹	nd

n/a = not applicable. nd = no data. ^aManufacturer uncomfortable with upstream use. ^bManufacturer would not supply for upstream use. ^cAs given by manufacturer. ^dUsing PLS analysis (chapter three). ^eSingle point. ^fMultipoint.

Engine manufacturer's limits are usually published in terms of total silicon per unit of methane, so the ability of the FTIR to differentiate between cyclic and linear siloxanes is more than sufficient. Individual siloxane speciation, achievable using GC, is not required. In fact, it may be argued that only cyclic siloxanes need to be measured as they make up 85 – 100% of the siloxanes measured in sewage-sludge derived gas (chapter three). The PLS analysis undertaken (chapter three) improved the correlation between FTIR spectroscopy and laboratory GC-MS results for linear siloxanes both upstream (RMSE = 11.7 to RMSE = 2.3) and downstream (RMSE = 7.4 to RSME = 0.44). Only eighteen FTIR spectra and corresponding laboratory GC-MS siloxane measurements from real biogas were available in this study, so further refinement of the PLS method will be possible if more samples are analysed. In particular, the downstream samples were over a limited concentration range, so expanding this range would be beneficial. FTIR spectroscopy also has several advantages over the other analytical techniques regarding ease of operation for the user (i.e. the water utility technicians): FTIR spectroscopy does not require the use of carrier or purging gas and is only calibrated once, during the initial set-up. GC and IMS require recalibrating daily and both require a supply of carrier gas (usually nitrogen) (Photovac, 2012; Rubinson and Rubinson, 2000), so additional technician time and training is needed. The Antaris FTIR spectrometer can run automatically, cycling through the sampling points including taking a daily background reading with the gas cell evacuated, or to take a manual reading or background reading requires a single mouse click. This minimises operator time requirement, which is a key consideration as employee costs account for 25% of water utilities' operating costs (Severn Trent Water, 2013a).

The Antaris IGS has been installed at Minworth Sewage Treatment Works (STW) for over ten months where it has provided useful data regarding both the extent of siloxane contamination in the biogas and the performance of the siloxane adsorption vessels. The data intensity provided by the Antaris is much greater than was previously achieved using bag sampling: bag samples were

taken twice a week (insufficient to capture siloxane breakthrough) whilst the Antaris takes hourly readings for each contactor. To achieve the data intensity provided by the Antaris (six data points per hour – one upstream of the carbon vessels and one downstream from each of the five carbon vessels / vessel pairs) using bag samples would cost £613,200 per annum (£60 per sample for total siloxanes analysis and £10 per gas bag). Bag sampling twice a week costs £43,680 per annum. The Antaris cost £50,000 (including installation and set-up) if multipoint sampling is required or £35,000 for single point sampling and requires an annual service costing £1500. This gives it a payback period of 14 months compared to the original bag sampling programme. This payback period estimate does not include savings due to reduced operator time requirement, increased engine availability, decreased oil change frequency or lower reactive maintenance costs (see chapter three). Breakthrough curves generated using data from the Antaris are much more data intense than those generated using bag sampling data – the discovery made in this thesis (chapter three) that siloxane concentrations could rise from the baseline to over 100 mg m⁻³ in less than four hours during breakthrough was only possible by using on-line data. This thesis produced the first usable siloxane breakthrough curves of full scale carbon vessels (chapter three). The other critical benefit of on-line data analysis is receiving immediate results, unlike bag sampling which incorporates a lag of around three to four days between taking the sample and receiving the results from the lab. In the three days after breakthrough, the mass of siloxane entering the engine can equal the mass that entered the engine over the 18 days before breakthrough, doubling the potential damage (chapter three). Under the current procedure, the adsorption vessels are run for four weeks between carbon changes, meaning for half of the time they are in use they provide no engine protection at all. It is estimated in chapter three, based on the experience of Tower and Wetzal (2006) in the United States, that over £237,000 per year can be saved at Minworth STW by using on-line analysis to detect breakthrough and manage the carbon vessels to enhance engine protection. This leads to a payback period for the Antaris of two months.

Allowing an engine to run after siloxane breakthrough in the associated carbon bed for even a short time can account for a significant proportion of the siloxane damage. According to J. Griffiths, head CHP technician at Minworth STW, the performance of the engines is noticeably impacted when breakthrough occurs (Griffiths, 2014). This problem is thought to be enhanced by the “rush” of linear siloxanes displaced by cyclic siloxanes just before cyclic siloxane breakthrough – an effect which was first practically demonstrated in this thesis (chapter six). Consequentially, the earliest possible warning of breakthrough is desirable. The changepoint detection algorithm (developed in chapter four) can provide an early warning of 25 – 45 hours and would be straightforward to incorporate into either the Macro designed by the author for data analysis and/or a new alarm system to alert engine operators to breakthrough. However this is only at proof-of-concept stage and requires further work to reduce false-positive errors before it can be implemented (chapter four). Another, potentially simpler method could be to use the Antaris to measure breakthrough of other VOCs. One of the most common uses of FTIR spectroscopy is identification of organic compounds and FTIR spectroscopy can explicitly measure over 200 VOC species (Stuart, 2004). It has been demonstrated that D5 displaces L2 on adsorption sites when the carbon nears D5 saturation, so L2 breakthrough precedes D5 breakthrough (chapter six). It is postulated that D5 may also displace other, smaller, adsorbed molecules, such as benzene (shown in chapter five to be adsorbed in the siloxane removal vessels). Under this assumption, benzene would break through before either linear or cyclic siloxanes as it is a smaller molecule. Benzene breakthrough would therefore be a sign of near-saturation of the carbon, and measuring benzene concentrations in the outlet biogas could provide early-warning of siloxane breakthrough (both linear and cyclic).

7.2 How do we best enhance media capacity in practice?

A significant proportion of research into siloxane adsorption has been focussed on finding the adsorbent with the highest capacity for siloxanes (chapter two). However, few have identified the criticality of process parameters to siloxane removal. A single activated carbon has been used throughout this thesis, which

has demonstrated that increases in capacity can be achieved by changing operational parameters (such as the Reynold's number and humidity of the biogas) which are as great as those achieved by changing adsorbent. The most important finding of this thesis is the effect of Reynold's number on media capacity. In dry model biogas, the adsorption capacity of activated carbon was found to increase by 36% when Reynold's number was increased from 31 to 107 (chapter six). This Reynold's number range sites gas flow on either side of the boundary between the laminar and transitional flow regimes ($Re = 40-55$ (Crittenden and Thomas, 1998; Chilton and Colburn, 1931)). Busmundrud (1993) identified a correlation between a rate constant and linear velocity over a similar Reynold's number range and Wakao and Funazkri (1978) demonstrate that axial dispersion is important for the gas phase mass transfer at low Re . At Reynold's numbers within the laminar regime, Taylor-Aris axial dispersion (characteristic of the laminar regime (Cussler, 2009)) is still dominant but as the Reynold's number increases turbulent dispersion begins to take over, increasing the media capacity (chapter six). In model gas at 100% humidity, the increase in media capacity was greater: 410% when Reynold's number was increased from 31 to 73 (chapter six). This phenomenon, first evidenced for siloxanes in this thesis, was also demonstrated at full scale: in real biogas also at 100% humidity, the media capacity increased by 400% when Reynold's number was increased from 30 to 80 (chapter five).

The effect of humidity on the adsorption capacity of the activated carbon is strongly affected by the Reynold's number. In model gas under near-laminar conditions ($Re = 31$) the capacity was increased by 95% by reducing the humidity from 80% to zero (chapter six). The pores in the carbon were too large for capillary condensation to occur at these humidities, so this is due to the reduction in the resistance to siloxane transport caused by the water film on the carbon particles (Habuka et al., 2013; McCoy and Rolston, 1992). However at $Re = 73$ the same reduction in humidity had little effect (chapter six). If a high Reynold's number is unattainable, then reducing humidity will enhance the media capacity. In practice this could be achieved by drying the biogas but for

Minworth STW this would require approximately 100 kW of power, costing around £250,000, equating to £100,000 per annum in lost revenue. If practical, increasing Reynold's number will be a cheaper and more effective way to improve media capacity.

Reducing competing VOCs may have a beneficial effect on the media capacity for siloxanes, but the evidence for this is not clear cut. VOCs other than siloxanes are also adsorbed by the activated carbon (chapter five) but many of the smaller VOC molecules may be adsorbed in pore space that cannot be accessed by siloxane molecules due to their size (chapter two). The average pore size of the carbon media used at Minworth STW is 2.2 nm, twice the molecular diameter of D5. The competition experiment carried out in chapter six also suggests that adsorbing a smaller molecule (in this case L2, but potentially other VOCs) does not affect the ultimate adsorption capacity for D5 as the L2 was desorbed when adsorption sites became scarce. This contradicts findings from other studies, for example Ricaurte Ortega and Subrenat (2009a) found that in batch adsorption adding 10 mg m⁻³ of toluene to their model biogas resulted in a 50 g kg⁻¹ reduction in the L2 adsorption capacity of activated carbon cloth. Anecdotally it is suggested that the VOC load might be significantly reduced by changing the pump housing of the gas mixing pumps in the anaerobic digester so oil cannot come into contact with sludge or biogas as BTEX compounds (benzene, toluene, ethylbenzene and xylenes) account for nearly 50% by mass of the VOC load (not including siloxanes) in the biogas (chapter five). However, further research is needed to validate this assertion and to ascertain whether this would be beneficial or economical.

The literature review (chapter two) identified that a wide variety of media have been tested for their suitability as siloxane adsorbents. Matsui and Imamura (2010) tested twenty-two different types of activated carbon and found adsorption capacities for D4 varied between 56 g_{D4} kg⁻¹_{carbon} and 192 g_{D4} kg⁻¹_{carbon}. This range is smaller than the range of capacities found in this thesis for a single activated carbon (69 - 369 g_{D5} kg⁻¹_{carbon}) by changing the Reynold's

number and humidity. The highest adsorption capacity evidenced in the literature ($878 \text{ g}_{\text{D3}} \text{ kg}^{-1}_{\text{carbon}}$; $3.95 \text{ mol}_{\text{D3}} \text{ kg}^{-1}_{\text{carbon}}$) was achieved with a specially modified adsorbent: activated carbon impregnated with copper salts (Finocchio et al., 2009; Montanari et al., 2010). This is approximately six times the mean capacity achieved by the activated carbon used in this thesis ($220 \text{ g}_{\text{D5}} \text{ kg}^{-1}_{\text{carbon}}$; $0.59 \text{ mol}_{\text{D5}} \text{ kg}^{-1}_{\text{carbon}}$). The price of the activated carbon tested by the research group of Finocchio and Montanari is not known but prices of standard activated carbon available from Norit Activated Carbon vary from $\text{£}1.57 \text{ kg}^{-1}$ to $\text{£}3.30 \text{ kg}^{-1}$, which suggests that the price of a specialised activated carbon is likely to be more than double that of the carbon used in this thesis, which is at the lower end of this scale. Further research may be needed before a cost-benefit analysis can be carried out to assess the benefits of using an alternative media, but this thesis has shown that it is as important to optimise the design of the adsorption vessel.

7.3 What is the optimum carbon vessel design for siloxane removal?

7.3.1 For new carbon contactors

When the carbon vessels at Minworth (STW) were designed, there was little data available relating to the design of adsorption vessels for siloxane removal, so the vessels are not optimally designed. This project has produced some guidelines for the design of carbon vessels. When siloxane removal is implemented at additional sewage treatment works these guidelines should be followed.

To ensure gas flow is evenly distributed across the carbon bed and to reduce the potential for channelling to occur near the walls of the carbon vessel, a minimum particle diameter to vessel diameter ratio should be observed; Chilton and Colburn (1931) suggest that a ratio above 10 gives negligible wall effects whereas Cooney (1999) recommends a minimum ratio of 20. The ratio used in the test rig experiment was 11 – 17, which indicates that the wall effect factors were relatively small. Further evidence for the industrial relevance of the data

provided by the test rig is the similarity in shape of breakthrough curves produced at full scale (chapter five) and at bench scale (chapter six). The carbon beds at Minworth (STW) have particle diameter to vessel diameter ratios of 129 – 229, giving wall effect factors approaching 1.0. For a new siloxane vessel, this ratio provides a minimum vessel diameter.

In chapters five and six it was shown that the media capacity is significantly increased (by 36% in dry gas or 410% at 80% humidity, chapter six) if the bed is operated at Reynold's numbers greater than 55, i.e. in the transitional regime (chapter six). The boundary between the laminar and transitional regimes in packed beds was significantly characterised by Chilton and Colborn (1931) who demonstrated general agreement across numerous studies for both gas and liquids that the critical Reynold's number for transition from viscous to transitional was 40 - 50. Further refinement from later researchers enabled correlations to be derived that explicitly describe the different mass transfer behaviour in these two discrete regions of flow, often separated at $Re = 40 - 55$ (e.g. (Chilton and Colburn, 1931; Lightfoot et al., 1962; Wilson and Geankoplis, 1966)). Most carbon vessels at Minworth STW have Reynold's numbers of above 55 ($Re = 65 - 162$) with the exception of GAC4 which has a Reynold's number of 30, although a benefit from increased Reynold's number was still noted in the higher Re range (chapter five). The increase in media capacity was observed to plateau above Reynold's numbers of approximately 100 (chapter five). It has been demonstrated by Wakao and Funazkri (1978) and Urban and Gomezplata (1969) that the axial Peclet number asymptotically approaches a value of 2 at Reynold's number of approximately 100, leading to no further increase in dispersion, and hence no further increase in media capacity. The diameter of the vessel should therefore be chosen so that the Reynold's number will be greater than 55, but increasing Re beyond 100 will not give further benefit. In general, a smaller diameter will lead to a larger Reynold's number, but the minimum diameter to prevent wall channelling should be observed.

The length can then be chosen based on: (i) the minimum empty bed contact time required; and, (ii) the desired time between bed changes. The empty bed contact time (EBCT) for a gas application is much shorter than those used in liquid applications (typically around 1.5 – 7.5 minutes for water (American Water Works Association, 1999)) as the low Schmidt number of gases compared to liquids leads to mass transfer rates which are several orders of magnitude higher (Wakao and Funazkri, 1978; Cooney, 1999). EBCTs used in full scale siloxane studies have varied from 0.25 s (Pirnie, 2011) to 28 s (Tower and Wetzel, 2004). The EBCTs of the Minworth carbon vessels range from 12 to 16 s although GAC4 has an unusually long EBCT of 56 s. Chapter six showed that increasing EBCT had a positive effect on adsorption capacity when EBCT and Re were varied independently. When designing a new carbon vessel, it is possible to decouple EBCT and Re by changing the aspect ratio. The longer the vessel, the longer the contact time and the operating time between bed changes. However the bed length is limited by the allowable pressure drop across the bed. Pressure drop (ΔP) can be calculated according to equations 3 and 4 (adapted from Crittenden and Thomas, 1998).

$$\text{Pressure drop} = \Delta P = \frac{LfQ^2}{2x\rho} \quad (3)$$

$$f = \frac{805}{Re} \quad \text{for } Re < 40 \quad (4)$$

$$f = \frac{38}{Re^{0.15}} \quad \text{for } Re > 40$$

in which L is the bed length, f is a dimensionless friction factor calculated using equation 4 (Chilton and Colburn, 1931), Q is the volumetric gas flowrate, x is the adsorbent particle diameter, ρ is the gas density and ϵ is the bed voids fraction. Bed lengths for full scale siloxane studies have ranged from 1.86 m (Tower and Wetzel, 2004) to 2.4 m (Pirnie, 2011), and bed lengths for Minworth carbon vessels range from 1.9 – 3.7 m.

7.3.2 Adapting existing vessels

The advice above is intended for the design of new vessels; this section considers how existing assets can be adapted or operated differently to improve performance. In most cases the aim is to maximise the Reynold's number in the adsorption vessel by maximising the superficial gas velocity (U_s). This can be achieved in two ways: (i) gas management or (ii) changes to contactor arrangement. CHP engines are often not operated at full load, so that spare capacity is available if gas production increases. In the case of an array of engines, each with a carbon contactor upstream, then the minimal number of engines should be run at maximum load. For example, rather than operating two engines at half load, one engine should be operated at full load, with the second engine only brought into service when the gas flow available exceeds the maximum for one engine. This will increase the gas velocity through the adsorption vessel which treats gas for the operating engine and therefore increase the Reynold's number. Running engines at full load rather than half load also improves the efficiency of CHP engines (Vale, 2014). Where multiple adsorption vessels are run in parallel at low Re (not duty-standby), these should be arranged to run in series. This increases both the gas velocity (and hence Re) and the empty bed contact time as the combined vessels can be treated as a single vessel with the same diameter but increased height. This rearrangement causes the Reynold's number to double, as the cross-sectional area is halved (equations 1 and 2). Based on results from this thesis, Cranfield University advised that two contactor pairs (GAC4 and GAC5, chapter five) at Minworth STW should be rearranged in this way. This has resulted in a significant increase in bed life (corresponding to enhanced adsorption capacity) (Griffiths, 2014). Rearranging vessels is a more expensive option than changing the gas load as new pipework may be required, but, once completed, operation is simpler and greater flexibility is attainable. Installation of new pipework for existing vessels costs around £5,000. Increasing the Reynold's number from 30 to 80 equates to a 400% increase in media capacity in full scale vessels (chapter five) so assuming the carbon was originally replaced

every four weeks (chapter five) at a cost of £5000 (£1.684 kg⁻¹ for 3000 kg, not including labour) then Replacing the carbon in a 3000 kg vessel costs £5000 (£1.684 kg⁻¹, not including labour) then the new pipework will be paid for in two months. Replacing the vessels is also feasible. The cost of two new 425 kg carbon contactors (£1430 per carbon change) and associated pipework is around £30,000, so if two vessels run at Re = 31 were replaced with two vessels run at Re = 73 (by increasing the vessel aspect ratio) then the payback time for the new vessels will be two years.

7.3.3 Vessel layouts

Many operators, for example the Orange County Sanitation District (Pirnie, 2011), use a single adsorption vessel to treat biogas, as this is the simplest and least capital intensive layout. This thesis proposes two further layouts (duty-standby and mother-daughter, Figure 2) which can provide better engine protection by reducing or eliminating the lag period between observing a high siloxane concentration measurement and either shutting down the engine for carbon replacement or switching to a new duty vessel. This period can be critical in terms of engine protection because high linear siloxane concentrations have anecdotally been observed during breakthrough when larger siloxane molecules displace smaller molecules on adsorption sites, as demonstrated in chapter six. In addition, many biogas sites cannot sacrifice the revenue whilst waiting for fresh carbon so instead run the CHP engines on untreated biogas.

The duty-standby vessel layout (Figure 7-2) is commonly used at larger sites (Tower and Wetzel, 2004) and in particular is often used for adsorbents or ion-exchange media which can be regenerated in situ, for example PpTek media (PpTek, 2014). Two vessels are connected in parallel; when the adsorbent in the duty vessel becomes saturated, the gas flow is switched to the standby vessel and the media in the duty vessel is replaced or regenerated. To prevent pressure surges in the pipework, the ATEX rated valve switching is actuated over a period of 30 minutes (Hunt, 2012). If the duty vessel is operated to a set point concentration (e.g. 30 mg m⁻³, chapter four), gas which exceeds the

engine manufacturer's siloxane concentration limit will be entering the engine during this period. It is recommended that the duty-standby layout is operated in conjunction with the changepoint detection algorithm (chapter four), which will give sufficient early warning (25 - 45 hours) to switch between vessels.

The mother-daughter layout (Figure 7-2) is the most complex of the layouts. Verdesis use three vessels connected in series and replace them as they saturate. The difference between the Verdesis system and the mother-daughter system is that using the mother-daughter layout, both vessels are changed at the same time. A large vessel (sized as described in the previous section) is connected in series with a small vessel, sized to adsorption siloxanes during the lag time between ordering and received adsorbent media. The siloxane concentration is monitored between the vessels and when breakthrough occurs in the large vessel, fresh adsorbent is ordered and both adsorbent beds are replaced at the same time. This minimises cost as only one call-out charge is incurred for both vessels whilst the media is used efficiently and continuous engine protection is provided.

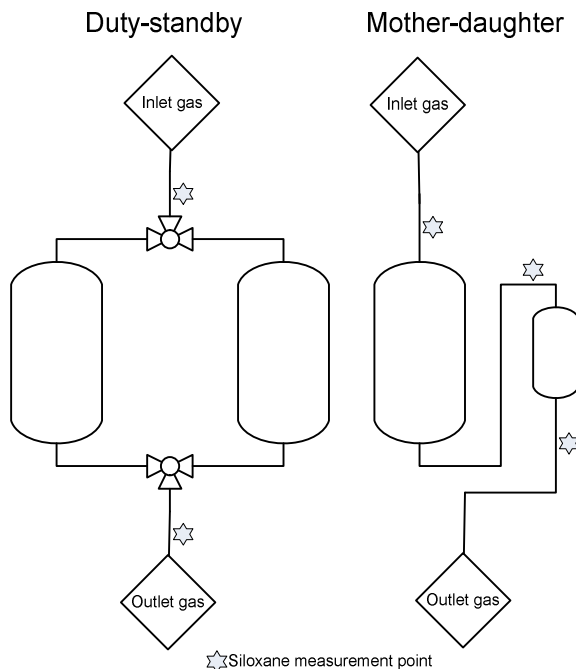


Figure 7-2. Proposed contactor layouts

7.4 How is this understanding of contactor design integrated into existing practice?

The new insight into contactor design developed in this thesis has already been put into practice by Severn Trent Water. An extreme case of siloxane contamination at Strongford Sewage Treatment Works (STW) led to the rapid implementation of new siloxane removal plant. Over a period of three months, siloxane concentrations of approximately $20,000 \text{ mg m}^{-3}$ were found in the biogas with $300 - 500 \text{ mg m}^{-3}$ reaching the CHP engines. Two engine decokes were required at a cost of £100,000 each and the activated carbon in the original siloxane removal system required changing twice a week at a cost of £800 per day for labour. The new plant was designed according to a technical note provided by the author, which incorporated some of the advice given in this and the previous section (7.3 and 7.4). Two 425 kg carbon vessels from another site were installed in series at Strongford STW giving a total carbon mass of 850 kg. The cost of installation, including moving the vessels and installing them with associated pipework at Strongford, was around £30,000 – 15% of the cost of the two decokes.

8 Conclusions and Future Work

8.1 Conclusions

This thesis has extended understanding of siloxane adsorption from biogas onto activated carbon. The following conclusions may be drawn from this work.

1. On-line Fourier transform infrared spectroscopy is a valuable tool for monitoring siloxane concentrations in biogas both upstream and downstream of activated carbon vessels. Good linearity was achieved between FTIR spectroscopy and the standard methodology. A limit of detection of 3.2 mg m^{-3} was achieved. (Objective 1)
2. On-line siloxane analysis can provide enhanced engine protection (compared to grab sampling) by timely identification of siloxane breakthrough, reducing the siloxane load on CHP engines by up to 80%, leading to cost savings of up to $\text{£}0.007 \text{ kWh}^{-1}$ and a payback period of two months. (Objectives 2 and 3)
3. Using on-line analysis, it has been shown that, prior to breakthrough, carbon vessels consistently remove siloxanes to below engine manufacturers' warranty limits despite fluctuations in the inlet gas concentration. (Objective 4)
4. Full-scale carbon vessels are commonly operated near the boundary between the laminar and transitional regimes. In this region, increasing the Reynold's number leads to increased dispersion, broadening of the breakthrough profile and enhanced capacity under dynamic adsorption conditions. (Objective 4)
5. Moving from the laminar into the transitional regime by increasing Reynold's number reduces the negative effect of humidity on media capacity by preventing the formation of a water film on the carbon particles. (Objectives 4 and 5)
6. Reynold's number may be decoupled from empty bed contact time by changing the aspect ratio of a carbon vessel. Carbon vessels should be

designed to be tall and thin – this maximises both Reynold's number and empty bed contact time. (Objective 4)

7. When activated carbon nears saturation, previously adsorbed smaller siloxane molecules (L2) are displaced by larger siloxane molecules (D5), leading to a surge of L2 in the outlet gas. (Objective 5)

8.2 Future Work

A number of areas where further work would be beneficial have been identified during this project.

1. The stability and precision of the partial least squares method developed for the Fourier transform infrared spectrometer may be improved by carrying out further calibration work using new FTIR spectra and corresponding GC-MS siloxane measurements.
2. The principle of using a statistical method to provide early warning of the onset of siloxane breakthrough was demonstrated in chapter four, but further work is needed to develop an algorithm with a reduced rate of errors, either by optimising the proposed changepoint detection algorithm or by developing a new algorithm.
3. Further investigation into the displacement of VOCs by siloxanes when carbon nears saturation could lead to a method of achieving early-warning of siloxane breakthrough by monitoring the outlet concentration of a smaller VOC (e.g. benzene).
4. More generally, further investigation into whether competition between siloxanes and other VOCs for adsorption sites affects the adsorption capacity for siloxanes would be welcome, as the evidence from batch experiments contradicts evidence from dynamic experiments (this thesis).
5. The role of the water film in controlling media capacity in the laminar and transitional regimes is not fully understood. In particular, at a Reynold's number of 73, a small positive effect on media capacity was evidenced when the humidity was increased (chapter six). The mechanism behind

this is not yet known. Further investigation into this mechanism would be welcome.

REFERENCES

- Abdel-Hadi, M. A. (2009), "Determination of methane content by measurements of flame temperature and voltage from biogas burner", *Misr Journal of Agricultural Engineering*, vol. 26, no. 1, pp. 498-513.
- Abiko, H., Furuse, M. and Takano, T. (2010), "Quantitative Evaluation of the Effect of Moisture Contents of Coconut Shell Activated Carbon Used for Respirators on Adsorption Capacity for Organic Vapors", *Industrial health*, vol. 48, no. 1, pp. 52-60.
- Accettola, F., Guebitz, G. M. and Schoeftner, R. (2008), "Siloxane removal from biogas by biofiltration: Biodegradation studies", *Clean Technologies and Environmental Policy*, vol. 10, no. 2, pp. 211-218.
- Adams, R. P. and MacKay, D. J. C. (2007), *Bayesian online changepoint detection*, Technical report, University of Cambridge, Cambridge.
- Ajhar, M., Travesset, M., Yüce, S. and Melin, T. (2010a), "Siloxane removal from landfill and digester gas - A technology overview", *Bioresource technology*, vol. 101, no. 9, pp. 2913-2923.
- Ajhar, M., Wens, B., Stollenwerk, K. H., Spalding, G., Yüce, S. and Melin, T. (2010b), "Suitability of Tedlar® gas sampling bags for siloxane quantification in landfill gas", *Talanta*, vol. 82, no. 1, pp. 92-98.
- American Water Works Association (1999), *Water quality and treatment: a handbook of community water supplies*, 5th ed, McGraw-Hill, New York.
- Anfruns, A., Martin, M. J. and Montes-Morán, M. A. (2011), "Removal of odourous VOCs using sludge-based adsorbents", *Chemical Engineering Journal*, vol. 166, no. 3, pp. 1022-1031.
- Appels, L., Baeyens, J., Degreè, J. and Dewil, R. (2008), "Principles and potential of the anaerobic digestion of waste-activated sludge", *Progress in Energy and Combustion Science*, vol. 34, no. 6, pp. 755-781.
- Applied Filter Technology (2011), *SAGPack information sheet*, , Applied Filter Technology, Available at: <http://appliedfilter.com/products/sagpack/> Accessed on: 24/10/11.
- Arnold, M. (2009), *Reduction and monitoring of biogas trace compounds*, , VTT Research notes 2496 VTT, Espoo. 74p. + app.5.
<<http://www.vtt.fi/inf/pdf/tiedotteet/2009/T2496.pdf>> (accessed on 10/10/11).

- Arnold, M. and Kajolinna, T. (2010), "Development of on-line measurement techniques for siloxanes and other trace compounds in biogas", *Waste Management*, vol. 30, no. 6, pp. 1011-1017.
- Bacsik, Z., Mink, J. and Keresztury, G. (2004), "FTIR spectroscopy of the atmosphere I: Principles and methods", *Applied spectroscopy reviews*, vol. 39, no. 3, pp. 295-363.
- Balanay, J. A. G., Crawford, S. A. and Lungu, C. T. (2011), "Comparison of toluene adsorption among granular activated carbon and different types of activated carbon fibers (ACFs)", *Journal of Occupational and Environmental Hygiene*, vol. 8, no. 10, pp. 573-579.
- Bansal, R. C. and Goyal, M. (2005), *Activated carbon adsorption*, CRC Press, Boca Raton, FL.
- Bendini, A., Cerretani, L., Di Virgilio, F., Belloni, P., Bonoli-Carbognin, M. and Lercker, G. (2007), "Preliminary evaluation of the application of the FTIR spectroscopy to control the geographic origin and quality of virgin olive oils", *Journal of Food Quality*, vol. 30, no. 4, pp. 424-437.
- Bertran, E., Blanco, M., Coello, J., Iturriaga, H., Maspoch, S. and Montoliu, I. (1999), "Determination of olive oil free fatty acid by Fourier transform infrared spectroscopy", *Journal of the American Oil Chemists' Society*, vol. 76, no. 5, pp. 611-616.
- Bletsou, A. A., Asimakopoulos, A. G., ††, S., A.S., Thomaidis, N. S. and Kannan, K. (2013), "Mass loading and fate of linear and cyclic siloxanes in a wastewater treatment plant in Greece", *Environmental Science and Technology*, vol. 47, no. 4, pp. 1824-1832.
- Bouhamra, W. S., Baker, C. G. J., Elkilani, A. S., Alkandari, A. A. and Al-Mansour, A. A. A. (2009), "Adsorption of toluene and 1,1,1-trichloroethane on selected adsorbents under a range of ambient conditions", *Adsorption*, vol. 15, no. 5-6, pp. 461-475.
- Boulinguez, B. and Cloirec, P.L., (2009), *Biogas pre-upgrading by adsorption of trace compounds onto granular activated carbons and an activated carbon fiber-cloth*.
- Boulinguez, B. and Le Cloirec, P. (2009), "Removal of trace compounds in biogas by adsorption onto activated carbon materials", *8th World Congress of Chemical Engineering: Incorporating the 59th Canadian Chemical Engineering Conference and the 24th Interamerican Congress of Chemical Engineering*, 23 August 2009 through 27 August 2009, Montreal, QC, .

- Boulinguez, B. and Le Cloirec, P. (2010), "Adsorption on activated carbons of five selected volatile organic compounds present in biogas: Comparison of granular and fiber cloth materials", *Energy and Fuels*, vol. 24, no. 9, pp. 4756-4765.
- Bramston-Cook, E. and Bramston-Cook, R. (2012), "Online, direct measurement of volatile siloxanes in anaerobic digester and landfill gases by gas chromatography with mass spectrometric detection", Air and Waste Management Association (ed.), in: *Air Quality Measurement Methods and Technology Conference 2012*, 24-26 April 2012, Durham, North Carolina, Curran Associates, New York, pp. 438-443.
- Branton, P. and Bradley, R. H. (2011), "Effects of active carbon pore size distributions on adsorption of toxic organic compounds", *Adsorption*, vol. 17, no. 2, pp. 293-301.
- Brunauer, S., Emmett, P. H. and Teller, E. (1938), "Adsorption of gases in multimolecular layers", *Journal of the American Chemical Society*, vol. 60, no. 2, pp. 309-319.
- Busmundrud, O. (1993), "Vapour breakthrough in activated carbon beds", *Carbon*, vol. 31, no. 2, pp. 279-286.
- Butt, H. J., Graf, K. and Kappl, M. (2006), *Physics and Chemistry of interfaces*, 2nd ed, Wiley, Weinheim, Germany.
- Cabrera-Codony, A., Montes-Morán, M. A., Sánchez-Polo, M., Martín, M. J. and Gonzalez-Olmos, R. (2014), "Biogas upgrading: Optimal activated carbon properties for siloxane removal", *Environmental Science and Technology*, vol. 48, no. 12, pp. 7187-7195.
- Cal, M. P., Rood, M. J. and Larson, S. M. (1996), "Removal of VOCs from humidified gas streams using activated carbon cloth", *Gas Separation and Purification*, vol. 10, no. 2, pp. 117-121.
- Cao, S. and Rhinehart, R. R. (1995), "An efficient method for on-line identification of steady state", *Journal of Process Control*, vol. 5, no. 6, pp. 363-374.
- Carrasco-Marín, F., Fairén-Jiménez, D. and Moreno-Castilla, C. (2009), "Carbon aerogels from gallic acid-resorcinol mixtures as adsorbents of benzene, toluene and xylenes from dry and wet air under dynamic conditions", *Carbon*, vol. 47, no. 2, pp. 463-469.
- CERAM (2012), *Analysis of landfill gas and biogas for siloxanes by automated thermal desorption-gas chromatography-mass spectrometry*, CERAM, Stoke-on-Trent, UK.

- Chandra, G. (ed.) (1997), *The handbook of environmental chemistry: Organosilicon materials*, Springer, Berlin.
- Chilton, T. H. and Colburn, A. P. (1931), "Pressure drop in packed tubes", *Industrial and Engineering Chemistry*, vol. 23, no. 8, pp. 913-919.
- Coates, J. (2000), "Interpretation of infra-red spectra, a practical approach", in Meyer, R. A. (ed.) *Encyclopedia of Analytical Chemistry*, Wiley, Chichester, UK, pp. 10815-10837.
- Cooney, D. O. (1999), *Adsorption design for wastewater treatment*, CRC Press LLC, Florida.
- Crittenden, B. and Thomas, W. J. (1998), *Adsorption Technology and Design*, Butterworth-Heinemann, Oxford.
- Crittenden, J. C., Cortright, R. D., Rick, B., Tang, S. R. and Perram, D. (1988), "Using GAC to remove VOCs from air stripper off-gas", *Journal of the American Water Works Association*, vol. 80, no. 5, pp. 73-84.
- Crittenden, J. C., Rigg, T. J., Perram, D. L., Tang, S. R. and Hand, D. W. (1989), "Predicting gas-phase adsorption equilibria of volatile organics and humidity", *Journal of Environmental Engineering*, vol. 115, no. 3, pp. 560-573.
- Cussler, E. L. (2009), *Diffusion: Mass transfer in fluid systems*, 3rd ed, Cambridge University Press, Cambridge.
- Das, D., Gaur, V. and Verma, N. (2004), "Removal of volatile organic compound by activated carbon fiber", *Carbon*, vol. 42, pp. 2949-2962.
- DECC (2013), *Digest of United Kingdom energy statistics chapter six: Renewable sources of energy*, DUKES, Department for Energy and Climate Change, London.
- DEFRA (2011), *Anaerobic digestion strategy and action plan*, DEFRA.
- Dewil, R., Appels, L. and Baeyens, J. (2006), "Energy use of biogas hampered by the presence of siloxanes", *Energy Conversion and Management*, vol. 47, no. 13-14, pp. 1711-1722.
- Dewil, R., Appels, L., Baeyens, J., Buczynska, A. and Van Vaeck, L. (2007), "The analysis of volatile siloxanes in waste activated sludge", *Talanta*, vol. 74, no. 1, pp. 14-19.
- Doczyck, W. (2003), "Reinigung von Deponiegasen, Erfahrungen mit organischen Siliziumverbindungen – Ursachen, Historie, Neue

- Reinigungskonzepte", *Deponiegas*, , pp. 175-187 Cited in: Ajhar, M., Travesset, M., Yüce, S. and Melin, T. (2010), "Siloxane removal from landfill and digester gas - A technology overview", *Bioresource technology*, vol. 101, no. 9, pp. 2913-2923.
- Ducom, G., Laubie, B., Ohannessian, A., Chottier, C., Germain, P. and Chatain, V., (2013), *Hydrolysis of polydimethylsiloxane fluids in controlled aqueous solutions*.
- Eklund, B., Anderson, E. P., Walker, B. L. and Burrows, D. B. (1998), "Characterization of landfill gas composition at the Fresh Kills municipal solid-waste landfill", *Environmental Science and Technology*, vol. 32, no. 15, pp. 2233-2237.
- European Parliament (2012), *Air and Noise Pollution Fact Sheet*, , Available at http://www.europarl.europa.eu/ftu/pdf/en/FTU_4.10.6.pdf Accessed on 26/10/12.
- Fairén-Jiménez, D., Carrasco-Marín, F. and Moreno-Castilla, C. (2007), "Adsorption of benzene, toluene, and xylenes on monolithic carbon aerogels from dry air flows", *Langmuir*, vol. 23, no. 20, pp. 10095-10101.
- Finocchio, E., Montanari, T., Garuti, G., Pistarino, C., Federici, F., Cugino, M. and Busca, G. (2009), "Purification of biogases from siloxanes by adsorption: On the regenerability of activated carbon sorbents", *Energy and Fuels*, vol. 23, no. 8, pp. 4156-4159.
- Foster, K. L., Fuerman, R. G., Economy, J., Larson, S. M. and Rood, M. J. (1992), "Adsorption characteristics of trace volatile organic compounds in gas streams onto activated carbon fibers", *Chemistry of Materials*, vol. 4, no. 5, pp. 1068-1073.
- Fulford, D. (1996), *Biogas stove design*, University of Reading, Reading, UK.
- Gaur, A., Park, J. -. , Maken, S., Song, H. -. and Park, J. -. (2010), "Landfill gas (LFG) processing via adsorption and alkanolamine absorption", *Fuel Processing Technology*, vol. 91, no. 6, pp. 635-640.
- GE Jenbacher (2006), *Jenbacher gas engines technical specification*, , US Power and Environment.
- Ghorbel, L., Tatin, R. and Couvert, A. (2014), "Relevance of an organic solvent for absorption of siloxanes", *Environmental Technology*, vol. 35, no. 3, pp. 372-382.

- Gislon, P., Galli, S. and Monteleone, G. (2013), "Siloxanes removal from biogas by high surface area adsorbents", *Waste Management*, vol. 33, no. 12, pp. 2687-2693.
- Glus, P. H., Liang, K. Y., Li, R. and Pope, R. J. (1999), "Recent advances in the removal of volatile methylsiloxanes from biogas at sewage treatment plants and landfills", *AWMA Annual Conference*, St Louis, Missouri, Air and Waste Management Association, .
- Griffiths, J., (2012), , Personal communication.
- Griffiths, J., (2014), , Personal communication.
- Gunn, D. J. (1987), "Axial and radial dispersion in fixed beds", *Chemical Engineering Science*, vol. 42, no. 2, pp. 363-373.
- Habuka, H., Ono, N., Sakurai, A. and Naito, T. (2013), "Molecular absorption and desorption behaviour on silicon surface in a complex ambient atmosphere containing vapors of diethylphthalate, acetic acid and water", *American Journal of Analytical Chemistry*, vol. 4, pp. 80-85.
- Hagmann, M., Hesse, E., Hentschel, P. and Bauer, T. (2001), "Purification of biogas - removal of volatile silicones", *Proceedings Sardinia 2001, Eighth International Waste Management and Landfill Symposium*, Vol. 2, 1-5 October, Cagliari, Italy, CISA, Italy, pp. 641-644.
- Hand, D. W., Hokanson, D. R. and Crittenden, J. C. (1999), "Air stripping and aeration", in Letterman, R. D. (ed.) *Water quality and treatment: A handbook of community water supplies*, 5th ed, McGraw-Hill, New York, pp. 5.1-5.68.
- Hayes, H. C., Graening, G. J., Saeed, S. and Kao, S. (2003), "A summary of available analytical methods for the determination of siloxanes in biogas", 2003, Tampa, Florida, .
- Hepburn, C. A., Brown, A., Roberts, J., Simms, N. and McAdam, E. J. "On-line detection of siloxanes for adsorption vessel characterisation using FTIR spectroscopy", *Manuscript in preparation*, .
- Hepburn, C. A., Martin, B. D., Simms, N. and McAdam, E. J. (2014), "Characterization of full-scale carbon contactors for siloxane removal from biogas using online Fourier transform infrared spectroscopy", *Environmental Technology*, vol. In press.
- Hepburn, C. A., Simms, N. and McAdam, E. J. "Siloxane adsorption from biogas in the transitional regime", *Manuscript in preparation*, .

- Huang, H., Haghghat, F. and Blondeau, P. (2006), "Volatile organic compound (VOC) adsorption on material: Influence of gas phase concentration, relative humidity and VOC type", *Indoor air*, vol. 16, no. 3, pp. 236-247.
- Hunt, N., (2012), , Personal communication.
- Huppman, R., Lohoff, H. W. and Schroder, H. F. (1996), "Cyclic siloxanes in the biological waste water treatment process - determination, quantification and possibilities of elimination", *Fresenius Journal of Analytical Chemistry*, vol. 354, pp. 66-71.
- International Organisation for Standardisation (2005), *General requirements for the competence of testing and calibration laboratories*, ISO/IEC 17025:2005, International Organisation for Standardisation, Geneva, Switzerland.
- Jeison, D. and van Lier, J. B. (2006), "On-line cake-layer management by trans-membrane pressure steady state assessment in Anaerobic Membrane Bioreactors for wastewater treatment", *Biochemical engineering journal*, vol. 29, no. 3, pp. 204-209.
- Khandaker, N. and Seto, P. (2010), "Novel application of vermiculite for siloxane removal from biogas", *International Journal of Green Energy*, vol. 7, no. 1, pp. 38-42.
- Kim, D., Cai, Z. and Sorial, G. A. (2006), "Determination of gas phase adsorption isotherms-a simple constant volume method", *Chemosphere*, vol. 64, no. 8, pp. 1362-1368.
- Kim, T. Y., Kim, S. J. and Cho, S. Y. (2004), "Effect of relative humidity on the adsorption characteristics of carbon tetrachloride in a fixed bed", *Journal of Industrial and Engineering Chemistry*, vol. 10, no. 2, pp. 188-195.
- Knaebel, K. S. (2000), *A "how to" guide for adsorber design*, Adsorption Research, Inc, Dublin, Ohio.
- Kuo, J. (1999), *Practical design calculations for groundwater and soil remediation*, CRC Press LLC, Boca Raton, Florida.
- Lai, T. L. (1995), "Sequential changepoint detection in quality-control and dynamical-systems", *Journal of the Royal Statistical Society Series B - Methodological*, vol. 57, no. 4, pp. 613-658.
- Lechner, B., Paar, H. and Sturm, P. J. (2001), "Measurement of VOCs in vehicle exhaust by extractive FT-IR-spectroscopy", Fujisada H., Lurie J.B., Ropertz A., et al (eds.), in: *Sensors, Systems, and Next-Generation*

Satellites IV, Vol. 4169, 25 September 2000 through 28 September 2000, Barcelona, pp. 432.

- Lee, J. -, Choi, D. -, Kwak, D. -, Jung, H. -, Shim, W. -. and Moon, H. (2005), "Adsorption dynamics of water vapor on activated carbon", *Adsorption*, vol. 11, no. 1 SUPPL., pp. 437-441.
- Lee, S. -, Cho, W., Song, T. -, Kim, H., Lee, W. -, Lee, Y. -. and Back, Y. (2001), "Removal process for octamethylcyclotetrasiloxane from biogas in sewage treatment plant", *Journal of Industrial and Engineering Chemistry*, vol. 7, no. 5, pp. 276-280.
- Lemar, P. (2005), "CHP systems for landfills and wastewater treatment plants", *Intermountain CHP Centre workshop*, 11/08/2005, Salt Lake City, UT, .
- Li, J., Jiang, X., Xiao, W., Li, Z. and Xi, H. (2010), "Adsorption breakthrough of benzene in the fixed bed of modified activated carbon under different humidity conditions", *Journal Wuhan University of Technology, Materials Science Edition*, vol. 25, no. 3, pp. 499-503.
- Li, Y., Wang, J. D., Huang, Z. H., Xu, H. Q. and Zhou, X. T. (2002), "Monitoring leaking gases by OP-FTIR remote sensing", *Journal of Environmental Science and Health*, vol. 37, no. 8, pp. 1453-1462.
- Liang, K. Y., Li, R., Tudman, S., Schneider, R. J., Sheehan, J. F. and Anderson, E. (2001), "Pilot testing case study: removal of volatile methylsiloxanes from anaerobic digester gas fired engines", *2001 Annual AWMA conference*, 24-28 June, Orlando, Florida, Air and Waste Management Association, pp. 1-10.
- Lightfoot, E. N., Sanchez-Palma, R. J. and Edwards, D. O. (1962), "Chromatography and allied fixed-bed separations processes", in Schoen, H. M. (ed.) *New Chemical Engineering Separation Techniques*, Interscience, New York.
- Lipp, E. D. and Smith, A. L. (1991), "Infrared, raman, near-infrared and ultraviolet spectroscopy", in Smith, A. L. (ed.) *The analytical chemistry of silicones*, Wiley, New York, pp. 305-245.
- Long, C., Li, Y., Yu, W. and Li, A. (2012), "Adsorption characteristics of water vapor on the hypercrosslinked polymeric adsorbent", *Chemical Engineering Journal*, vol. 180, pp. 106-112.
- Lorberau, C. (1990), "Investigation of the determination of respirable quartz on filter media using Fourier transform infrared spectrophotometry", *Applied Occupational and Environmental Hygiene*, vol. 5, no. 6, pp. 348-350.

- Lorimier, C., Subrenat, A., Le Coq, L. and Le Cloirec, P. (2005), "Adsorption of toluene onto activated carbon fibre cloths and felts: Application to indoor air treatment", *Environmental technology*, vol. 26, no. 11, pp. 1217-1230.
- Marshik, B. and Perez, J. E. (2013), "Novel improvements in FTIR analysis of specialty gases", in Geiger, W. M. and Raynor, M. W. (eds.) *Trace analysis of specialty and electronic gases*, Wiley, Hoboken, NJ, pp. 43-70.
- Marshik, B. and Zemek, P. G. (2012), "Real-time siloxanes measurements at landfill and digester sites using FTIR", Air and Waste Management Association (ed.), in: *Air Quality Measurement methods and Technology Conference*, 24-26 April 2012, Durham, North Carolina, Curran Associates, New York, pp. 464-468.
- Matsui, T. and Imamura, S. (2010), "Removal of siloxane from digestion gas of sewage sludge", *Bioresource technology*, vol. 101, no. 1 SUPPL., pp. S29-S32.
- Mayer, B., Collins, C. C. and Walton, M. (2001), "Transient analysis of carrier gas saturation in liquid source vapor generators", *Journal of Vacuum Science and Technology A: Vacuum, Surfaces, and Films*, vol. 19, no. 1, pp. 329-344.
- McBean, E. A. (2008), "Siloxanes in biogases from landfills and wastewater digesters", *Canadian Journal of Civil Engineering*, vol. 35, no. 4, pp. 431-436.
- McCoy, B. J. and Rolston, D. E. (1992), "Effect of combined adsorption and absorption in migration of soil contaminants", Suzuki, M. (ed.), in: *Fundamentals of Adsorption: Proceedings of the 4th International Conference on Fundamentals of Adsorption*, May 17-22, Kyoto, Japan, Elsevier, Tokyo, Japan, pp. 429-436.
- Metcalf & Eddy Inc, Tchobanoglous, G., Burton, F. L. and Stensel, H. D. (2004), *Wastewater Engineering Treatment and Reuse*, 4th ed, McGraw-Hill, New York.
- Miller, J. N. and Miller, J. C. (2005), *Statistics and chemometrics for analytical chemistry*, 5th ed, Pearson Education, Harlow, UK.
- Miyauchi, T., Kataoka, H. and Kikuchi, T. (1976), "Gas film coefficient of mass transfer in low Péclet number region for sphere packed beds", *Chemical Engineering Science*, vol. 31, no. 1, pp. 9-13.
- Mohan, N., Kannan, G. K., Upendra, S., Subha, R. and Kumar, N. S. (2009), "Breakthrough of toluene vapours in granular activated carbon filled packed bed reactor", *Journal of hazardous materials*, vol. 168, no. 2-3, pp. 777-781.

- Montanari, T., Finocchio, E., Bozzano, I., Garuti, G., Giordano, A., Pistarino, C. and Busca, G. (2010), "Purification of landfill biogases from siloxanes by adsorption: A study of silica and 13X zeolite adsorbents on hexamethylcyclotrisiloxane separation", *Chemical Engineering Journal*, vol. 165, no. 3, pp. 859-863.
- Nam, S., Namkoong, W., Kang, J. -, Park, J. -. and Lee, N. (2013), "Adsorption characteristics of siloxanes in landfill gas by the adsorption equilibrium test", *Waste Management*, vol. 33, no. 10, pp. 2091-2098.
- Narros, A., Del Peso, M. I., Mele, G., Vinot, M., Fernandez, E. and Rodriguez, M. E. (2009), "Determination of siloxanes in landfill gas by adsorption on Tenax tubes and TD-GC-MS", *Sardinia 2009, 12th International Waste Management and Waste Symposium*, 5-9 October, S. Margherita di Pula, Caligari, Italy, Italy, .
- Ohannessian, A., Desjardin, V., Chatain, V. and Germain, P. (2008), "Volatile organic silicon compounds: The most undesirable contaminants in biogases", *Water Science and Technology*, vol. 58, no. 9, pp. 1775-1781.
- Oshita, K., Ishihara, Y., Takaoka, M., Takeda, N., Matsumoto, T., Morisawa, S. and Kitayama, A. (2010), "Behaviour and adsorptive removal of siloxanes in sewage sludge biogas", *Water Science and Technology*, vol. 61, no. 8, pp. 2003-2012.
- Parliamentary Office of Science and Technology (2007), *Postnote number 282: Energy and Sewage*, .
- Pei, J. and Zhang, J. S. (2012), "Determination of adsorption isotherm and diffusion coefficient of toluene on activated carbon at low concentrations", *Building and Environment*, vol. 48, no. 1, pp. 66-76.
- Perry, R. H. and Green, D. W. (1998), *Perry's Chemical Engineers' Handbook*, 7th ed, McGraw-Hill.
- Persson, M. and Wellinger, A. (2006), *Biogas upgrading and utilisation*, , International Energy Agency, Paris.
- Photovac (2012), *Photovac sentry online siloxane monitor*, , Photovac, Waltham, MA Available at <http://www.photovac.com/sentry-form.aspx> Accessed on 28/10/11.
- Pirnie, M. (2011), *Retrofit digester gas engine with fuel gas clean-up and exhaust emission control technology - Pilot testing of emission control system plant one engine one*, J-79, Orange County Sanitation District, Irvine, California.

- PpTek (2014), *PpTek siloxane removal systems*, available at: <http://www.pptek.co.uk/index.php> (accessed 02/09/2014).
- Prabucki, M. J., Doczyck, W. and Asmus, D. (2001), "Removal of organic silicon compounds from landfill and sewer gas", *Proceedings Sardinia 2001, Eighth International Waste Management and Landfill Symposium*, Vol. 2, 1-5 October, Cagliari, Italy, CISA, Italy, pp. 632-639.
- Ramirez, D., Qi, S., Rood, M. J. and Hay, K. J. (2005), "Equilibrium and heat of adsorption for organic vapors and activated carbons", *Environmental Science and Technology*, vol. 39, no. 15, pp. 5864-5871.
- Rasi, S., Läntelä, J. and Rintala, J. (2011), "Trace compounds affecting biogas energy utilisation - A review", *Energy Conversion and Management*, vol. 52, no. 12, pp. 3369-3375.
- Rasi, S., Lehtinen, J. and Rintala, J. (2010), "Determination of organic silicon compounds in biogas from wastewater treatments plants, landfills, and co-digestion plants", *Renewable Energy*, vol. 35, no. 12, pp. 2666-2673.
- Rasi, S., Veijanen, A. and Rintala, J. (2007), "Trace compounds of biogas from different biogas production plants", *Energy*, vol. 32, no. 8, pp. 1375-1380.
- Read, A. and Hofmann, F. (2011), "Does biogas scrub up?", in *Materials Recycling World*, 2nd December 2011 ed, EMAP Publishing, London.
- Ricaurte Ortega, D. and Subrenat, A. (2009a), "Elimination of siloxanes by adsorption process as a way of upgrading biogas", *2nd International Conference on Energy and Sustainability, Energy and Sustainability 2009*, Vol. 121, 23-25 June, Bologna, pp. 49.
- Ricaurte Ortega, D. and Subrenat, A. (2009b), "Siloxane treatment by adsorption into porous materials", *Environmental technology*, vol. 30, no. 10, pp. 1073-1083.
- Ross, G. J. (2013), "Modelling financial volatility in the presence of abrupt changes", *Physica A: Statistical Mechanics and its Applications*, vol. 392, no. 2, pp. 350-360.
- Ross, G. J., Tasoulis, D. K. and Adams, N. M. (2011), "Nonparametric Monitoring of Data Streams for Changes in Location and Scale", *Technometrics*, vol. 53, no. 4, pp. 379-389.
- Royal Society of Chemistry (2014), *ChemSpider*, available at: <http://www.chemspider.com/Search.aspx> (accessed October 14th).

- Rubinson, K. A. and Rubinson, J. F. (2000), *Contemporary instrumental analysis*, Prentice-Hall, Upper Saddle River, NJ.
- Ruyken, M. A., Visser, J. A. and Smilde, A. K. :. (1995), "Online detection and identification interferences in multivariate predictions of organic gases using FT-IR spectroscopy", *Analytical Chemistry*, vol. 67, no. 13, pp. 2170-2179.
- Sager, U. and Schmidt, F. (2010), "Binary adsorption of n-butane or toluene and water vapor", *Chemical Engineering and Technology*, vol. 33, no. 7, pp. 1203-1207.
- Schweigkofler, M. and Niessner, R. (1999), "Determination of siloxanes and VOC in landfill gas and sewage gas by canister sampling and GC-MS/AES analysis", *Environmental Science and Technology*, vol. 33, no. 20, pp. 3680-3685.
- Schweigkofler, M. and Niessner, R. (2001), "Removal of siloxanes in biogases", *Journal of hazardous materials*, vol. 83, no. 3, pp. 183-196.
- Severn Trent Water (2013a), *Delivering the future of water: Annual report and accounts*, , Severn Trent Water, Coventry.
- Severn Trent Water (2013b), *Working hard for our customers: our performance in 2012/13*, , Severn Trent Water, Coventry.
- Sherwood, T. K., Pigford, R. L. and Wilke, C. R. (1975), *Mass Transfer*, McGraw-Hill, New York.
- Shih, Y. -. and Li, M. -. (2008), "Adsorption of selected volatile organic vapors on multiwall carbon nanotubes", *Journal of hazardous materials*, vol. 154, no. 1-3, pp. 21-28.
- Shin, H. -. , Park, J. -. , Park, K. and Song, H. -. (2002), "Removal characteristics of trace compounds of landfill gas by activated carbon adsorption", *Environmental Pollution*, vol. 119, no. 2, pp. 227-236.
- Sigot, L., Ducom, G., Benadda, B. and Labouré, C. (2014), "Adsorption of octamethylcyclotetrasiloxane on silica gel for biogas purification", *Fuel*, vol. 135, no. 0, pp. 205-209.
- Silvestre-Albero, A., Ramos-Fernández, J. M., Martínez-Escandell, M., Sepúlveda-Escribano, A., Silvestre-Albero, J. and Rodríguez-Reinoso, F. (2010), "High saturation capacity of activated carbons prepared from mesophase pitch in the removal of volatile organic compounds", *Carbon*, vol. 48, no. 2, pp. 548-556.

- Smith, A. L. (1991), "Introduction to silicones", in Smith, A. L. (ed.) *The analytical chemistry of silicones*, Wiley, New York, pp. 3-19.
- Smith, A. L. and Parker, R. D. (1991), "Trace analysis involving silicones", in Smith, A. L. (ed.) *The analytical chemistry of silicones*, Wiley, New York, pp. 71-95.
- Song, Y., Kwon, S. and Woo, J. (2004), "Mesophilic and thermophilic temperature co-phase anaerobic digestion compared with single-stage mesophilic- and thermophilic digestion of sewage sludge", *Water research*, vol. 38, no. 7, pp. 1653-1662.
- Soreanu, G., Beland, M., Falletta, P., Edmonson, K., Svoboda, L., Al-Jamal, M. and Seto, P. (2011), "Approaches concerning siloxane removal from biogas - a review", *Canadian Biosystems Engineering*, vol. 53, no. 8, pp. 1-18.
- Srivastava, A. K., Shah, D., Saxena, A., Mahato, T. H., Singh, B., Verma, A. K., Shrivastava, S., Roy, A., Shrivastava, A. R. and Gutch, P. K. (2012), "Vapour breakthrough behaviour of carbon tetrachloride - A simulant for chemical warfare agent on ASZMT carbon", *Journal of Scientific and Industrial Research*, vol. 71, no. 11, pp. 748-756.
- Štandeker, S., Novak, Z. and Knez, Z. (2009), "Removal of BTEX vapours from waste gas streams using silica aerogels of different hydrophobicity", *Journal of hazardous materials*, vol. 165, no. 1-3, pp. 1114-1118.
- Stuart, B. (2004), *Infrared spectroscopy: Fundamentals and applications*, John Wiley & Sons, Chichester, England.
- Surita, S. C. and Tansel, B. (2013), "Emergence and fate of cyclic volatile polydimethylsiloxanes (D4, D5) in municipal waste streams: Release mechanisms, partitioning and persistence in air, water, soil and sediments", *Science of the Total Environment*, vol. 468-469, pp. 46-52.
- Tadros, M. E., Hu, P. and Adamson, A. W. (1974), "Adsorption and contact angle studies: I. Water on smooth carbon, linear polyethylene, and stearic acid-coated copper", *Journal of colloid and interface science*, vol. 49, no. 2, pp. 184-195.
- Tagliabue, M., Farrusseng, D., Valencia, S., Aguado, S., Ravon, U., Rizzo, C., Corma, A. and Mirodatos, C. (2009), "Natural gas treating by selective adsorption: Material science and chemical engineering interplay", *Chemical Engineering Journal*, vol. 155, no. 3, pp. 553-566.
- Tower, P. (2003), "Removal of siloxanes from landfill gas by SAGTM polymorphous porous graphite treatment systems", *SWANA 26th Landfill Gas Symposium*, 27/03/2003, Tampa, FL, .

- Tower, P. M. and Wetzel, J. V. (2004), "Reducing biogas power generation costs by removal of siloxanes", *NZWWA 46th Annual Conference*, 6-8/10/2004, Christchurch, NZ, .
- Tower, P. M. and Wetzel, J. V. (2006), "Making power generation make sense by removing siloxanes from digester gas", *CWEA Annual Conference*, 5-7 April, Sacramento, CA, California Water Environment Association, .
- Tower, S. and Tower, P. (2007), *Guaranteed removal of siloxanes from digester and landfill gas*, 425.334.5505, Applied Filter Technology.
- Turner, R. (2010), "Bayesian change point detection for satellite fault prediction", *Proceedings of interdisciplinary graduate conference*, 28-29 June, Cambridge, UK, pp. 213-221.
- Urban, J. C. and Gomezplata, A. (1969), "Axial dispersion coefficients in packed beds at low Reynolds numbers", *The Canadian Journal of Chemical Engineering*, vol. 47, no. 4, pp. 353-359.
- USEPA (2006), *Off-gas treatment technologies for soil vapour extraction systems: State of the practice*, EPA-542-R-05-028, USEPA, Cincinnati, Ohio.
- Vale, P., (2014), , Personal communication.
- van Egmond, R., Sparham, C., Hastie, C., Gore, D. and Chowdhury, N. (2013), "Monitoring and modelling of siloxanes in a sewage treatment plant in the UK", *Chemosphere*, vol. 93, no. 5, pp. 757-765.
- Vargaftik, N. B., Volkov, B. N. and Voljak, L. D. (1983), "International tables of the surface tension of water", *Journal of Physical and Chemical Reference Data*, vol. 12, no. 3, pp. 817-820.
- Veksha, A., Uddin, A., Sasaoka, E. and Kato, Y. (2012), "Adsorption and desorption behavior of benzene on activated carbons from different precursors in dry and humid conditions", *Journal of Chemical Engineering of Japan*, vol. 45, no. 6, pp. 387-394.
- Vizhemehr, A. K., Kholafaei, H., Haghghat, F. and Lee, C. -. (2011), "The effect of relative humidity level, VOC type and multiple VOCs on the performance of full-scale GAC filters", *12th International Conference on Indoor Air Quality and Climate 2011*, Vol. 3, 5 June 2011 through 10 June 2011, Austin, TX, pp. 1791.
- Wakao, N. and Funazkri, T. (1978), "Effect of fluid dispersion coefficients on particle-to-fluid mass transfer coefficients in packed beds: Correlation of

- sherwood numbers", *Chemical Engineering Science*, vol. 33, no. 10, pp. 1375-1384.
- Weber Jr., W. J. (1983), "Evolution of a technology", *Journal of Environmental Engineering*, vol. 110, no. 5, pp. 899-917.
- Weber Jr., W. J. and Smith, E. H. (1987), "Simulation and design models for adsorption processes", *Environmental Science and Technology*, vol. 21, no. 11, pp. 1040-1050.
- Welty, J. R., Wicks, C. E., Wilson, R. E. and Rorrer, G. (2001), *Fundamentals of momentum, heat and mass transfer*, 4th ed, John Wiley and Sons, New York.
- Wheless, E. and Gary, D. (2002), "Siloxanes in landfill and digester gas", *25th Annual Landfill Gas Symposium*, 25-28 March, Monterey, California, SWANA, pp. 29.
- Wheless, E. and Pierce, J. (2004), "Siloxanes in landfill and digester gas update", *SWANA 27th Landfill Gas Conference*, 22-25 March 2004, San Antonio, Texas, .
- Williams, S., Leung, Y., Aleixo, J. and Hu, R. (2014), *Understanding FTIR formaldehyde measurement and its influence on the RICE NESHP rule*, , DCL International, Ontario, Canada.
- Wilson, E. J. and Geankoplis, C. J. (1966), "Liquid mass transfer at very low Reynolds numbers in packed beds", *Industrial and Engineering Chemistry Fundamentals*, vol. 5, no. 1, pp. 9-14.
- World Health Organisation (2010), *WHO guidelines for indoor air quality: selected pollutants*, , WHO European Office for Environment and Health, Bonn, Germany.
- Xu, L., Shi, Y. and Cai, Y. (2013), "Occurrence and fate of volatile siloxanes in a municipal Wastewater Treatment Plant of Beijing, China", *Water research*, vol. 47, no. 2, pp. 715-724.
- Yang, R. T. (1997), *Gas separation by adsorption processes*, Imperial College Press, London.
- Yi, F. -, Lin, X. -, Chen, S. -. and Wei, X. -. (2009), "Adsorption of VOC on modified activated carbon fiber", *Journal of Porous Materials*, vol. 16, no. 5, pp. 521-526.

Yu, M., Gong, H., Chen, Z. and Zhang, M. (2013), "Adsorption characteristics of activated carbon for siloxanes", *Journal of Environmental Chemical Engineering*, vol. 1, no. 4, pp. 1182-1187.

Zaitan, H., Bianchi, D., Achak, O. and Chafik, T. (2008), "A comparative study of the adsorption and desorption of o-xylene onto bentonite clay and alumina", *Journal of hazardous materials*, vol. 153, no. 1-2, pp. 852-859.